Needle Intervention System with Mirror Ultrasound Imaging

Final Project Report

Major Qualifying Project by:
Aditya Malik
Isaac Abouaf

Advised by:
Professor Haichong Zhang

Acknowledging:
Yichuan Tang
Jakub Tomasz
Ryosuke Tsumura
Dr. Igor Sorokin

05/06/2020

Table of Contents

Abbreviations:

Ultrasound (US)
Percutaneous Nephrolithotomy (PCNL)
Obstetrics and Gynecology (OB/GYN)
Time Gain Compensation (TGC)
Needle and Camera System (NCS)
Degree(s) of Freedom (DOF)
Internal Measurement Unit (IMU)
Integrated Circuit (IC)
Lithium Polymer (li-poly)
Graphical User Interface (GUI)
Radio Filter (RF)
Computer Aided Design (CAD)
Printed Circuit Board (PCB)

Table of Figures

Table of Tables

Abstract:

Procedures such as Percutaneous Nephrolithotomy often face problems with ineffective needle insertion due to the unknown geometric relationship with the needle, fascia, and ultrasound probe. The goal of the project is to develop a needle insertion device with mirror ultrasound imaging, which provides an intuitive and simple solution to guide the needle insertion path. This is achieved by visualizing the forward-view of needle insertion by changing the relative angle between mirror and US probe.

Client Statement:

Common clinical procedures, such as PCNL, that require needle insertion into the patient's body often require highly skilled technicians. In approximately 3 to 12 percent of PCNL cases, there is excessive bleeding caused by fault needle passage [1]. Image guidance using ultrasound is a great low-cost, real-time imaging procedure that can be used to visualize and monitor the position of the needle and its target during insertion, making the needle insertion process more effective. Unfortunately, the scale and shape of the current design, along with difficulty aligning the needle and ultrasound probe, makes it difficult and sometimes near to impossible to view the needle tip during insertion.

“The need for extensive experience and the unknown geometric relationship between the needle and ultrasound probe leads to difficulties with finding the optimal position and angle for needle insertion.”p

Background:

Ultrasound (US) technology

Ultrasound is commonly used in medical imaging to help diagnose causes of pain, swelling, infection in internal organs, and to examine a baby during pregnancy. The reason behind ultrasound's popularity is that it is safe, noninvasive, and does not use radiation. Ultrasound procedures use a small probe, called a transducer, and gel placed directly on the skin. Because images are captured in real-time, ultrasound can be used to capture the structure and movement of the body's internal organs [2].

Ultrasound is a series of tiny mechanical pressure waves propagating through the body. These sound waves are generated, transmitted, and received by US transducers. The US transducer contains several piezoelectric elements that are excited by an electric current. The electric current applied to the piezoelectric elements causes the element to expand and contract, creating a pressure wave. The typical frequencies of ultrasound range from 1 to 20 MHz Smaller piezoelectric elements vibrating faster leads to higher sound frequencies. Similarly, larger piezoelectric elements vibrating relatively slower, lead to lower sound frequencies. These pressure waves then propagate through tissue and different organs in the body. As ultrasound waves pass through tissue, they are reflected to the US transducer, where they are processed by an ultrasound engine to produce a black and white US image [3]. The image below shows the internal structure of a convex array transducer, and the piezoelectric elements that convert electric current to ultrasound waves.

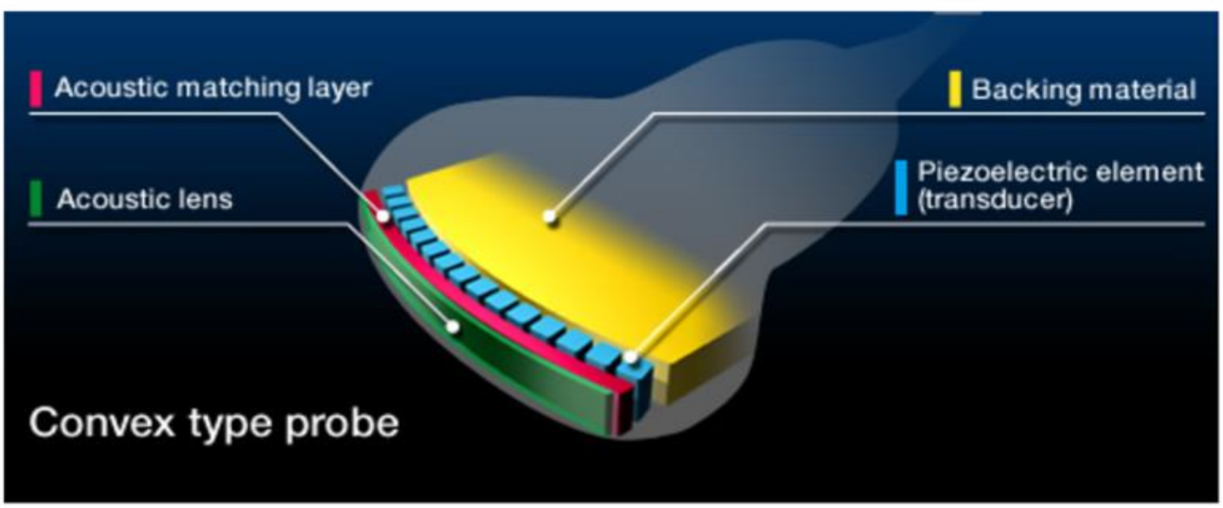

Figure 1: Convex Array Ultrasound Probe

An US image is a cross-section inside the patient that is formed line-by-line in front of the transducer. The US transducer is positioned at different angles to observe different 'slices' of the object in consideration. Sound waves are propagated through tissue rapidly, at approximately 1540 m/s. As the sound wave reaches internal structures, reflected waves are sent back to the transducer surface. Since the sound travels at a known speed, the system can interpret the signal and display structures at their exact location on the screen. Shallow structures, which reflect first, will be displayed at the top of the image. Echoes from deeper structures take longer to return and are displayed at the bottom of the image. This processing is done rapidly enough to display moving images in real-time [3]. With ultrasound, the major source of soft tissue absorption, is attenuation. Attenuation is the conversion of acoustic energy into heat, which results in the US waves becoming weaker over distance. Therefore, deeper structures are more difficult to see due to attenuation. Most ultrasounds compensate for attenuation by increasing the time gain compensation (TGC), also known as gain at deeper levels. Increasing TGC levels, brighten deeper structures to improve visibility.

The reflection of ultrasound waves against an acoustic mirror is dictated by Snell's Law. Snell's law is a formula used to describe the relationship between the angle of incidence and the angle of refraction when ultrasound waves pass through a boundary between two different isotropic media [4]. Following Snell's Law, total reflection occurs when the angle of incidence of ultrasound beam is equal to, or greater than, the critical angle. The critical angle can be determined by the equation below, where c1 is the speed of sound in the medium where the ultrasound waves originate from, and c2 is the speed of sound in the second medium.

$$\theta_c = \sin^{-1}(\frac{c_1}{c_2})$$

To apply Snell's law to our application, the value for c1 would be approximately 1480 m/s. This is the typical speed of sound in water. The value for c2 would depend on if we used metal or glass to reflect the ultrasound beam. If we used glass, the value for c2 would be 5700 m/s. Therefore, the critical angle can be calculated as follows:

$$\theta_c = \sin^{-1}(\frac{1480}{5700}) = 15.05°$$

Similarly, if we used a steel sheet to reflect to the ultrasound beam, the critical angle could be calculated as follows. The value of the speed of sound in steel is 5960 m/s:

$$\theta_c = \sin^{-1}(\frac{1480}{5960}) = 14.38°$$

For our application, the angle of incidence of the ultrasound beam is 45 degrees. Therefore, for both cases, since the critical angle is less than 45 degrees, there would be total reflection and no transmission of the ultrasound beam through the reflective surface. Furthermore, following Snell's Law, the angle of incidence will be equal to the angle of reflection as seen in the image below.

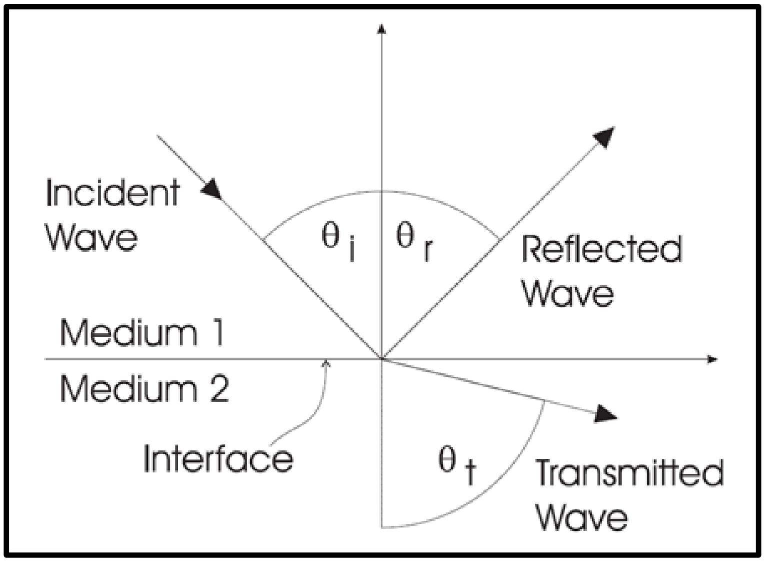

Figure 2: Snell's Law

As the angle of the mirror changes, the angle of incidence and the angle of reflection alter by the same amount. Therefore, in an instance where a mirror is adjusted by 1 degree, the angle of incidence and the angle of reflection both increase by 1 degree. This is a total change of 2 degrees, meaning that the angle of the reflected waves is influenced by the mirror's change in angle by a factor of two.

For sound to travel through the body, the medium must be acoustically coupled. This is due to the US being reflected and shadowed by air, given its low acoustic impedance. Acoustic impedance is a physical property of tissue. It describes how much resistance an ultrasound beam encounters as it passes through a tissue [4]. Acoustic impedance depends on the density of the tissue (d) and the speed of sound in the medium (c). A formula relating these factors can be seen below:

$$Acoustic\ Impedance\ (Z)$$
$$Z = d * c$$

Examples of impedance for bodily tissues (in kg/(m2s)) can be seen in the following table:

Table 1: Acoustic Impedance for Mediums Found Within the Body

Medium	Acoustic Impedance (kg/(m^{2}s))
air	0.0004×10^6
lung	0.18×10^6
fat	1.34×10^6
water	1.48×10^6
kidney	1.63×10^6
blood	1.65×10^6
liver	1.65×10^6
muscle	1.71×10^6
bone	7.8×10^6

Furthermore, because US is reflected by air, we need to use gel and there must be proper contact between the transducer and the patient. When air is trapped in between the transducer and the patient's skin, it reflects sound waves and creates shadowing. Structures like bones are strong reflectors, which means that most of the incoming wave is reflected by the structure, creating an acoustic shadow. Scatter occurs when US waves encounter a medium with a non-homogenous surface, where a portion of the sound wave is scattered in random directions. Scatter leads to a phenomenon known as Speckle, which produces miscellaneous types of grainy appearances in US images [3].

Clinical US mainly use 2 types of imaging: brightness-mode (B-mode) and Doppler mode. These modalities are based on varying sorts of US waves radiated by the transducer and are utilized for diverse applications. B-mode ordinarily utilizes a linear array of transducers to show morphological highlights of vessels by picturing a plane through the body. Doppler mode, on the other hand, can be part of a few diverse categories of imaging applications. The two major types are pulse-wave doppler and continuous wave doppler. An example of a B-mode ultrasound of a kidney can be seen below:

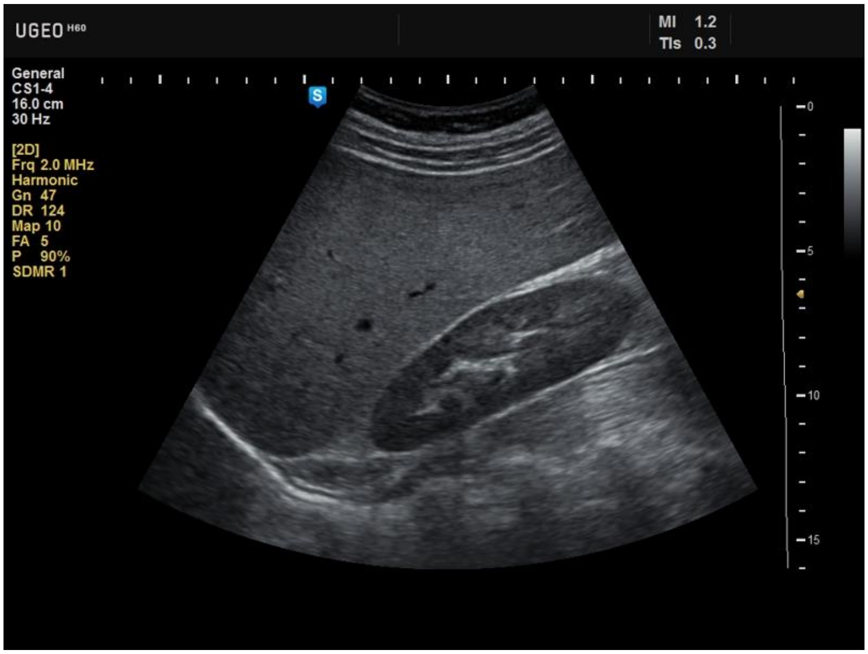

Figure 3: B-mode ultrasound of Kidney

There are several factors that affect the clarity of an ultrasound image. One of the factors is frequency. Lower frequencies are less attenuated and provide better penetration which is good for deeper structures. On the other hand, high frequencies provide better resolution for shallow structures. For optimal imaging, it is critical to select an US transducer with the right frequency for the anatomy being examined. It is essential to make sure the transducer is capable of adequate penetration, reasonable resolution, sufficient frequency, reasonable wavelength.

There are three types of US transducers that all have different medical applications. These are curved array, phased array, and linear array transducers. The active elements in a linear array transducer are arranged in a straight line and are typically non-steered. This results in evenly spaced beams and the best possible resolution. Convex array transducers utilize high frequencies, making them suitable for vascular and soft-tissue studies [3]. In our application, we will be using a Clarius C3 convex array transducer to guide a PCNL procedure. The image below shows the different types of ultrasound probes and the way they transmit ultrasound beams.

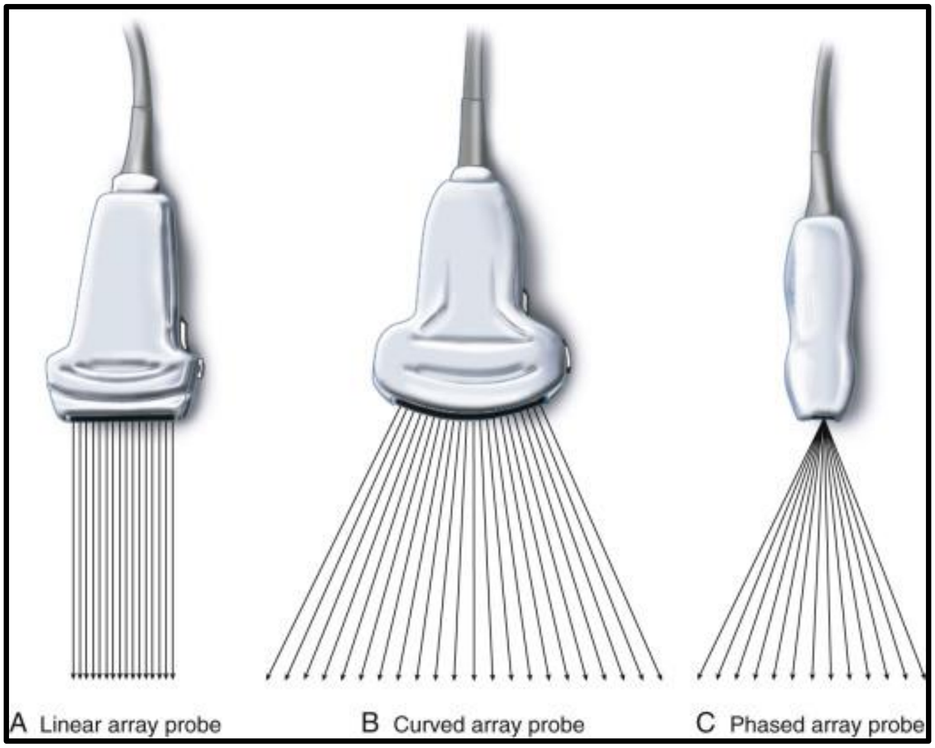

Figure 4: Types of Ultrasound Probes

Traditional Needle Intervention and PCNL

Currently, guided needle injections are separated into two different categories: augmented haptic force feedback and ultrasound-guided injections. To understand the need for these 2 procedures, background on how surgeries were completed before their creation must be detailed.

Before the ability to "look" inside a patient's body was created, blind injections were the only option for doctors. Blind injections are procedures done with needles where the doctors have no imaging device to show the path ahead. Complications with these types of procedures can range from hitting bones or nerves (causing paralysis in spinal injections), injecting into surrounding soft tissue when aiming for the joint space, or nicking an artery in the neck while trying to inject into the thyroid- ending in internal bleeding. In 2016, an article was published titled "Blind Injections: Ethical but not Eligible" [5] which added itself to the growing number of papers concerned with the continuation of blind injections. The main concern of the medical community was two-fold: are blind injections ethical, and if they are determined as such, are their shortcomings too drastic to be ignored.

One of the most common applications for percutaneous needle insertion procedures is PCNL. PCNL, since its development in the 1970s, has now become the gold standard for treating staghorn stones and other large kidney stones. The surgical procedure of PCNL usually comprises three main steps. The procedure starts with the insertion of a ureteral catheter to perform a retrograde study to evaluate the kidney anatomy and to analyze whether a kidney stone is blocking the urinary tract. Once this is accomplished, a puncture is performed by inserting a needle from the skin toward the calculi location. The final step deals with stone fragmentation and extraction using surgical tools such as nephoscopes, forceps, baskets, and stone lithotripters [6].

The procedure is traditionally guided by fluoroscopy and hence may pose a significant risk of radiation to the patient and practitioners performing the procedure. The images below show a fluoroscopy guided PCNL procedure.

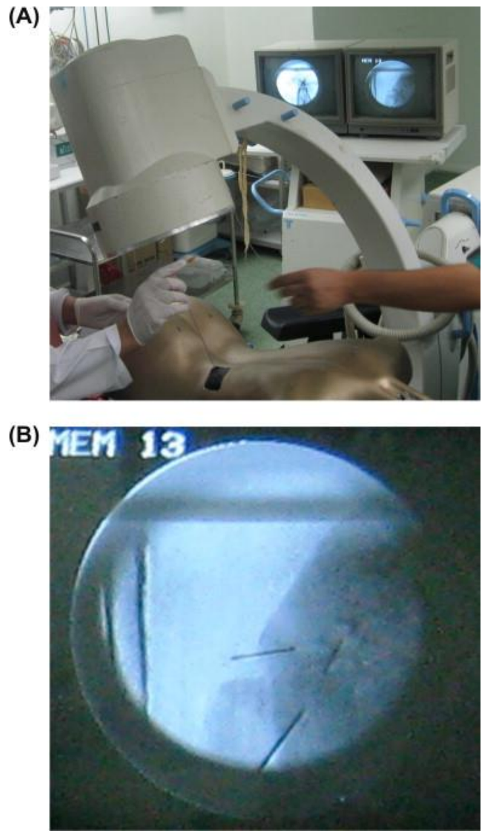

Figure 5: Fluoroscopy Guided PCNL Procedure

To perform a successful PCNL, an accurate puncture into the desired calyx is extremely important. It is essential that the puncture takes place through the center of the calyceal papillae to avoid causing damage to the interlobar and accurate branches of the renal artery. According to a study reported by Sampio et al, injury to the interlobar vessels occurs approximately 67 percent of upper pole and 13 percent of lower pole punctures [7]. Precise needle puncture of the kidney is a challenging and essential step for successful PCNL, which is challenging to accomplish without the help of an imaging guidance system. Although fluoroscopy allows accurate identification of the desired calyx to puncture, it does not allow for “real-time simultaneous bi-plane fluoroscopy " [8], making the procedure of getting an accurate puncture into the desired calyx a fastidious process for even experienced surgeons. Furthermore, essential organs adjacent to the kidney, such as the bowels and pleura, are not visualized during the procedure which poses additional risk of injury. There is, therefore, a need for a better imaging system that can add additional benefit for real-time imaging and include the visualization of organs adjacent to the kidney that are at risk during PCNL procedures. Next, we will look at ultrasound guided needle intervention procedures and its application in PCNL procedures.

US Guided Needle Intervention

Ultrasound imaging is widely used for clinical operations that require needle insertion due to a lack of radiation, low cost, and its ability to provide real-time imaging. The image shown below demonstrates the use of ultrasound image guidance during PCNL procedures.

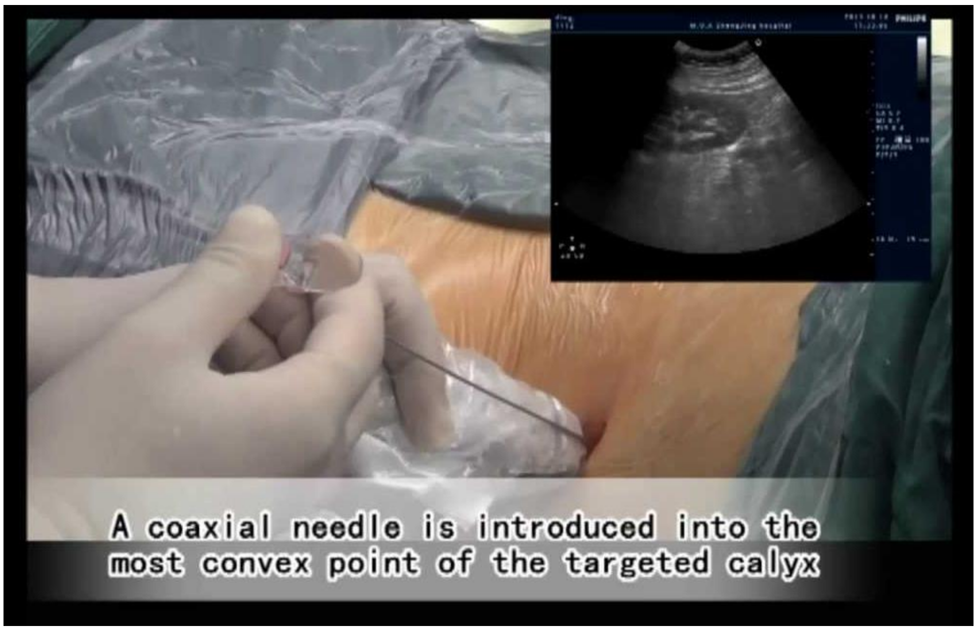

Figure 6: Ultrasound Guided PCNL Procedure

The use of US is widely recognized as being a safe and effective method of conducting needle surgical needles in percutaneous procedures. This is due to its ability to enable real-time image acquisition, has versatility, and is a much more cost-effective alternative compared to other imaging options, such as MRI. Furthermore, given the absence of radiation, US is the imaging option of choice for pregnant patients and other patients with transplanted organs. Recent technological advances have also made it possible to acquire 3D ultrasound images that provide volumetric measurements and a 360-degree view of anatomic structures [8].

Following the drawbacks of fluoroscopy in PCNL mentioned in the section above, access with ultrasound-guided puncture during PCNL will allow for real-time tracking of the route of the puncture into the desired calyx. It would also give practitioners visualization of adjacent organs thus avoiding any accidental injury to them. This increased optimization to the access point for PCNL procedures will result in fewer bleeding complications and increased postoperative stone free rates [8].

However, current methods of ultrasound guided PCNL procedures also face certain challenges. Currently, physicians performing needle intervention procedures must hold the needle with their dominant hand, while manipulating the ultrasound probe with their other hand to find the optimum position and angle to insert the needle with. The underlying issue with this process is the need for physicians to have extensive experience with needle insertion procedures to successfully perform them [9]. This is due in part to physicians being unaware of the geometric relationship between the needle and the ultrasound probe, which means there is often a lot of trial and error before the physician can find the optimal point for insertion [10].

The safe and successful performance of ultrasound-guided procedure requires that the physician always know exactly where the needle tip is always. Therefore, the visualization of the needle tip requires alignment with the ultrasound beam. In this paper, we propose an ultrasound image-guided needle insertion system that provides an intuitive and simple solution to guide the needle insertion path. This can be done by visualizing the forward-view of the needle insertion by changing the relative angle between a mirror and the ultrasound beam.

State of the Art:

Current Solutions

There are currently products available that seek to improve the effectiveness of ultrasound guided procedures by ensuring proper needle alignment with the ultrasound imaging plane. These products do so by creating universal attachments for multiple US probes or marketing a device to a certain probe. An example of one such product was created by a group of students from Harvard University [11]. An image of their design can be seen below.

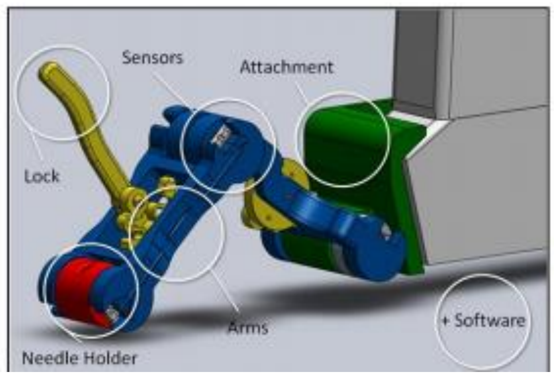

Figure 7: Needle Guide Attaching to the Ultrasound Probe

The system above would provide a practitioner with the ability to lock the guide to prevent needle deviation from the desired position during the procedure. The system also eliminates the need for extensive experience to develop the fine hand movement needed for traditional ultrasound guided procedures. However, an issue with the current design is that there are certain applications that require the needle to be in the same plane as the ultrasound image, such as percutaneous nephrolithotomy (PCNL) where the forward-view of the needle insertion is required. In this case, the current solution proposed would not be suitable. Furthermore, there is a need for a system to provide real-time visualization of the needle insertion process, so that a practitioner can always see the needle and determine its optimal position.

Another current product strays from the idea of a needle-guided attachment system and follows the ideology of needle tracking systems. This device "uses a pair of cameras to track the needle location so that a standard needle can be used without attaching a separate sensor to the needle" [5]. In layman's terms, this device can cut down extraneous additions and in turn- cut down cost, size, and complications.

Below shows the expected positions and degrees of freedom of the needle with respect to this ultrasound device.

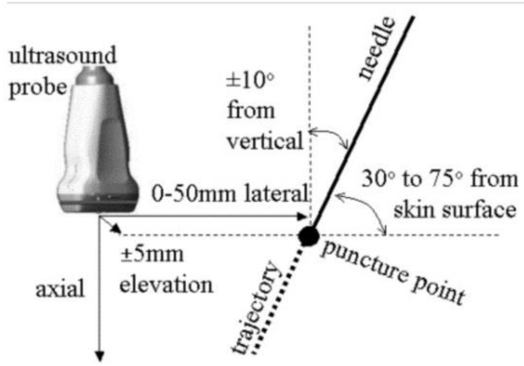

Figure 8: Expected Workspace of the Needle with Respect to the Ultrasound Probe [5]

Positives of this device focus on major improvements with the needle tracking with respect to the US beam. By mounting a miniature camera system on the ultrasound probe, common problems with line of sight are near to fully addressed (no obstructions in the line of sight). The clear line of sight also makes placement of the device far more flexible than others on the market due to the removal of markers usually needed for direct tracking. Another plus of this device is its ease of use. As mentioned in the article, “many...percutaneous procedures are recognized as challenging tasks and considerable expertise is required to perform the procedure with a single insertion” [5]. By removing the need for complicated, expensive, and time-consuming training- this device is attractive for both hospitals who may not have the funds/resources larger, or city hospitals may and/or ones with few extensively trained staff.

Drawbacks, however, of this device include the position operators must hold the device in prior to use, limited needle trajectory, sterility concerns, and the year this device went onto market. As mentioned in the product outline, “the operator is required to hold the needle such that a small segment just above the puncture point is visible to the cameras...by holding the base or...shaft with a precision fingertip grip” [5]. So, while this device can take out a majority of traditional operator training for this type of device, such a precise grip leaves much room for error. As the needle and camera system (from here on, this system shall be referred to as NCS) are both exposed to open air and are such a small apparatus; should the grip block the cameras in any way the device is rendered useless, and an operator must go back and readjust.

Another concern with this device, as mentioned previously, is the limited needle trajectory for surgery. Unfortunately, due to the limited geometry of needle guides in 2005 (being as this year was when this device was created), the geometry to hold these guides would not be compliant with those in 2020. This in turn creates another problem for the device: the necessity of these needle guides for accurate expected trajectory of the US image. The simulation software projecting these values is based around the slot direction (and thus the needle) being a fixed, constant variable takes away the option to have surgeons work with more than one degree of freedom and the accuracy needed for such a sensitive surgery.

A final drawback for this device, sterility is a major component for all surgical equipment to pass inspections and be safely used on patients. In this device’s case, the attachment off the ultrasound is detailed as bare (allowing cameras to have an unobstructed view) which, in other words, means all the delicate components (including what is to go into the patient) sits out for dust, bacteria, and more to gather on it. Additionally, as mentioned above, this device was created in 2002 so while many of the principles will be the same with our device- technology has far improved since 2005 and shortcomings with this device must be kept in mind with the creation of a far more modern version.

While the previous device was limited by the technology 15 years ago, the next device was developed mere months ago by alumni of Georgia Tech. This device, the Ethos *Iris* was originally developed for lumbar punctures (more commonly known as spinal taps) to replace the outdated palpation-guided process used since 1891.

The *Iris*, akin to our projected device, uses ultrasound to create a projected needle pathway image that surgeons can use to reduce needle pokes, pain, and increase accuracy. Finding the correct spot to inject reduces complications with surgery (multiple sticks can lead to infection, increased hospital stays times, and expensive bills) and allows for one device to be used on patients with very different anatomy. For instance, obese patients commonly have issues with the palpation method due to amount of adipose insulating their bodies in the subQ region of the dermis. Other positives of this device include having an attachment system that works with ultrasound wands with a “disposable, rotatable needle guide insert” [12], and software programmed to display the needle path on the ultrasound image. By attaching to the head of the device, most of the problems with visualization are mitigated and sensors in a reusable insert on the ultrasound head can correctly orient the image should the device rotate. While the *Iris* does not completely remove the need for training, the years traditionally spent to prepare are now majorly shortened with the length of training dependent on how proficient the user is with ultrasound.

Drawbacks of the device include further development still needed, training, and limited testing in the field. Further development refers to the company being founded in 2018 then this device being brought into the spotlight only two years later. Much of the specifics still need to be looked over, including a training plan for surgeons. Currently, the CEO/founders of the company have been personally going into hospitals to show how the device works however when the product goes to market, they must have something organized. The plan for this project is to attempt to remove training needed for use to reach more hospitals and technicians than currently. However, this device was created and has only been tested on the Philips Lumify portable ultrasound which greatly reduces the number of hospitals this can be marketed to. In an interview on March 18, 2020 one of the founders talked about an attachment system being worked on for carted options (an example given is the SonoSite model) but with the product going to market in Q3 of 2021, this model may not be fully tested in time.

The third and final device is the EpiGuide two dimensional (2D) created for neuraxial procedures in relation to lumbar punctures, epidurals, or combined-spinal epidural placements. As with the other devices discussed in this paper, this device was created to give surgeons the ability to visualize a needle pathway without falling to palpation/blind injections. Especially in the case where injections must be made near to the spine (where parts of the kidneys fall), inaccurate insertion can lead to spinal cord damage and fully puncturing through the kidney accidently which then leads to extended hospital stays and pain.

Benefits of this device begin with the year it was created. Though not the 7 months prior design of the *Iris*, 2019 is still quite modern. The insertion and imaging accuracy testing was a massive positive for this device as well with benchtop, water bath, and in vivo porcine models utilized. In total, “n=424 needle insertions (were) performed” [13] and “visible range and contrast-to-noise ratios” [13] were analyzed after each insertion. Below are two charts explaining the methods for testing the EpiGuide and data from the water bath testing to show the success in the field.

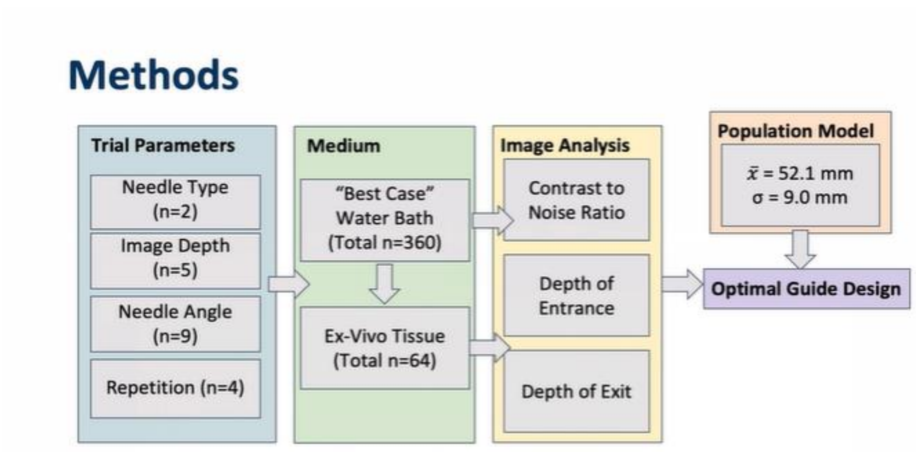

Figure 9: Visualization of Determined Methods for EpiGuide Testing

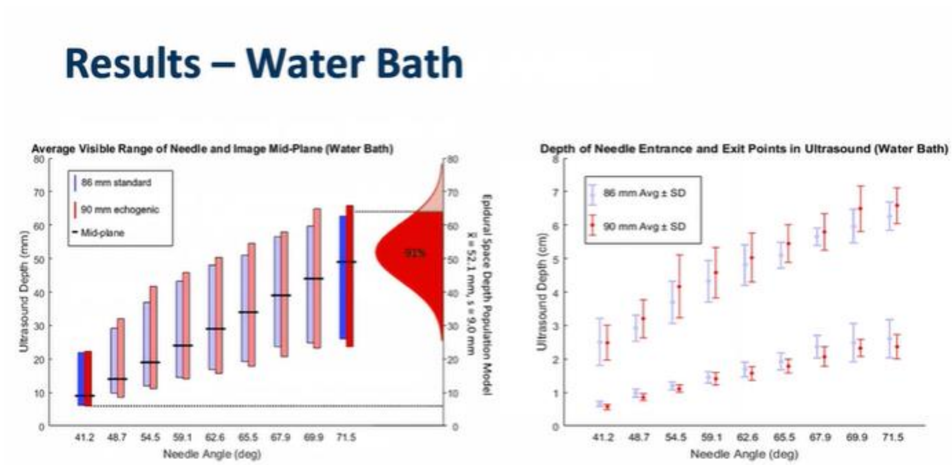

Figure 10: Example Results from One of Three Testing Methods

In addition to the testing completed for the product, a universal clip designed to attach to “latest-generation curvilinear transducer(s) (such as) C-3, Clarius Mobile Health Corp., Burnaby, BC, Canada” [13]. The face of the EpiGuide also rests against the patient's back such that “a continuous seal around the transducer face” is created and an even pad of gel is retained during the surgery. A final positive of this product is the cost: with several pieces 3D printed, many others prefabricated (bought off the shelf), and the ability for this product to change between multiple ultrasound wands the cost to both the hospital and patient are dramatically decreased.

Unfortunately, with so many positives to one device, there are negatives that must also be discussed. These include limited *in vivo* testing, being designed for pre-procedure imaging instead of a full surgery process, and where the image is aligned due to 2D imaging instead of 3D. At this time, the device has only been tested with porcine or pig subjects which dramatically lowers the accuracy of tests. While pigs are a common animal for *in vivo* testing, their kidneys are a different size than humans, a pig skin (epidermis and dermis) has a permeability of 21% (vs humans at 34%), and the epidermis and stratum corneum of a pig skin are respectively 51.89±1.49μm and 12.28±0.72μm vs humans with an 80μm epidermis and a 10μm stratum corneum. While these numbers may not seem dramatic on paper, when deciding on needle length to reach internal organs and it needs to pass through these layers, any difference in the model versus the actual system can lead to issues when doing the procedure.

The device is also created not only for a different procedure than PCNL (epidural insertion), but for pre-procedure imaging versus being used for the entire surgery. While the article does mention that "pre-procedure imaging has been shown to improve success rates of insertions" it does not say by how much. Additionally, due to the natural curvature of the back and the size of the targets to be injected with this device, pre-procedure imaging will not prove to be successful unless the device were to be firmly fixed to the patients back and not move between the time it takes to insert the needle and appurtenance then inject. Unfortunately, this scenario simply is not realistic.

A final negative is how the needle and ultrasound image are aligned. How ideal 2D ultrasound "results in a single point of visibility" [13] goes directly against our devices' need for imaging of a section of the kidney in relation to the needle as a center point. Surgeons can manually move the needle to change the ultrasound image freely before fine-tuning the image with a series of belts running off a knob system. Taking this freedom away from them could both prolong the surgery as they must scan slowly over the kidney with a limited area being reflected on the screen for them to search in. The image on this device is also aligned with the midline of the transducer which can be off center with the ultrasound beam. Our device is used to see the optimum path of travel in relation to the entry point (instead of the flipped logic of the EpiGuide 2D) and inject relative to the best position. A final negative is how the needle and ultrasound image are aligned. How ideal 2D ultrasound "results in a single point of visibility" [13] goes directly against our devices' need for imaging of a section of the kidney in relation to the needle as a center point. Surgeons can manually move the needle to change the ultrasound image freely before fine-tuning the image with a series of belts running off a knob system. Taking this freedom away from them could both prolong the surgery as they must scan slowly over the kidney with a limited area being reflected on the screen for them to search in. The image on this device is also aligned with the midline of the transducer which can be off center with the ultrasound beam. Our device is used to see the optimum path of travel in relation to the entry point (instead of the flipped logic of the EpiGuide 2D) and inject relative to the best position. Below is a table comparing the positives and negatives to the devices described in this section. Below is a table comparing the positives and negatives to the devices described in this section.

Table 2: Pros and Cons of Each Device Highlighted

Device	Needle tracking software?	Sterile?	Positives	Negatives	Link
PCNL SD	Yes	No	-Sensors to decrease pokes -Cost, size, complication mitigation -Degrees of freedom	-Limited needle trajectory -Odd grip -Sterility -Blocked line of sight -Made in 2005	ScienceDirect PCNL
Ethos *Iris*	Yes	Yes	-Modern -Disposable needle guide -Able to be used on patients with different anatomy -less training	-Limited testing -Development/design not yet fully completed -Training program not yet developed	Medadget Iris Interview Georgia Tech Iris
EpiGuide 2D	No	Yes	-Modern -Many types of testing utilized	-Limited *in vivo* testing -Best for pre-procedure -Image is aligned through the midline of the transducer -Image adjustment	BMJ EpiGuide Spie EpiGuide
Harvard Biodesign Lab	No	No	-Guide can be locked into position -Fine hand movements (training required) removed	-Needle can be in same plane as US image -Real time visualization not developed	Biodesign

From this table and the explanations of each product, this group will be able to build off what other companies have fallen short on to ensure a strong competitor to that already on the market. To summarize, this device must have an integrated software to display the needle trajectory in the body, work on patients of vastly different anatomy, attach to a variety of ultrasound devices/wands, be intuitive enough to reduce training needed to use the product dramatically, be sterile, and be well tested. The *Iris*, while a strong competitor for spinal taps, is not built for PCNL surgery; however much of their design/injection geometry mirrors that needed for this device. The EpiGuide, while a solid epidural injection device, has major drawbacks by nature of its design. Lack of *in vivo* testing, being designed for pre-procedure imaging, and the alignment of the ultrasound beam and the needle do not make up for the multiple types of testing, universal attachment system, and low cost. These negatives identified are things that this team must mitigate for their design and should not be overlooked.

Methodology:

The current state of the art techniques for percutaneous needle insertion either require the operator to hold the ultrasound and the needle separately in each hand or fixed together without enough range of motion. We have developed a potential solution that would provide an intuitive method to guide the needle insertion path which could improve the effectiveness of treatment and diagnosis. The concept uses a mirror to reflect the ultrasound waves to be parallel to the needle, offering a full view of the needle during the insertion process. This method is like the long-axis approach for current techniques but improves upon it by allowing the needle to be perfectly in line with the ultrasound waves rather than at an angle. This solution could help reduce complications such as hematomas (injury to the wall of a blood vessel) and tissue damage from mis punctures in non-visible areas. Additionally, the device would remove the need to manually align the needle with the ultrasound probe, making the needle tip identification more intuitive.

Mirror and Needle Mechanism:

The proposed needle intervention device will include an ultrasound probe and a mirror that can rotate with a minimum of 1 degree of freedom (DOF), and ideally 2 DOFs if possible. This improves upon the current fixed solution because it enables the user to manipulate the needle in line with the ultrasound waves automatically. A needle can be inserted through the mirror, allowing the user to rotate the needle and mirror simultaneously. An important design consideration is how the rate of rotation of the needle will need to be different from the rate of the rotation of the mirror for there to be no distortion.

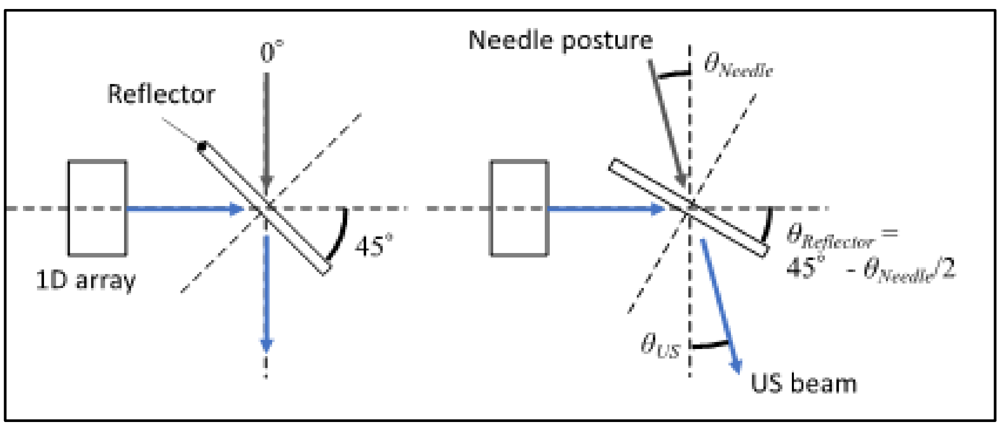

Figure 11: The Relationship Between Needle Posture and US Beam Path Direction with Mirror.

As shown in the figure above, in the simplistic case of where the needle is pointing straight down and the mirror is at a 45-degree angle, the ultrasound waves will be reflected to be in the same plane as the needle. However, if the needle is to rotate in either direction, the mirror would need to rotate half the amount. This is because of how reflections operate within the laws of physics. If the angle of incidence is altered by a given angle, the angle of reflection will be equally affected. For example, a one-degree rotation of the mirror would result in a 2-degree difference in the new ultrasound view; this means the needle should rotate 2 degrees as well. The proposed design for the device would utilize a 2:1 gear ratio, as the mirror and needle assembly will be in the disposable portion of the device and to make the device as cost effective as possible, gears can be 3D printed with ABS (or PLA, depending on final choice) plastic. One design challenge is the need for the mirror and needle to rotate on the same axis, meaning the gear ratio must be collinear rather than traditionally parallel alignments. To measure the change in angle, an encoder will be used to read the values and the angle will be displayed on a small screen mounted on the device.

Pairwise Comparison Chart:

To guide our design process and determine parameters to guide our product so we decided on a series of parameters to base our design on. These were cost, sterility, ease of use, image quality, and adaptability. The reason for choosing these parameters can be seen below:

Cost:

One main goal of this device is to provide a more simplistic and cost-effective solution for hospitals compared to other the next generation solutions that could offer a circular ring array ultrasound transducer. That said, when dealing with patients and hospital settings, quality is of the utmost importance so while we aim to reduce cost wherever possible, it should not be at the expense of the device’s performance or safety.

Sterility:

In the operating room it is essential to maintain a sterile environment, to reduce the number of microbes present and prevent the patient from getting an infection. It is therefore, of paramount importance to design our device to maintain sterility either by having a protective case or by making a disposable attachment.

Ease of Use / Portable:

Needle intervention procedures need a high degree of accuracy. Users need to handle the ultrasound probe with one hand and manipulate the needle with the other. Given how manual the procedure is, an important design consideration is to make our device lightweight and portable so there is less strain on the user. Furthermore, the user interface that displays ultrasound information needs to be easy to use and understand, so that there is minimal preventable harm arising from device complexity.

Image Quality:

In the current state of ultrasound procedures, it can be incredibly difficult to visualize what is being viewed and from what perspective. In cases such as PCNL procedures where a larger organ is being viewed, an additional challenge lies in the fact that the user needs to visualize a 3-dimensional shape when given only 2 dimensional images. Having a high-quality image gives the user the best chance at identifying anatomical structures.

Adaptability:

It is common for PCNL procedures to require different needle diameters; therefore, the device would benefit the user if it could support all potential needles easily. Additionally, for the device to be useful in other procedures aside from PCNL, the device could be compatible with different ultrasound transducers.

Table 3: Pairwise Comparison Chart to Determine Priorities for Requirement Categories

Pairwise Comparison Chart						
	Cost	Sterility	Ease of Use/Portable	Image Quality	Adaptable to different procedures	Total
Cost	--	0	1	0	0	1
Sterility	1	--	1	0	1	3
Ease of Use/Portable	0	0	--	0	1	2
Image Quality	1	1	1	--	1	4
Adaptable	1	0	0	0	--	0

Conclusion:

In terms of adaptability, the pairwise comparison clearly shows that it is not a high priority compared to the other categories. This means the device should instead focus on using one needle size and based on recommendations by Dr. Sorokin and Dr. Zhang, this will be an 18-gauge needle. This is the largest needle used in PCNL procedures and its size offers more rigidity and ease of viewing on the ultrasound image. In terms of the device being compatible with different transducers, based on the pairwise comparison chart, the focus for this prototype should be PCNL procedures, simplifying the design to only make use of the typical linear array transducer. We also aim to design the device to be a cost-effective ultrasound guided needle intervention system, compared to more expensive solutions such as ring-array transducers. The next weighted design consideration is ease of use/portability. Since needle insertion procedures are very manual and place a lot of strain on users, the device will be lightweight and portable. We aim to add portability by using the Clarius C3 ultrasound probe, which is wireless and easily maneuverable. The second most important design consideration is to make sure the device is sterile in use, to prevent a patient from getting infected during the procedure. To do this, the ultrasound probe will have a sterile covering, and the mirror attachment for the probe will be disposable. The most important design consideration is to make sure that our system provides users with high image quality so that the user has all the information they need to identify anatomical structures and make informed decisions during the procedure.

Ultrasound Probe:

The ultrasound probe is the backbone of this project, offering the user the appropriate imaging to make informed decisions about where a needle should be inserted. There are numerous options for ultrasound transducers, and each is appropriate for a specific application. In our case, we plan to focus on deep organ needle insertions, more specifically percutaneous nephrolithotomy (PCNL), a procedure to remove stones within the kidney. Therefore, the ultrasound transducer required would need to be able to focus on these deep organs, meaning a larger elevation focus would be needed. Even though it is possible to change the focal depth using changing frequencies, it is not recommended to significantly do so as higher frequencies are attenuated quicker in tissues compared to lower frequencies [14]. Based on sample PCNL procedures performed in the last two years and documented by Urology Times, Dove Medical Press, and Precision Urology Hospital, the ultrasound transducer of choice seems to be a convex array transducer that offers 2D imaging and an elevation focus of at least 60mm.

Figure 12: Clarius C3 1st Generation Ultrasound Transducer

As shown in the figure above, the ultrasound transducer offers a wireless solution that would allow the device to be fully portable. Additionally, the device's transducer can view a maximum depth of 320 mm which is more than suitable for the desired procedures. Due to the convex nature of the transducer, it has a wide footprint of 73 degrees for imaging, giving the user greater context of the area they are viewing. By designing the device to attach to this transducer, it would greatly reduce the cost and improve the practicality of the device because the ultrasound transducer can be reused for different applications and attached to our device when applicable.

Electronic Components:

The electronic components of the device will be powered separately from the ultrasound transducer, allowing the device to be changed separately and then attached to the transducer for a quick and easy installation before a procedure.

Encoders:

The electronics needed in the device to measure the change in angle of the mirror and needle are encoders. Given that the range of motion is relatively small and the changes in angle could be less than one degree, the encoders would need an appropriate resolution to suit the task. We believe an option that offers a minimum pulse per resolution of 720 would be ideal as this still would provide measurements with increments of 0.5 degrees.

Figure 13: EMS22A Absolute Encoder (Bourns, 2020)

The encoder depicted above is an example of an absolute encoder that offers a resolution of 1024 ppr, and a small form factor. One key benefit of this encoder design is its capability of continuously rotating 360 degrees meaning there is no mechanical stop preventing the encoder from rotating past a certain point. This could prove to be very useful in calibration phases where the user could attach the disposable needle and mirror component, then rotate the needle to the minimum and maximum positions. Using the range of values provided from the calibration, the relative position of the needle would then be possible to measure.

Microcontroller:

The ideal microcontroller to interface with these components is the ESP32 due to its very small footprint of 18 mm x 20 mm x 3 mm and can easily fit in the device. Additionally, it offers plenty of SPI and I2C pins to connect an encoder, an IMU, and a small display.

Figure 14: ESP32-WROOM-32 Microcontroller (Espressif 2018)

A bonus feature of the ESP32 is that it includes WIFI and Bluetooth support, which could be used to interface with the software without the need for a wired connection. That said, a wired connection would provide quicker transfer rates and potentially far superior real-time imaging as well as rapid 3D view generation. The ESP32 can be programmed in C++ and has the benefit of two cores that can potentially be used to improve performance.

Sterilization:

A major concern with all equipment used in healthcare settings is sterilization. The device will make use of a disposable attachment that the needle passes through to avoid the issue of needing to thoroughly clean the entire device. A protective cover can be placed over the rest of the device as is standard practice today. This way, only the mirror portion of the device is disposable, which is also one of the less expensive components. Given that the disposable portion could be manufactured and assembled in a clean room, it would offer the cheapest and easiest option for sterilization for end users.

Materials:

The device housing will be primarily 3D printed for our prototypes using PLA plastic. For manufacturing we plan to redesign components with injection molding in mind with the disposable portion ideally made of PVC plastic as that is the most common plastic used in pre-sterilized single use medical applications. The mirror itself will need to be tested as the reflective properties of ultrasound are far different than light. We plan to test the effectiveness of multiple materials with high acoustic impedances, including steel sheets, glass mirrors, and a thin glass mirror with an adhesive back.

Software and GUI:

The software developed for the device will provide a packaged solution that will provide the user with a high-quality ultrasound image and intuitive metrics about the orientation of the needle. Ideally, the software could utilize encoder readings to measure angle of the mirror and process the image to account for any changes in the angle of the mirror in relation to the ultrasound probe. The encoder data can be used to display the angle at which the needle is being held so that the user can keep a record of all the orientations viewed and more precisely decide the orientation they will set the needle before insertion. With real-time ultrasound imaging and improved maneuverability for the user to position the needle, the device will provide users with enhanced abilities to perform procedures.

In the case of the Graphical User Interface (GUI) for the user, the main goal is to focus on the real-time ultrasound image, but also compliment the image with details that could help to understand more quickly what is being viewed. This mitigates one common concern with ultrasound imaging as it can be difficult to visualize and identify what is being viewed within the ultrasound image.

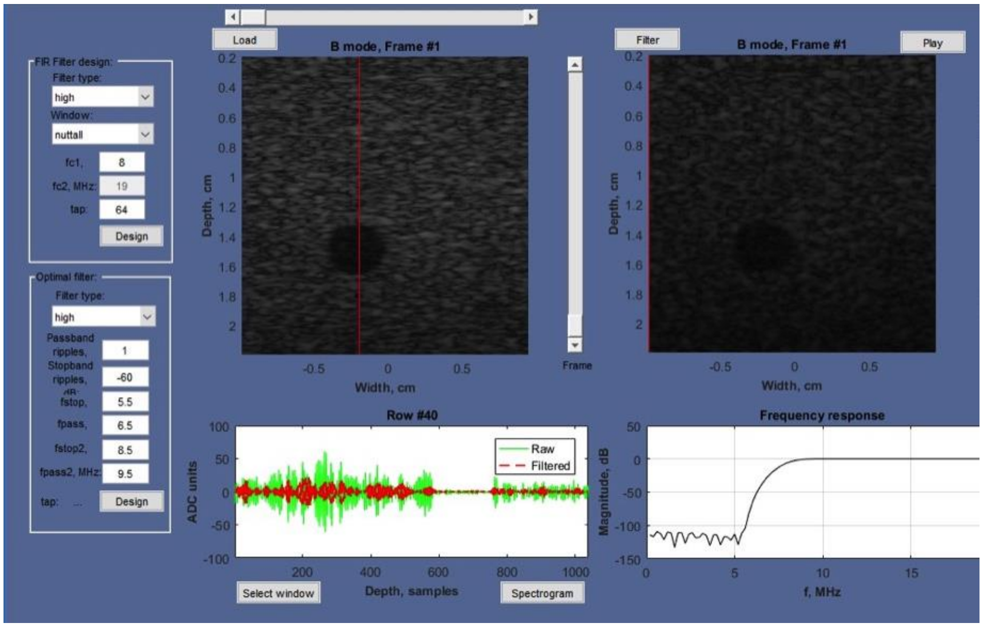

Figure 15: Example GUI for Ultrasound Imaging [15]

The figure above is an example of a GUI designed in MATLAB for radio filter (RF) filter analysis, but it also serves as a potential goal for the UI we hope to develop. Ideally, we could provide an additional view of the region that uses all the angles captured to stitch together a 3D model of the region. This would use the encoders to analyze the angle of the needle and would likely need to make use of an IMU or some equivalent that could provide rotational and translational data in the other DOFs. Given that the main priority is the real-time ultrasound image, the GUI should allow for the user to hide alternate views to allow for the main image to occupy a larger area. Lastly, the GUI could help the user identify regions of interest such as the calyx of the kidney so that the user can be assisted to interpreting the US image they are viewing.

Deliverables:

To design, construct, and test this device, we must complete the following objectives.

Minimum

- Select and incorporate an ultrasound probe.
- Select electronic components such as encoders, and display.
- Accommodate the design of the device to comply with sterilization standards.
- Design circuit schematic for device and implement and test electronics.
- Model and 3D print CAD components of the device.
- Develop software and GUI that compliments the device, providing the user with a high-quality ultrasound image and intuitive metrics about the orientation of the needle.

Expected

- Add 3D volume generation for ultrasound image based on device orientation and position and stitching together frames.
- Design the device to operate with at least one degree of freedom for needle/mirror rotation.
- Test device on phantoms.
- Incorporate principles of ergonomics to improve feel and comfort of device.

Reach (maximum)

- Design device to utilize 2 degrees of freedom in terms of needle and mirror rotation.
- Development of a custom PCB to minimize electronics components footprint.
- Use computer vision to identify potentially key areas of the kidney to help users locate calyx.
- Develop a version of GUI outside of MATLAB to allow for users to view information on a phone or website.

Project Timeline:

Table 4: Full Project Timeline Through Terms A, B, C, D

Order	TASK TITLE	START DATE	DUE DATE	DURATION
A Term	Project Planning and Proposal			
1	Background research	9/1/20	9/14/2020	13
2	Proposal	9/16/20	10/16/2020	30
3	Product design iteration 1	9/30/20	10/7/20	7
4	Product design iteration 2	10/7/20	10/14/20	7
5	Circuit schematic	10/7/20	10/14/20	7
6	Develop material and components list	10/7/20	10/16/20	9
7	Order components	10/16/20	10/16/20	1
B Term	Product development and prototyping			
1	Produce and test mirror/needle rotation mechanism	10/21/20	11/2/20	11
2	Produce and test circuitry on breadboard with test code	10/21/20	11/2/20	11
3	Translate circuit design to PCB	11/4/20	11/18/20	14
4	GUI phase 1: Implement real-time ultrasound imaging	11/18/20	12/2/20	14
5	3D print and assemble final components	12/2/20	12/9/20	7
6	GUI Start phase 2: Implement stitched 3D view	12/2/20	12/9/20	8
C Term	Testing and product improvements			
1	GUI Continue phase 2: Implement stitched 3D view	1/13/21	1/27/21	15
2	GUI phase 3: Computer Vision to detect calyx	1/25/21	2/10/21	16
3	Perform device trials on phantom	1/13/21	3/3/21	51
4	GUI Reach: Make GUI accessible outside of MATLAB (via app or website)	2/10/21	3/3/21	24
5	Device optimizations and improvements for ease of use as well as comfort	1/13/21	2/17/21	35
D Term	Presentations and Project Conclusions			
1	Market research and analysis	3/17/21	3/31/21	15
2	Design poster and presentation slide show	3/26/21	4/20/21	25
3	Project Presentation	4/20/21	4/22/21	3
4	Final Project Report	3/17/21	4/28/21	42
5	Product showcase to medical experts	4/21/21	4/28/21	8
	Project Complete			

Risk Management Plan:

Table 5: Risk Management Plan for Potential Obstacles Regarding Design and Development

Risk	**Mitigation Strategies (Plan A)**	**Backup Solution (Plan B)**
3D printed components are not high enough quality	Plan early and reduce part size and complexity when possible.	Laser cut structural components and either 3D print or sand outer components.
Ultrasound signal is not clear enough through mirror	Design the device to be airtight and allow for a great deal of gel to be applied.	Use a tank of water to submerge the device.
Encoders do not provide precise enough readings due to the nature of very delicate and small changes in angle.	Use an encoder with an appropriate resolution, likely a pulse per resolution greater than 360.	Mechanically improve resolution by designing a compact gear reduction.
Disposable portion of device being too costly.	Design disposable portions to be only plastic and simple to manufacture and assemble.	Revert to a non-disposable option where the device could be easily cleaned.
Device is bulky and heavy for the user, causing fatigue.	Design the device with lightweight materials and ergonomics in mind.	Create a sling that the user could wear to help distribute weight from arms to the upper body.

Design Process:

System Overview:

To meet our goal of creating a device that provides an intuitive method to guide the needle insertion path during PNCL procedures, we focused our improvements this term on the needle-mirror synchronized mechanism, a cover attachment with a needle insertion mechanism, and image visualization software.

The needle-mirror synchronized mechanism was designed to provide a simple and intuitive way for a user to rotate the ultrasound view while keeping the needle aligned with it. A mechanical system using 2 sets of timings belts and pulley wheels was developed to maintain a 2:1 ratio between the rate of rotation of the needle to the mirror. To attach the needle-mirror mechanism to the Ultrasound probe, a fixture was created that contains the needle-mirror mechanism within it and attaches to an ultrasound probe using a friction fit. The design was also modified to include bolts and bearings to provide smoother and more precise rotation for the needle arch, mirror, and belt wheels. The material used to reflect ultrasound waves was modified to be acrylic, and laser cut to perfectly fit into the needle arch. In terms of electronics components, the device includes an ESP 32 microchip, a 2.2-inch TFT display, a multidirectional switch for menu navigation, and an encoder to give the user the information about the orientation of the needle. Furthermore, a PCB was developed that can be implemented on the top of the device and showcases the user encoder readings and other useful information.

Given the current configuration of the device, there is a lot of negative space between the ultrasound probe, the mirror mechanism, and the surface of the device that contacts the patient. To overcome this, a cover attachment was developed that fits around the needle-mirror mechanism and probe attachment and can be filled with gel thus allowing ultrasound waves to pass through cleanly. The cover attachment was also designed to have a pathogen tight seal to reduce the risk of contamination during the procedure.

To aid the user and provide meaningful information as they are manipulating the device to rotate the ultrasound view, an image visualization software was developed. The Graphical User Interface developed aimed to provide the user with high quality ultrasound images, intuitive metrics about the orientation of the needle, and the ability to visualize a 3D volume of the area being scanned. Using the GUI, the user can choose between streaming real-time ultrasound images during the procedure or collect raw data and ultrasound images for offline viewing. The GUI was also designed to interface with the electronics to display encoder data about the current orientation of the needle. The GUI is also designed to utilize IMU data collected from the probe, to showcase the volume visualization based on current orientation of the device.

Needle-mirror Synchronized Mechanism:

Requirement:

The function of the needle-mirror synchronized mechanism is to provide an easy way for a user to rotate the ultrasound view and keep the needle aligned with the reflected ultrasound waves. Given that the required ratio between the rate of rotation of the needle to the mirror must be 2:1, a mechanical system must be capable of allowing the needle and mirror to rotate together on an axis yet at separate rates. To achieve this, 2 sets of timing belts and pulley wheels were used. Additionally, the needle-mirror mechanism needs the ability to connect to the Clarius C3 ultrasound transducer, in a manner where it can easily be attached or detached. This enables the device to serve as an attachment system useful in certain applications and does not interfere with the user's ability to use the probe by itself. To measure the angle at which the needle is positioned, an absolute encoder is used, and interfaced with a small ESP32 microcontroller, the device can provide valuable real-time information for the user as well as for the 3D visualization software that will require the angle of the slice that the ultrasound image is being taken.

To develop the device in an efficient yet thorough manner, multiple iterations will be designed, built, and tested. The first and second iteration prioritize the development of a mirror and needle mechanism capable of rotating the mirror and needle together but at different rates. The first iteration was designed to use a vertical mirror orientation, but this was later modified in iteration 2 to be a horizontal orientation. The third iteration of the design incorporates how the mirror and needle mechanism will attach to the device and was designed to be 3D printed and assembled.

Iteration 1:

In the first iteration of the device, the primary focus was designing a mechanism for the mirror and needle to rotate simultaneously, yet at different speeds. Initially we experimented with a gear train but quickly realized that to achieve the 2:1 gear ratio, it would not be possible to have the driven gears rotate colinearly with the use of only 4 gears. We would have needed to add additional gears for the system to work properly, and we could achieve the same 2:1 gear ratio with a simpler mechanism using timing belts. Additionally, iteration 1 utilized a tall mirror to reflect the ultrasound transducer, meaning the probe would need to be mounted perpendicular to the patient's body. This was later changed in iteration 2 to use a wide mirror instead so that the probe could be oriented parallel to the patient's body and provide unique ultrasound readings for every degree of rotation along a sweep. This is a crucial detail to generate 3D visualizations since the unique views will later be spliced together to create a holistic view of the region.

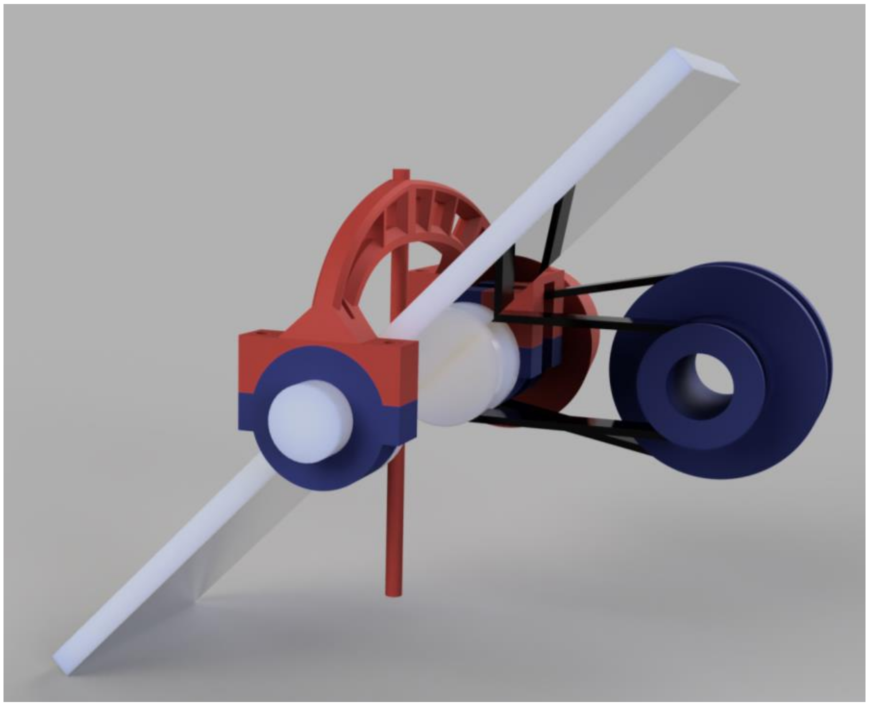

Figure 16: Partial Isometric View of Needle Mirror Mechanism

The isometric view of the design showcased above, designed in Fusion 360, demonstrates a working model of the needle and mirror attachment. The design provides 1 DOF and allows the user to manipulate the needle in line with the ultrasound beam, by rotating the knob on the far side of the image so that the needle and mirror can rotate simultaneously. The 2:1 gear ratio enables the user to easily rotate the orientation of the mirror and needle without worrying about if they are aligned properly as this is handled by the timing belt system.

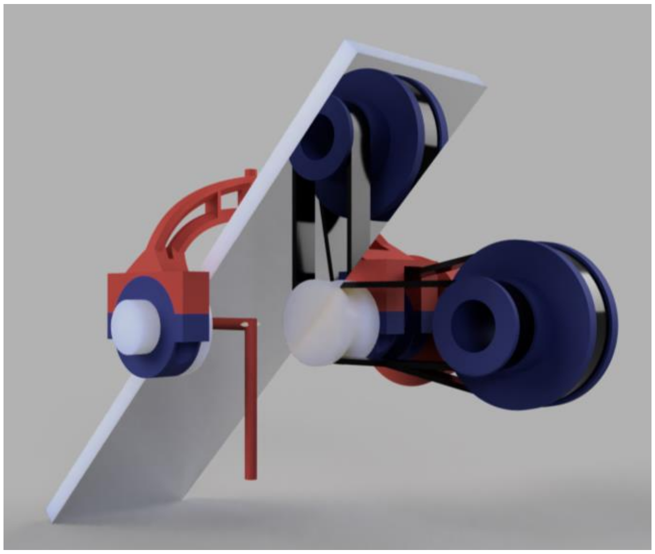

Figure 17: Isometric View of Mirror Set to 45 Degree Angle.

The first component to design was the mirror holder component, shown in white in the image above, that holds the needle sheath in place, and it is used to change the angle of reflection of the US beam. While designing the mirror component, we realized that using a glass mirror could be cumbersome given that it is difficult to cut and drill holes into. There also is a need for the component to be fixed to the main driven axel and have a way to help the needle rotate about that same axis. This led us to experiment with a plastic design that would have a reflective surface applied to the front so that the mirror component could have more complex geometry. The reason more complex geometry is needed is because as the needle rotates in relation to the mirror, if the hole that the needle sheath passes through is too small, the needle sheath will be restricted from rotating the required amount. By developing the mirror holder in plastic, it would allow the hole to have a significant chamfer, allowing the needle sheath to rotate unrestricted. Given that US waves reflect based on acoustic impedance, the reflective surface would likely need to be a mirror sticker or a thin sheet of metal that is incredibly smooth.

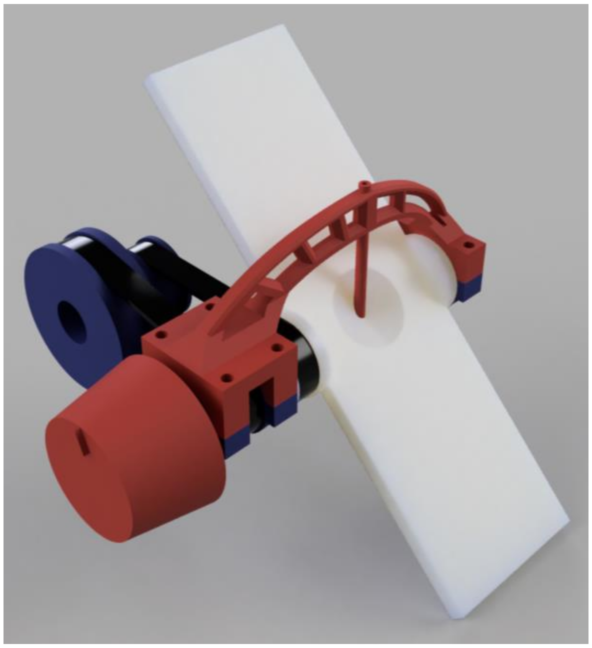

Figure 18: Isometric View of Device Knob and Arch

The image above showcases the design of the arch to hold the needle sheath, the timing belts, and knob used to manipulate the rotation of the needle and mirror. As mentioned above, the gear ratio was designed to be 2:1 to enable the needle and mirror to rotate so that the needle is always aligned with the ultrasound's angle of reflection. The inner belt manipulates the mirror, and the outer belt manipulates the needle. The arch is also attached to the outer wheel for stability and holds the needle sheath in the center.

Iteration 2:

The key improvement made in iteration 2 of the design shifts the mirror to a wide orientation. This allows the ultrasound probe to be mounted parallel to the surface of the patient.

With this orientation, as the needle and mirror mechanism are rotated, each view is unique and provides complimentary information for the user, potentially allowing a 3D view to be generated with a simple sweep motion.

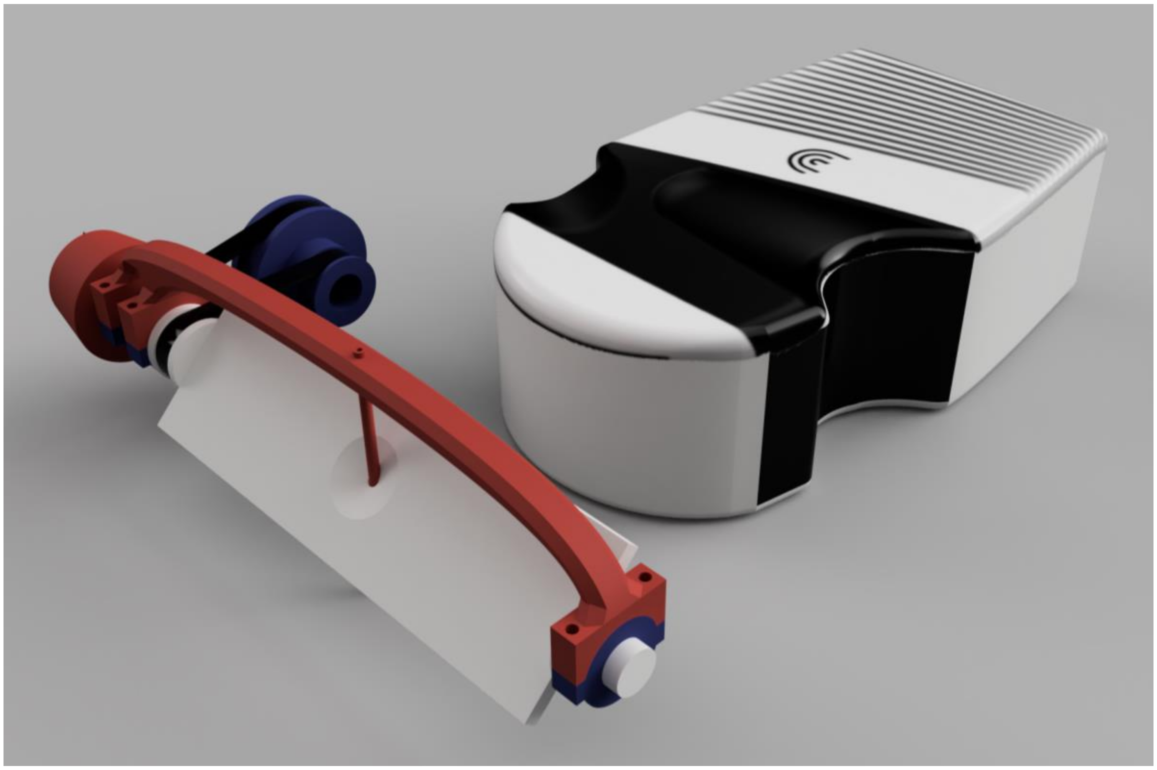

Figure 19: Top Isometric View of Horizontal Mirror System and Clarius C3

As shown in the figure above, the Clarius C3 US transducer can rest parallel to the patient's body. The main benefit of this is that the reflected view is different along every axis of rotation, whereas in the perpendicular approach of iteration 1, there is a significant overlap in redundant information upon rotating the view. A secondary benefit is that with a mirror that is not as tall, the needle sheath can be positioned closer to the patient's skin, reducing any error between the desired puncture location and actual puncture location as well as the amount of gel required.

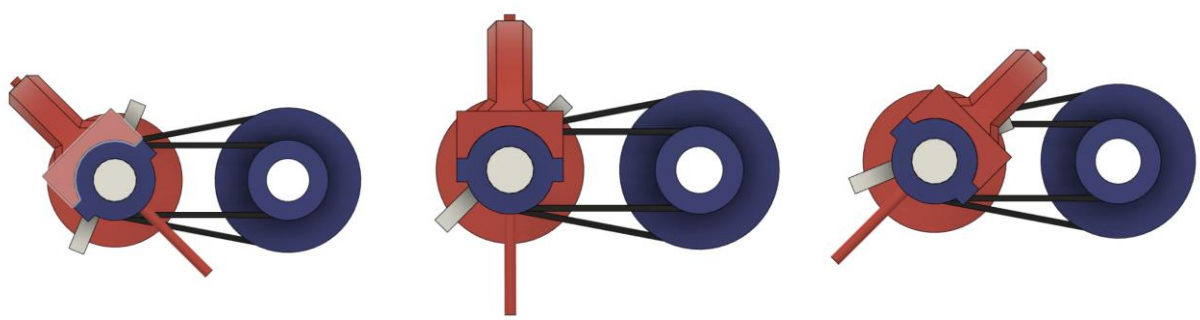

Figure 20: Side View, Full Range of Motion (Starting from Left (-45°), Origin (0°), Right (+45°))

The image above demonstrates the full range of motion of the needle and mirror mechanism. The range of motion goes from -45 degrees to +45 degrees, giving the user a 90-degree range of motion to utilize and a broader perspective of the target area being scanned with US. The knob also enables the user to make fine adjustments to the needle position compared to manually manipulating the needle.

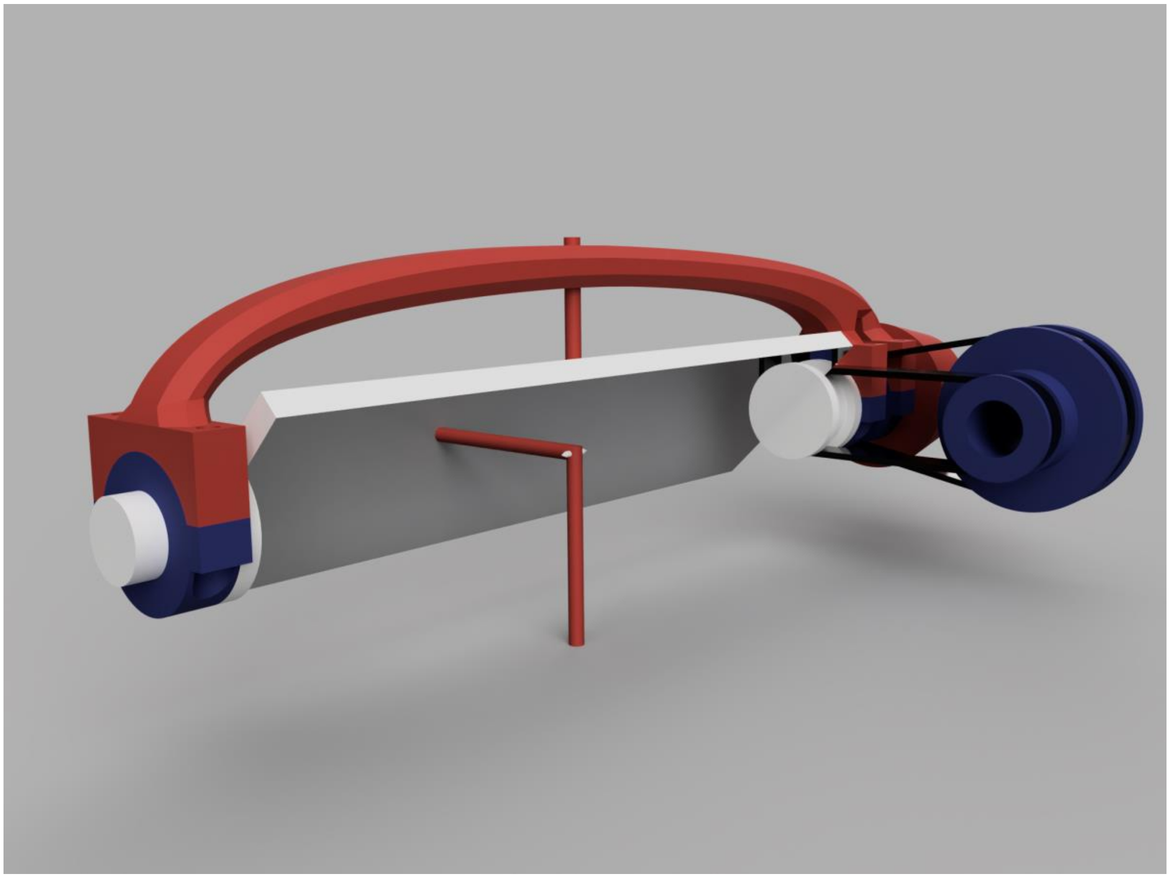

Figure 21: Isometric View of Horizontal Mirror Design

The figure above displays a view of the reflective surface and arch that holds the needle sheath, given that the mirror is wider in iteration 2, the arch was altered accordingly to satisfy the new dimensions. A key result is now the needle sheath reaches below the mirror no matter the angle of rotation, as opposed to in iteration 1 where the mirror was always below the needle sheath adding distance between the sheath and patient. All the negative space where the US waves will pass through must be filled with gel, mimicking the acoustic impedance of human tissue so that the US waves can pass through cleanly. Without the gel, the US waves can be reflected or shadowed by air particles, significantly reducing the quality of the US image.

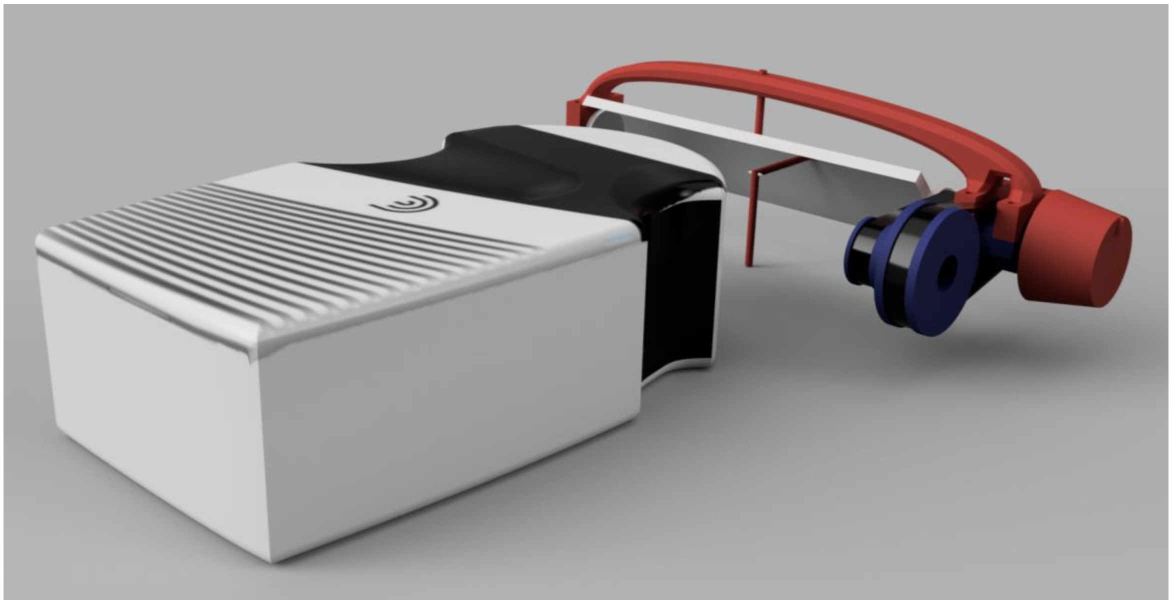

Figure 22: Back Isometric View of Needle Guidance Device and Clarius C3

The figure above shows a holistic view of the device mechanism from the perspective that the user may be holding it. In the current iteration there is no attachment mechanism connecting the device to the US probe, but this will be added in the next iteration, as well as a protective covering for the device.

Iteration 3:

Building upon iteration 1 and 2 of the needle mirror mechanism, the key additions were adding a fixture so that the mechanism could be easily attached to the ultrasound probe and redesigning the components for manufacturability so that the device could be assembled and tested. The material of the mirror was also changed to be acrylic as acrylic has a suitable acoustic impedance to reflect ultrasound waves and it can be laser cut. A 3D printer was used for all mechanical components and a laser cutter was used to create the acrylic mirror. Additionally, the circuit schematic was updated to include the encoder and the printed circuit board was designed and purchased to test the electrical components of the device.

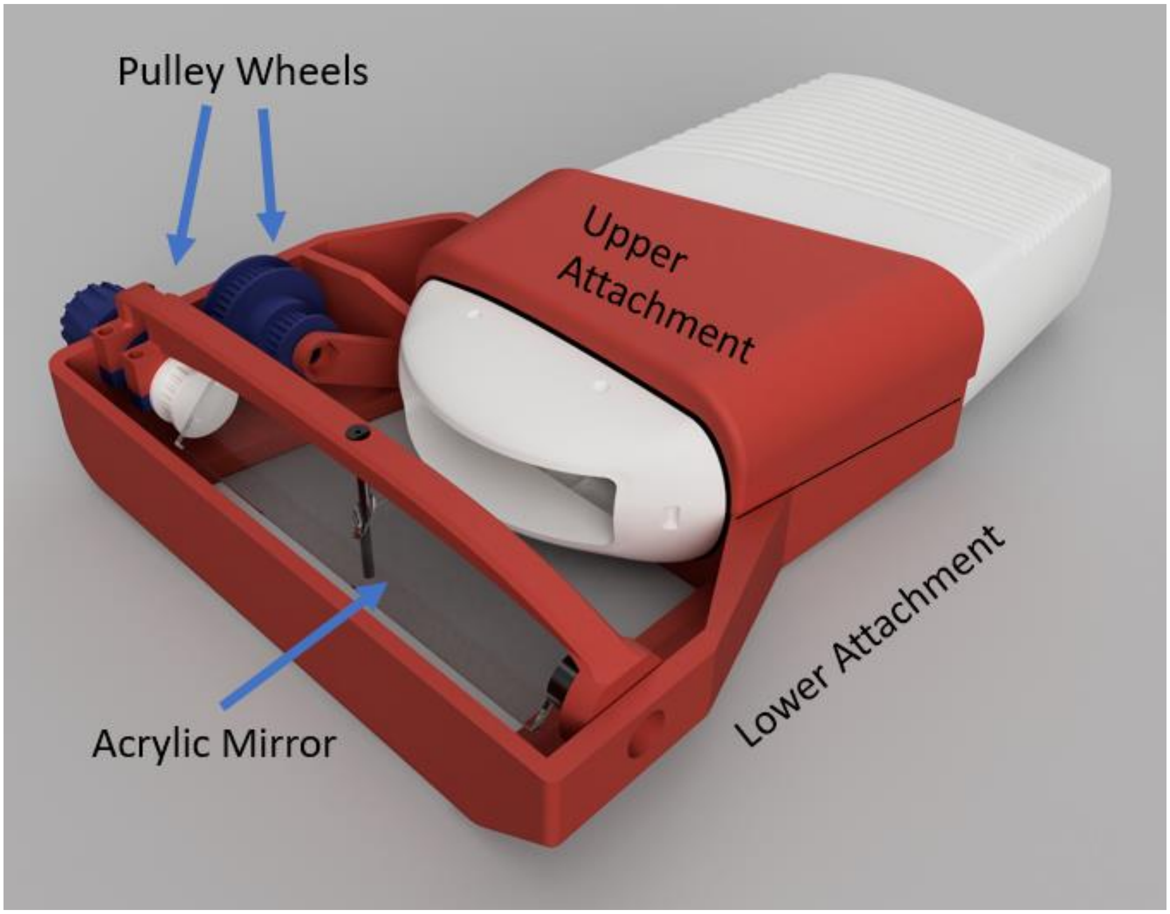

Figure 23: Isometric View of Needle-Mirror Mechanism CAD Model

As shown in the figure above, iteration 3 of the device improves upon the previous iterations by incorporating an attachment mechanism to the ultrasound probe by way of a friction fit. Essentially, all the mechanical components are assembled to the lower half of the attachment and the top half clips to the bottom to create a friction fit around the rubber grip of the Clarius. This allows the Clarius to be held in place, reducing the chance that the device moves in relation to the mirror which would cause a discrepancy between the expected viewing angle and the actual viewing angle. A limitation of this configuration is that it replaces the area the user is meant to hold the device, therefore in future iterations a new method to grip the device is required.

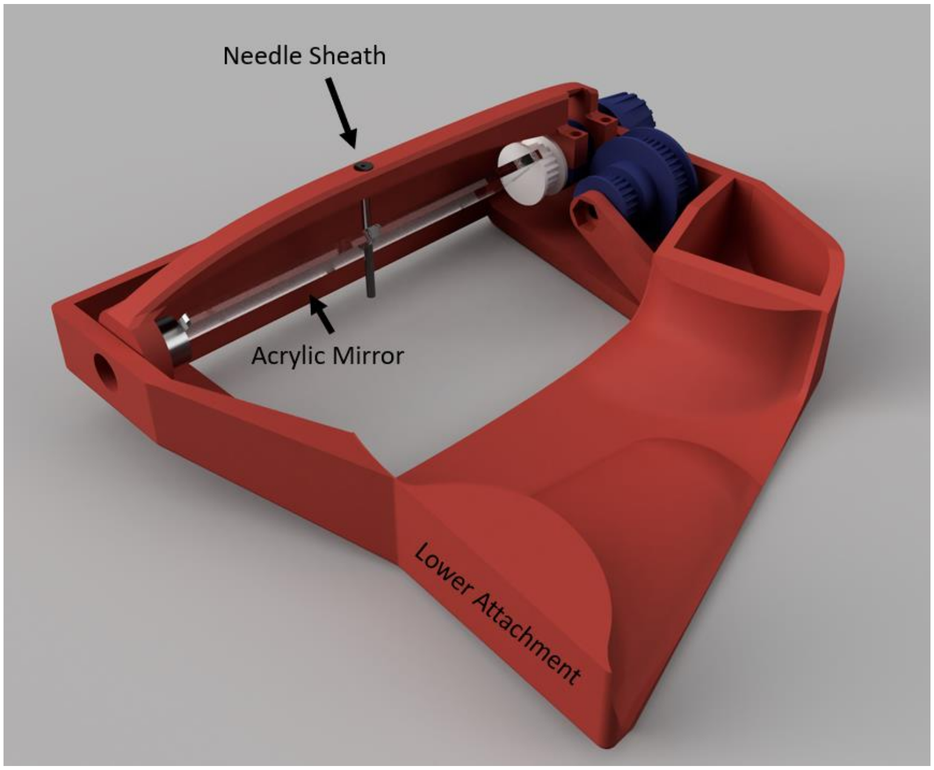

Figure 24: Isometric View of Lower Attachment and Needle-Mirror Mechanism

The figure above highlights the lower portion of the device, where all the mechanical components are attached to. It includes six 4mm bearings and three M4 bolts to provide smoother and more precise rotation for the needle arch, mirror, and belt wheels. This improves the ease of assembly and reduces the friction from the previous iteration which lacked these components. The complex curves on the portion that fits to the Clarius were modelled by taking the negative space of the rubber grip on the Clarius, providing a secure fit.

Figure 25: Right Isometric View of Needle-Mirror Mechanism Assembled

The fully assembled version of iteration 3 can be viewed above, featuring a laser cut acrylic mirror to reflect the ultrasound waves and belts around the pulley wheels to allow for the mechanism to rotate the mirror and needle simultaneously. Unfortunately, in this iteration of the design, there is no feature to adjust the tension of the pulley or tensioner wheel, so the two belts are not properly tensioned. In the next iteration of the device, both mechanisms will likely need to be added to ensure the rotation is smooth and that the belt does not slip over any teeth on the pulley wheel.

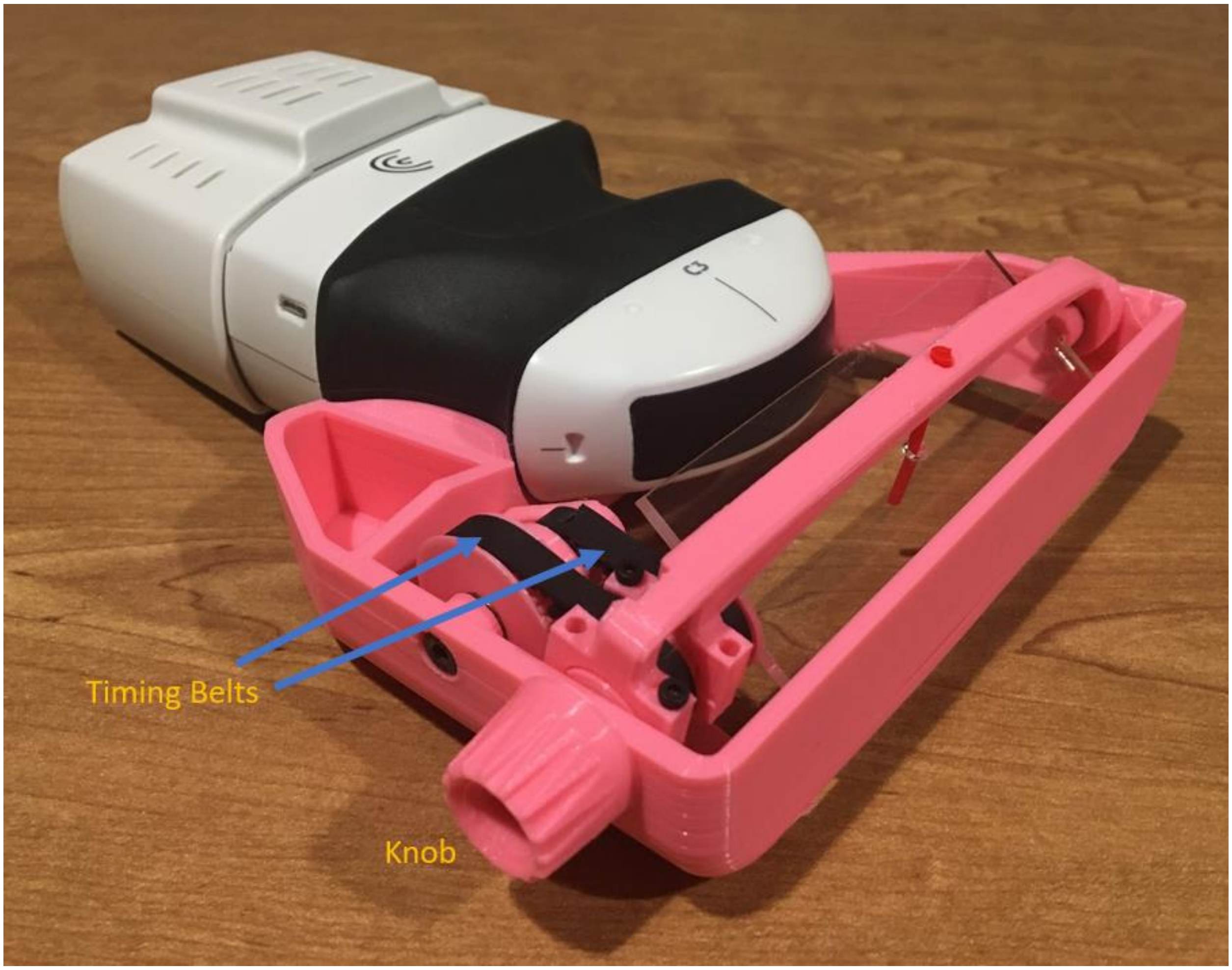

Figure 26: Isometric View of Needle-Mirror Mechanism Assembled

The view of the assembled device above shows the knob that can be used to rotate the mirror and needle synchronously. Iteration 3 improves upon many features of the previous iterations, enabling the device to be attached to the Clarius, and smoother rotations using bearings and bolts. Additionally, the device was redesigned with manufacturability in mind and the device was fully assembled by 3D printing components and laser cutting the acrylic mirror. However, there are also many shortcomings of the device that will need to be fixed in iteration 4, where the objective will be to test the device while the probe is completely submerged in water to sufficiently test the system in a controlled environment.

- Enlarge distance between pulley wheels and incorporate adjustable tensioning system. This will help tension one belt, and the other belt can be tensioned using a tensioner wheel.
- Incorporate electronics and encoder to design. Ideally this can be done in one compact version of the device, but the next iteration will focus on elevating the electronic components above the surface of the water while the entire probe is submerged in a water tank.

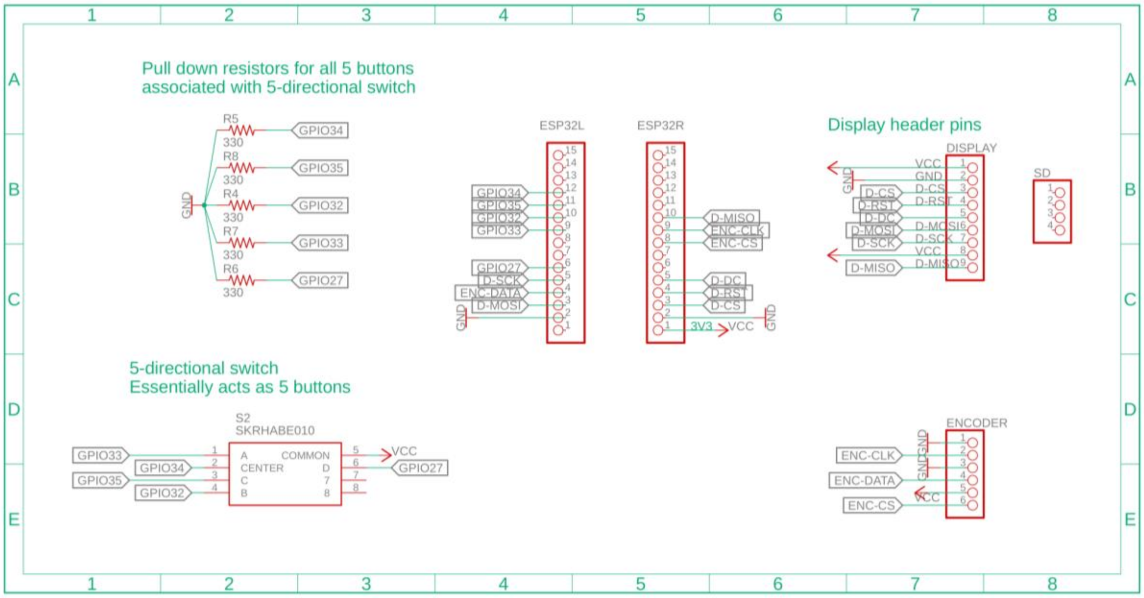

Figure 27: Circuit Schematic of Onboard Electronics

The figure above showcases the circuit schematic for the onboard electronics that will be included on the device. These include the ESP32 microchip, a 2.2-inch TFT display, a multidirectional switch for menu navigation, and a connection for the encoder cable to be soldered to so that it can be mounted on the device. The configuration was tested on a breadboard with success and then translated to a digital circuit schematic so that a printed circuit board could be developed.

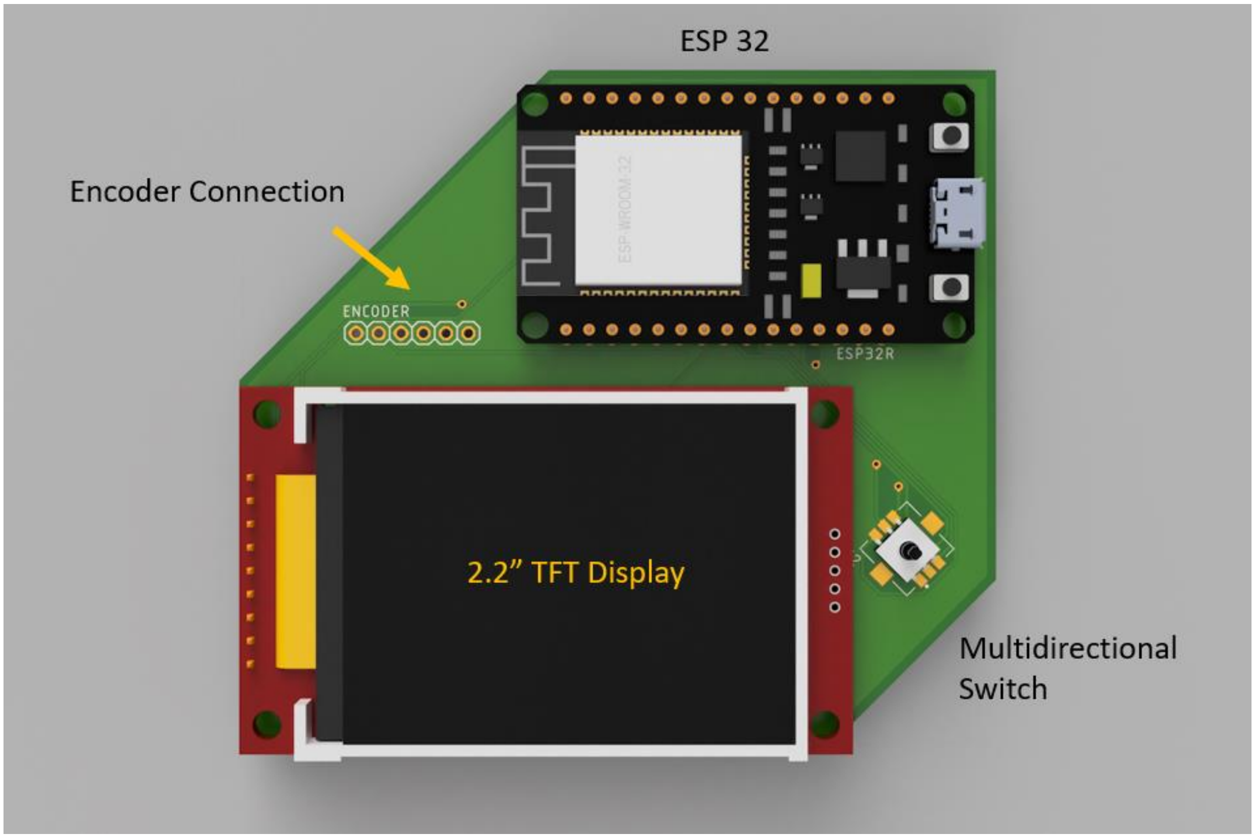

Figure 28: Printed Circuit Board Rendering

The figure above shows the PCB rendering including the ESP32, Display, and Multidirectional Switch. The PCB is designed to be compact so that it can easily be implemented on the top of the device, offering the user an intuitive view of the encoder readings and any other information that might be able to assist the user during a procedure. A limitation of the PCB is that it is not battery powered as originally planned because for early prototyping it is much more stable to use a serial connection to interface with the encoder, as this improves the rate of transmission and reduces the chance of packet loss over a wireless connection. We believe this may help simplify the process of matching encoder readings to the respective ultrasound readings in terms of time stamps.

Figure 29: Partially assembled PCB

In the figure above the PCB is simply fitted with the ESP32 and display, however the encoder, multidirectional switch, and the 5 corresponding 330-ohm resistors still need to be soldered to the board. Due to complications caused by the COVID 19 pandemic, access to the appropriate resistors and soldering iron were not available on campus, but thanks to a collection of tools at home, the PCB can be completed over winter break.

Preliminary experimental result:

To test the device, any space between the probe and patient must be filled with gel or water for the ultrasound waves to propagate through the desired regions. Iteration 3 was designed to be able to hold gel, in the central pocket, using saran wrap to hold the gel on the underside of the device. However, when tested, it was difficult to fill the entire area with gel and obtain high quality ultrasound readings. Given this shortcoming, we reapproached the testing processes by using an acrylic tank filled with water instead. The Clarius C3 ultrasound probe is fully waterproof aside from the optional fan attachment so we were able to submerge a great deal of the probe in water and test the effectiveness of the acrylic mirror to reflect ultrasound waves.

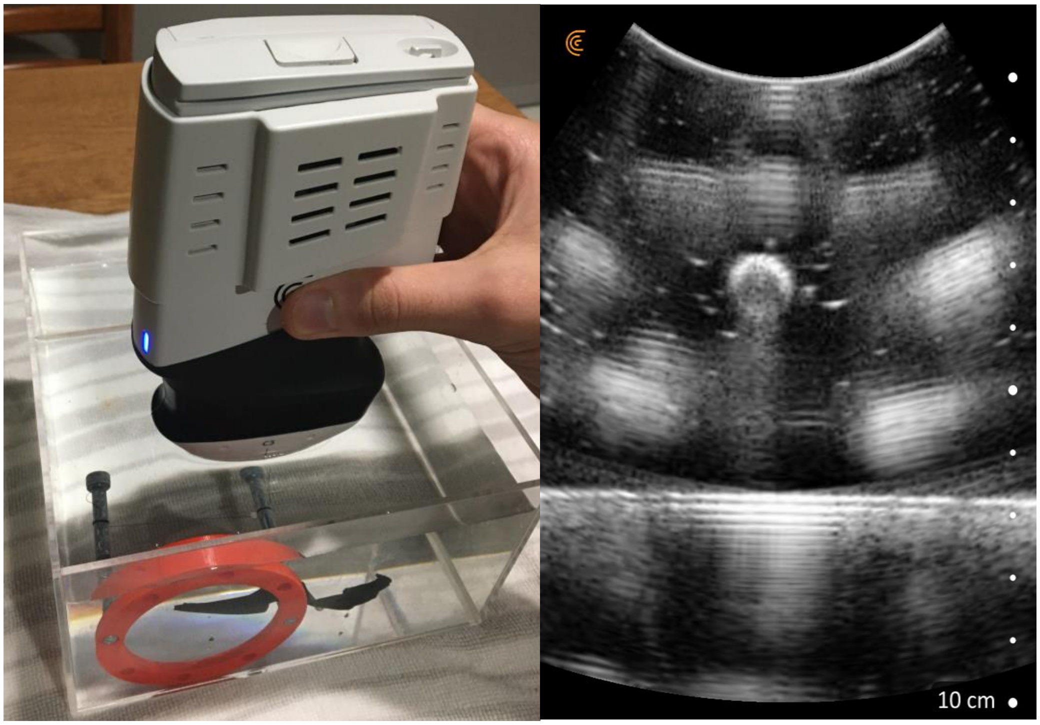

Figure 30: Control Test Viewing Cross Section of Metal Bolt

The figure above showcases the best-case result while looking directly at a recognizable object such as a metal bolt. Metal has a high acoustic impedance, and this means it is the bright circle viewed in the center of the ultrasound image on the right. This test is done to provide a benchmark for what we hope to see when using acrylic to reflect the ultrasound waves at an angle.

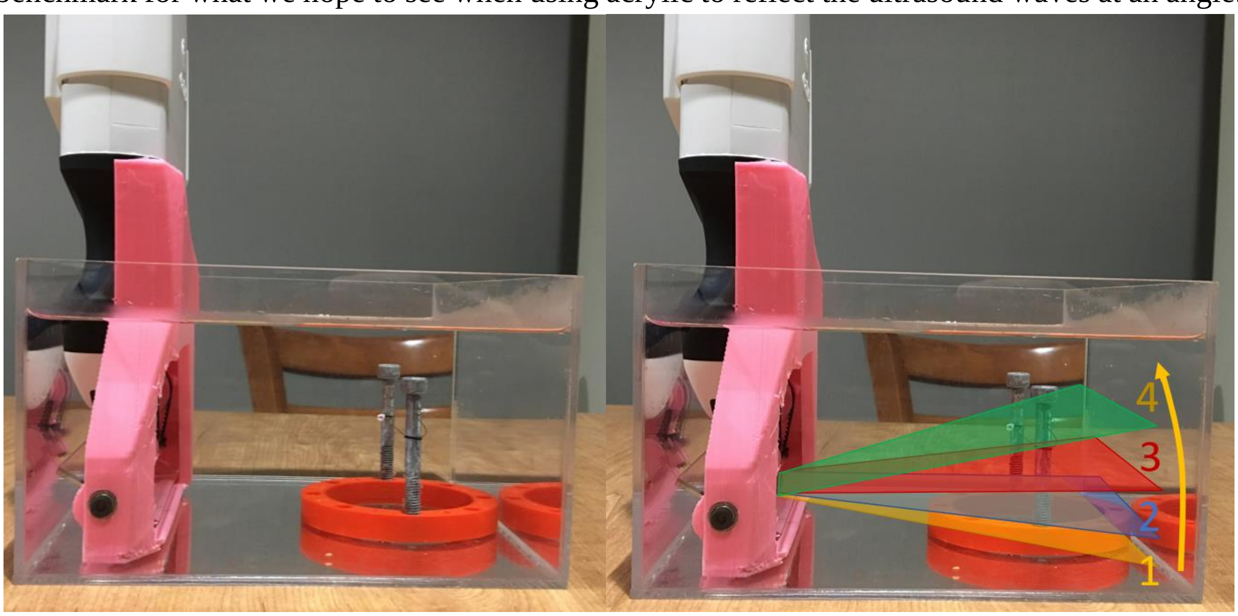

Figure 31: Experimental Setup for Rotational Sweep in Water Tank

The experimental setup used to test the rotational sweep within a tank filled with water is depicted in the figure above. On the left is a plain view of the configuration, where the device is mounted perpendicular to the surface of the water and submerged so that the transducer array is fully submerged along with the acrylic mirror and needle assembly. The image on the right shows the 4 points at which the ultrasound readings were obtained, starting at the bottom of the plastic and metal test piece, and rotating upwards to the heads of the bolts.

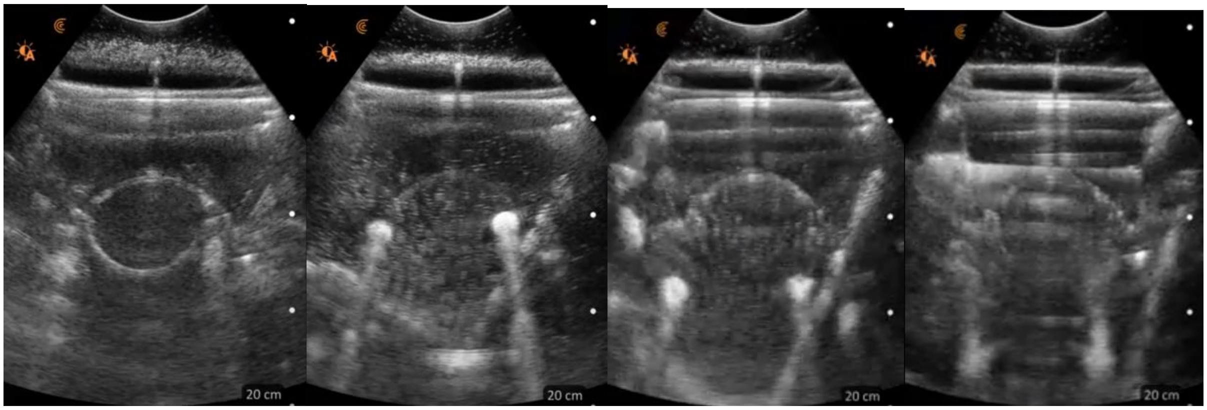

Figure 32: Raw Data from Rotational Sweep

The results of the experiment can be viewed above, in the 4 separate ultrasound readings at 4 points of interest. The expected result was for the bolts to translate downwards, indicated as a greater depth in the ultrasound reading as the ultrasound image rotated upwards. This is because the distance between the point on the acrylic where the ultrasound waves are reflected and the point on the bolts where the ultrasound waves intersect increases as the ultrasound view is rotated upwards. The labeled images below indicate this trend.

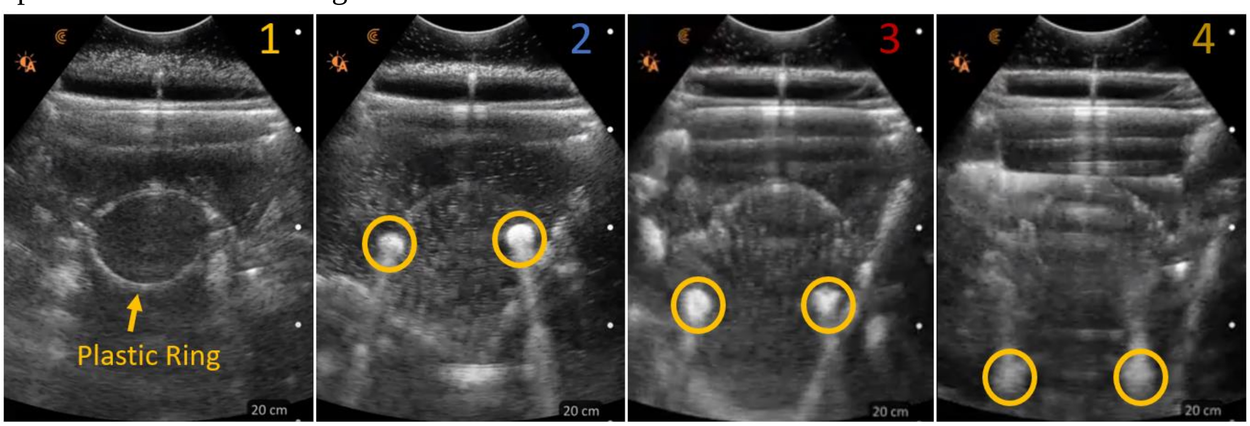

Figure 33: Highlighted Features of Each Ultrasound Image

Image 1 in the figure above shows the bottom of the plastic ring, before the bolts are easily visible. In the next image, the cross section of the bolts can be seen more clearly, and as the angle of the mirror is adjusted along the sweep, the bolts can be seen translating downwards in the ultrasound view in images 3 and 4. Overall, the initial test completed with the acrylic mirror that was laser cut proved to be very effective and promising. Given the size of the water tank there is a great deal of noise in the images, so to improve this testing configuration, a larger tank could help provide even clearer results.

Iteration 4:

With the improvements made in iteration 3, we were able to demonstrate the effectiveness of the acrylic piece as a mirror. However, iteration 3 did not include any of the electronics or the encoder, so there was no easy way to measure the change in angle. Given that the electronics are a key component of the device, iteration 4 had the primary goal of integrating the electronics and encoder into the design. Additionally, the testing in iteration 3 showed that a tank filled with water is a good testing environment for the device because the transducer and mirror can be fully submerged. Unfortunately, this is not ideal for a real case scenario, where ultrasound gel would be used, and a water tank would be cumbersome. With that said, given the early stages in the device's development, a water tank is the most consistent way to test the device. That is why a secondary design goal of iteration 4 was to elevate the electronics above the surface of the water so that there is no risk of water damage to the components. Ideally in a final product, the electronics could be housed in a more compact, watertight enclosure.

Figure 34: Iteration 4 Overview

As shown above in Figure 35, iteration 4 has a significant redesign compared to the previous iterations. The PCB is mounted at the top of the device, elevated 2.75 cm above the

Clarius transducer and the PCB has been fully assembled and soldered to the board including the directional button, TFT display, ESP32 Microcontroller, and all the surface mounted components such as resistors. The electronics are currently powered by a micro-USB port to allow for a real-time serial connection to a computer. This will help integrate the software component to the device given there will be less delay to receive the encoder readings compared to a wireless connection.

Figure 35: Encoder Angle Reading

The device uses a directional button for menu navigation allowing the user to press up, down, left, right and click in to select an option. The scripts in charge of the display and menu were written in C++ and are running on the ESP32 Microcontroller. The device can display encoder readings in real time, connecting to Wi-Fi networks, and updating firmware remotely. A full overview of the menu options can be viewed in Figure 37 below.

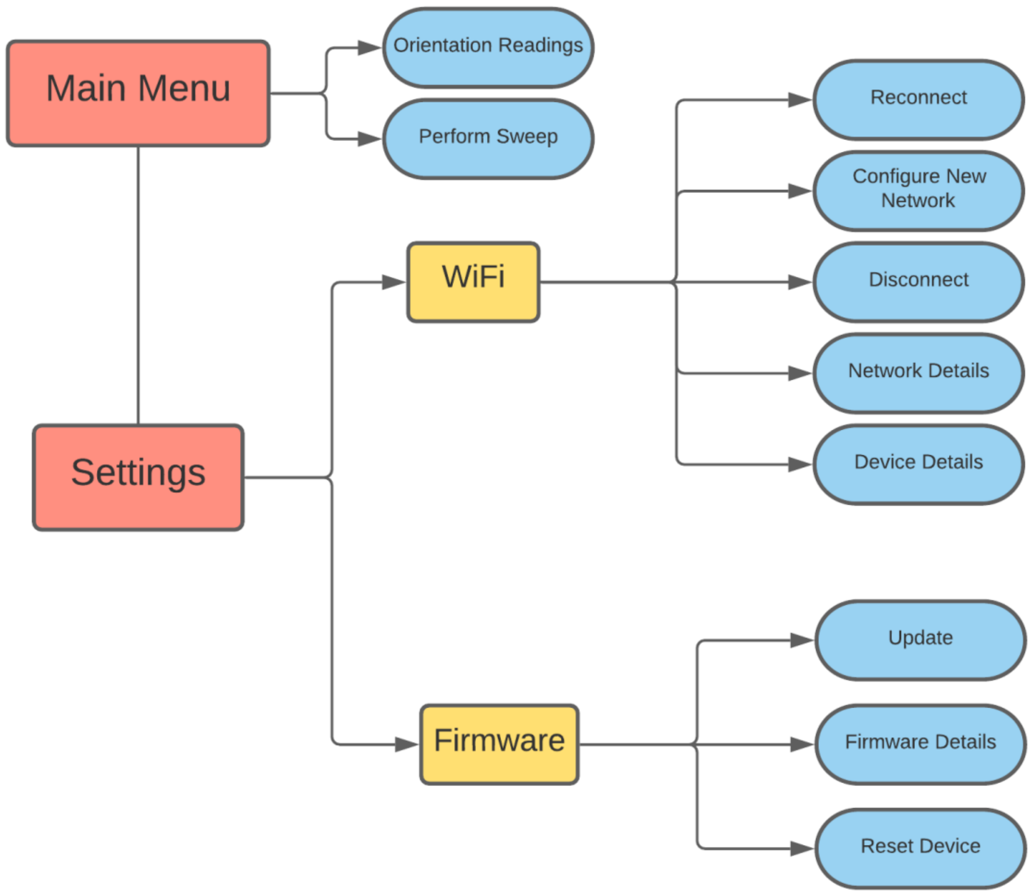

Figure 36: Menu Navigation Options

As shown above, the menu navigation the user interfaces with on the device follows a simple to follow layout. There are two main pages, the main menu, and the settings page. These have their respective features, with the main menu accessing the common functions such as viewing the encoder readings and details about how to perform a sweep. In the settings menu, this branches into two categories, the Wi-Fi options, and the firmware options, each with a variety of selectable functions such as viewing details, updating firmware, connecting to new or existing networks, and resetting the device.

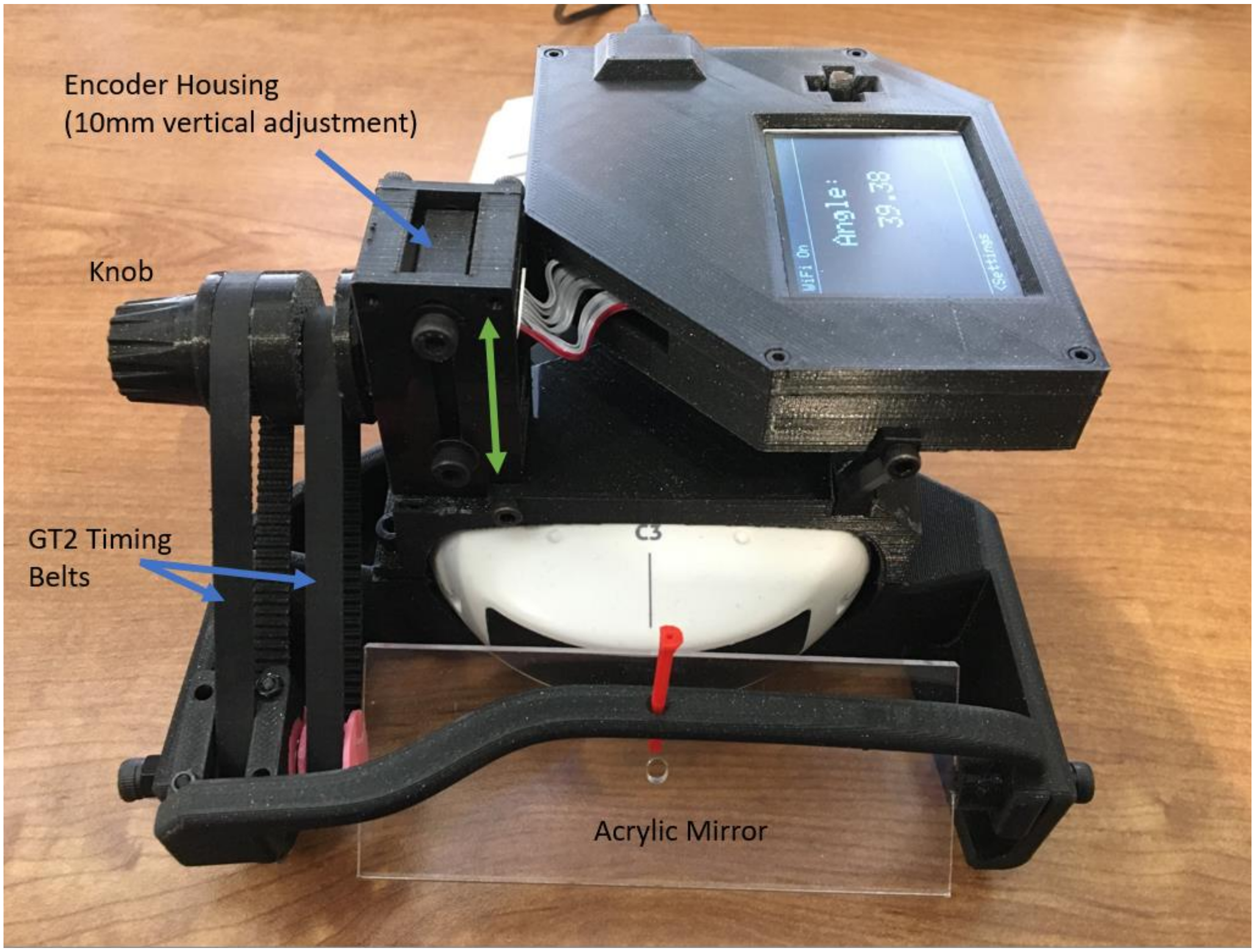

Figure 37: Front View of Iteration 4

The encoder readings are displayed on the TFT display in degrees to two decimal places. Given that the knob is connected to the encoder, as the user rotates the knob, they are also moving the 6mm wide GT2 timing belts, which is rotating the mirror and needle mechanism. This allows for the encoder readings to be updated as the knob is being rotated. To properly tension the belts, the encoder is housed in a 3D printed component that allows it to be translated vertically by +-5mm. Once the encoder and housing are configured properly, the M5 bolts can be tightened, securing the encoder in position. This allows the encoder to be positioned in a way such that the belts can be tensioned. Unfortunately, we found that using only one tensioning method for two belts was not sufficient to tension both belts. To remedy this, we will be using tensioner springs mounted to the belts. An example of a tensioner spring on a belt can be viewed below.

Figure 38: Tensioner Spring Mounted to GT2 belt

The benefit of using a spring is that the tensioning can be variable given that the spring can compress or expand. We believe this will allow the springs to adjust as the belts are moving to retain proper tensioning. The tensioner springs cannot be mounted on the belts in a configuration where they would pass over the pulley wheels, however they can be placed along the long stretch of belt between the wheels such that they will never contact the wheels.

Figure 39: View of TFT display and Wi-Fi Menu

Even though the device is currently using a wired connection, the ESP32 can use Wi-Fi, so in future developments of this device, wireless capabilities could be integrated into the software component of the device. Additionally, this could allow the device’s firmware to be updated remotely, a useful feature for any device that is sold commercially.

Preliminary experimental result:

Based on preliminary testing of the device, the belts slip due to improper tensioning and low-resolution 3D prints for the gear teeth on the belt wheels. This prevented us from gathering usable data on how accurately the mirror and needle mechanism could rotate together. It also requires reprinting the belt wheels on a higher resolution printer and with different gear teeth profiles. In the current state, the difference between the expected needle angle and the actual needle angle was 3 degrees. In the high precision setting of PCNL procedures this is likely not suitable for the practitioner’s needs. However, given the proper tensioning of the belts, this inaccuracy should be reduced.

Iteration 5:

Iteration 5 was the last iteration of the device, and successfully fixed the issues plaguing previous iterations. Firstly, and most importantly, the tensioning issues with the belts was solved by improving rigidity and support to both axes as well as allowing for variable tensioning with springs and upper axis placement. Secondly, we purchased precision rods and new bearings to improve the smoothness of rotation and double supported all belt wheels which greatly reduced the moments that were being applied on the belt wheels. Given these successful developments in the device, we were able to test using an US phantom and at UMass Memorial Hospital using a kidney phantom.

Figure 40: Iteration 5 Final implementation

As shown above, the electronics are still mounted to the top of the device, elevated 2cm above the surface of the US probe. This is necessary because the lower half of the device will be submerged in water so that there is a medium for the Ultrasound waves to pass through between the probe, mirror, and phantom. Additionally, as can be seen on the left of the image, spring tensioners were added to the belts to allow for tensioning while the device is in use and the belt wheels are being turned. We found that this significantly helped make both belts properly tensioned. To improve the support for the upper axis, we extended the left wall up to provide support on both sides of the upper axis and encoder which helped reduce the moments applied on the belt wheels. The arch piece was also redesigned and lengthened, allowing for a new support to fit between the two lower pulley wheels. The curved design in the arch piece prevents the belts from contacting the arch along the 40-degree range of motion. During our initial testing, we found that the acrylic mirror we were using was not as effective as glass, so we changed the design to incorporate a glass mirror and a 3D printed frame to hold the glass in place. We used a diamond glass cutter and carefully sanded the glass to obtain the 35mm x 85mm shape we needed and used a carbide tip drill bit to drill a hole for the needle to pass through.

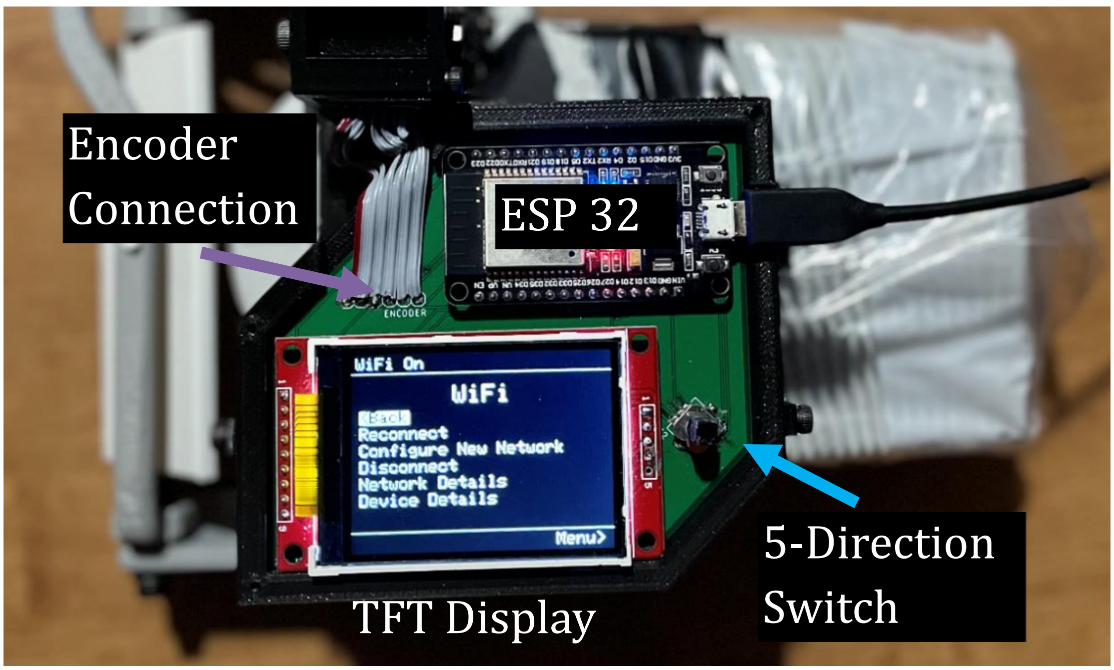

Figure 41: PCB Mounted on Device

The menus are controlled using the 5-direction switch and the user has the capability to view encoder readings, remotely update firmware, and connect to Wi-Fi networks. The encoder is soldered to the board using a ribbon cable and this allows for the encoder and upper axis to be adjusted without effecting the electrical connection to the board. The ESP 32 uses a serial connection with the GUI and sends encoder readings multiple times per second to update the 3D visualization of the US scans. Unfortunately, an unexpected issue we encountered was that the Clarius US probe was not as waterproof as we originally thought. The battery could not be submerged under water, complicating our testing process because there was no easy way to keep the probe out of the water at this point. Our solution was to create a watertight seal around the back of the probe and with the help of Yichuan, a Ziploc bag was cut and placed surrounding the battery compartment. To replace the battery, we could simply unzip the bag, swap the battery, then close the bag again. We experience small leaks during testing but with paper towels placed in the bag to absorb the leaks, the device was able to be submerged for the duration of testing.

Image Visualization:

Requirement:

With the software designed for this device, we aimed to provide a packaged solution that would provide the user with all the information they need, accessible in one place so that they could carry out the procedure effectively. We aimed to provide the user with high quality ultrasound images, intuitive metrics about the orientation of the needle, and the ability to visualize a three-dimensional view of the area being scanned. Using the software, the user would have the ability to choose between streaming real-time Ultrasound images as they are performing the scans or be able to collect ultrasound images for offline viewing. The software also provides the user with encoder data that can be used to display the angle at which the needle is being held. This way, the user can keep track of all the needle orientations viewed and has more information to decide the orientation to be set before needle insertion. With the ability to view real-time ultrasound imaging and enhanced maneuverability for the user to position the needle, the user will have all the information they need to make informed decisions during the procedure. The overall idea for the workflow of the software can be visualized with the tree map below:

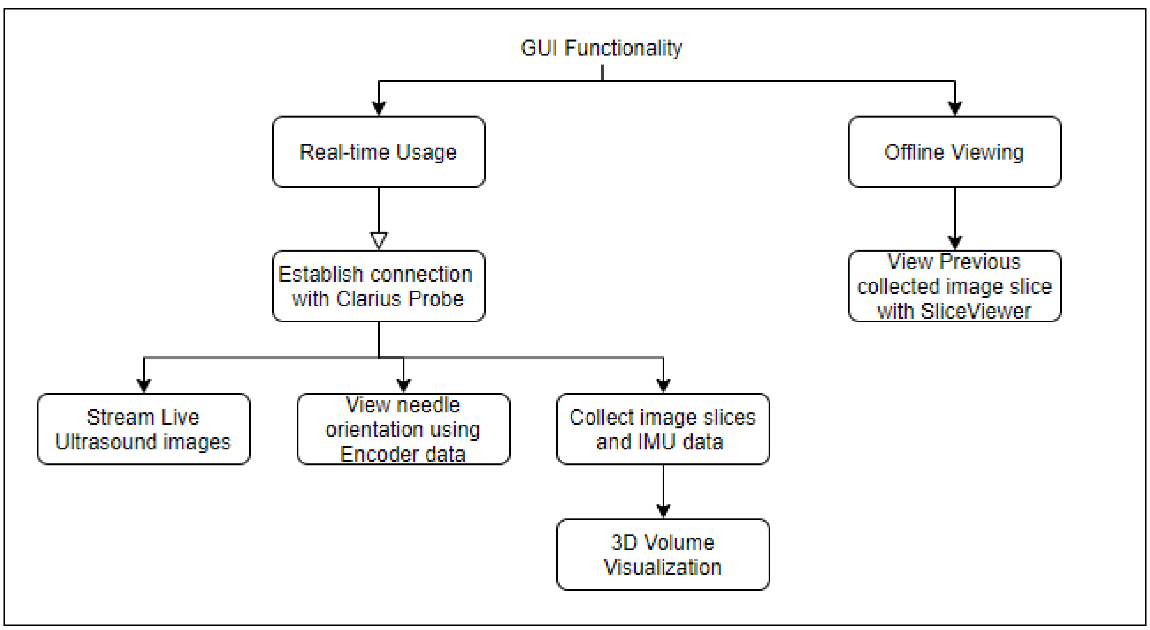

Figure 42: General GUI Workflow

As you can see from the tree map above, we aimed to design and develop a GUI with functionality to enable the user to choose between real-time usage and offline viewing. The primary motive for the real-time usage is to enable the user to stream live ultrasound scans as they are performing an ultrasound procedure on a patient. Additionally, they will be able to view the current orientation of the needle as they perform the scans and can decide what orientation to maintain before needle insertion. Lastly, the user will also have the option to collect image slices and IMU data from the Ultrasound probe that can then be used to develop a three-dimensional visualization of the area they scanned. Having this 3D volume visualization would be useful for the user to identify and visualize structures that cannot be easily identified using 2D scans and could potentially prevent complications during the procedure. Furthermore, there might also be a case where the user would want to look back at previously collected ultrasound scans to identify key features that might have been overlooked during the live scans. In this case, the user can utilize the Slice Viewer functionality to load in Ultrasound images collected previously and use the GUI to iterate through them.

Software architecture:

To view ultrasound images, export raw data, and utilize different modes of operation provided by the Clarius Scanners, we need to establish a workflow between the Clarius Scanner, the Clarius Mobile App, and the PC based GUI. The Clarius Scanner uses Direct-Wi-Fi to communicate with the Clarius Mobile App, and can be used to view live ultrasound scans, and other advanced modes such as M-mode and PW. This can be seen in Figure 36 below.

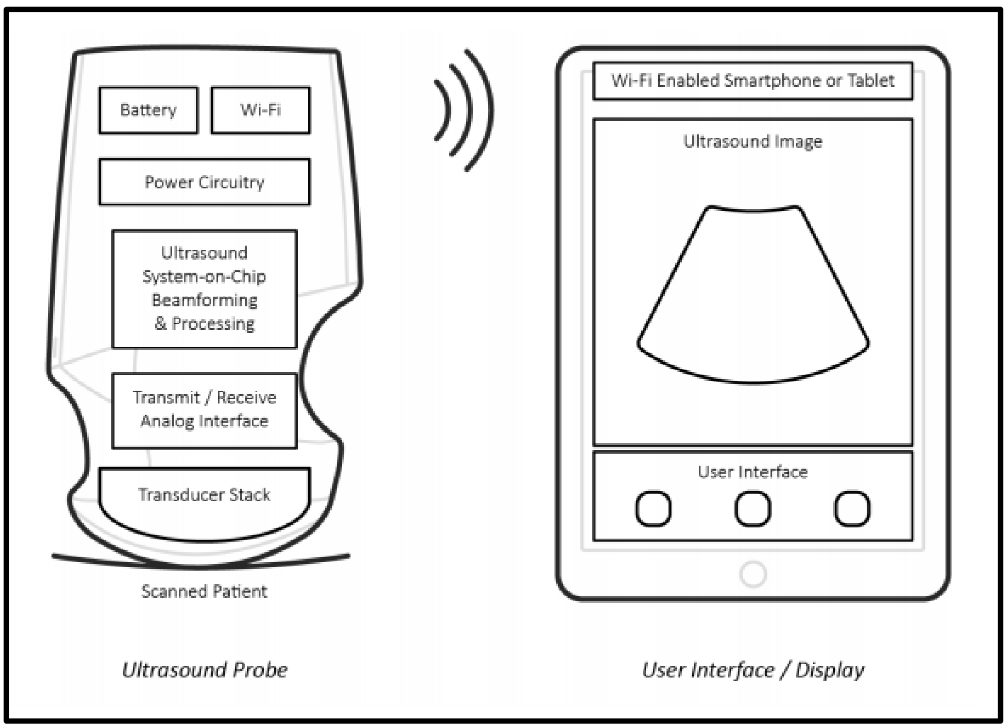

Figure 43: Clarius Probe Interfacing with Mobile App [3]

Live Stream ultrasound scans, and raw data can be collected from the Clarius probe and displayed onto the GUI using the Clarius Cast API. The Clarius API can be used to obtain grayscale and color Doppler images, or raw images, in real-time over the wireless network. Furthermore, 9 degree-of-freedom IMU data can be obtained real-time as well. The Clarius Cast API must be executed while the Clarius App is running and has established a connection to the probe. Furthermore, the Clarius probe, phone using the mobile app, and the PC displaying the GUI must all be on the same Wi-Fi network.

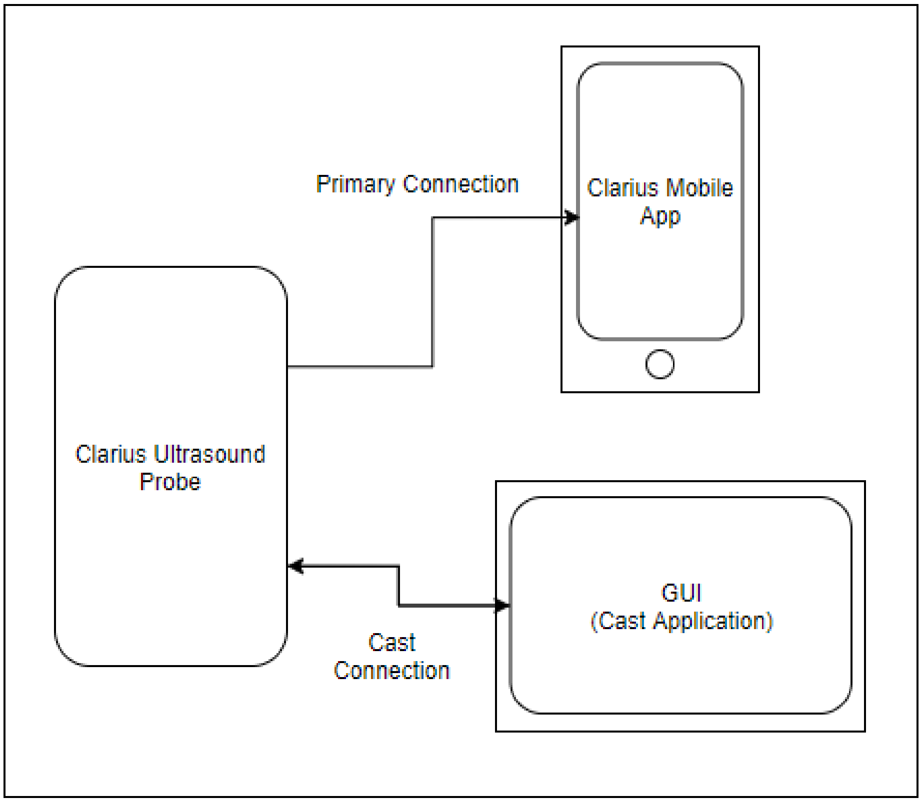

Figure 44: Clarius Interfacing with Mobile App and GUI

Figure 43 shown above demonstrates the Clarius Cast API architecture. The Cast API communicates directly with the Clarius scanner directly and utilizes TCP technology to create a secondary connection to the device that is receiving the ultrasound images. In this case, the secondary connection is initialized with the GUI that is receiving the ultrasound images.

To add functionality to the GUI to be able to stream live ultrasound images, collect images slices with their time stamps for offline viewing, and collect raw IMU data, python scripts were created that handled several independent functions. This can visualize with the workflow shown in the figure below:

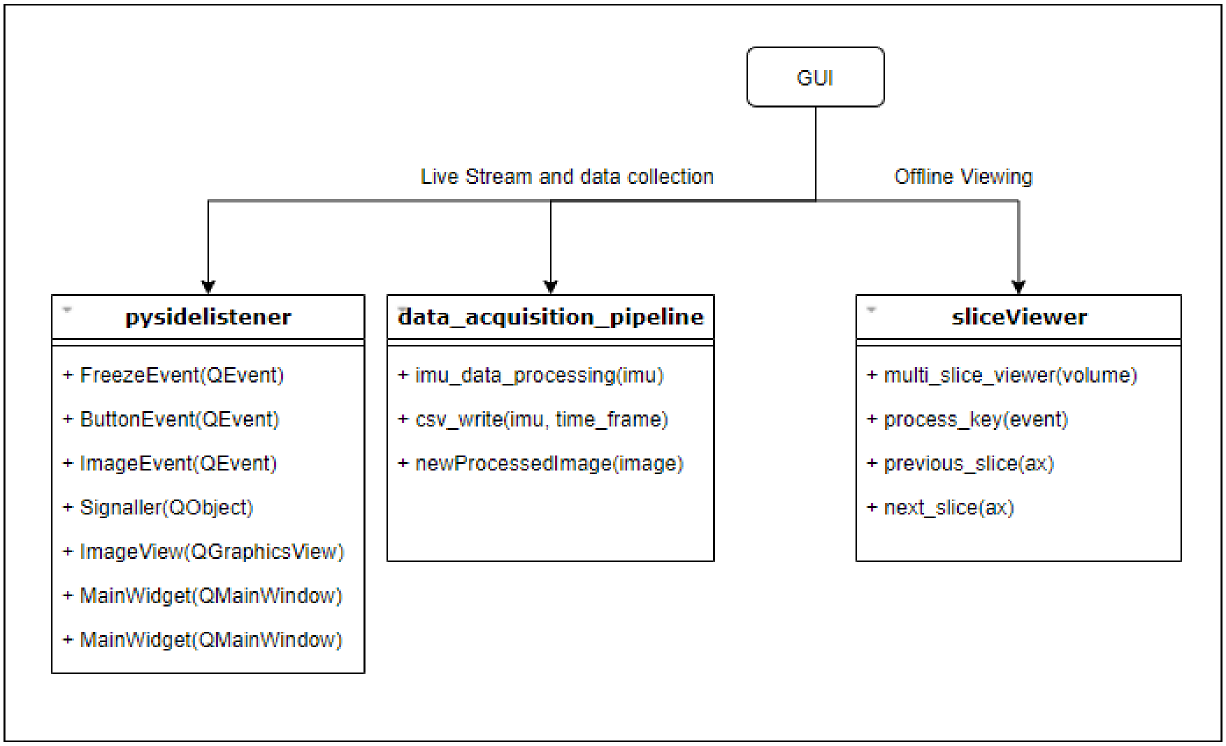

Figure 45: Visualization of Task Handling in GUI

The GUI can be split into two main workflows: live stream and data collection (which require a connection to the probe), and offline viewing. The real-time viewing of the ultrasound stream is implemented with the help of **PySideListener**, that creates a graphical program using Pyside2. Pyside2 is a python binding for the cross-platform GUI toolkit, Qt. Within the module, a Main window first initialized that contains controls and UI for the application. Thereafter, a connection is established with the Clarius Ultrasound probe and new processed ultrasound images are received to the GUI, which are then resized and drawn to the mainwindow. There are also custom events that handle changes in freeze state, button clicks, and for handling new images. The next module is the **data_acquisition_pipeline** that handles the raw data collection. It has two main functionalities. They can collect individual image slices with their respective time stamps and can collect raw IMU data. When a new image is received, a set of new inertial data is passed into the new image callback function. The inertial data for each measurement include a data timestamp, 3 gyroscope axes, 3 accelerometer axes, 1 magnetometer axes, a real component of the quaternion orientation, and three imaginary components of the quaternion orientation. Similarly, each time a new image is received, it is saved with its time stamp for later viewing. Lastly, **the SliceViewer** module handles offline data viewing. Firstly, Matplotlib subplots are initialized to plot and visualize the individual image slices collected through the data_acquisition_pipeline module. Using event-based handling, specific keys are mapped to allow the user to scroll through image slices. Each time the user iterates through an image slice, new subplots are drawn and appended to the mainwindow.

Iteration 1 Experimental Results and Demo:

The GUI was designed in a way that maximizes the screen usage and provides the user with all the information required in a modular fashion. The GUI uses two tabs to switch between viewing the live ultrasound stream, and the SliceViewer to view offline image data. By doing so, we could make sure that the user is able to see encoder readings and the 3D volume visualization irrespective of whether they are viewing a live ultrasound stream or viewing offline image data.

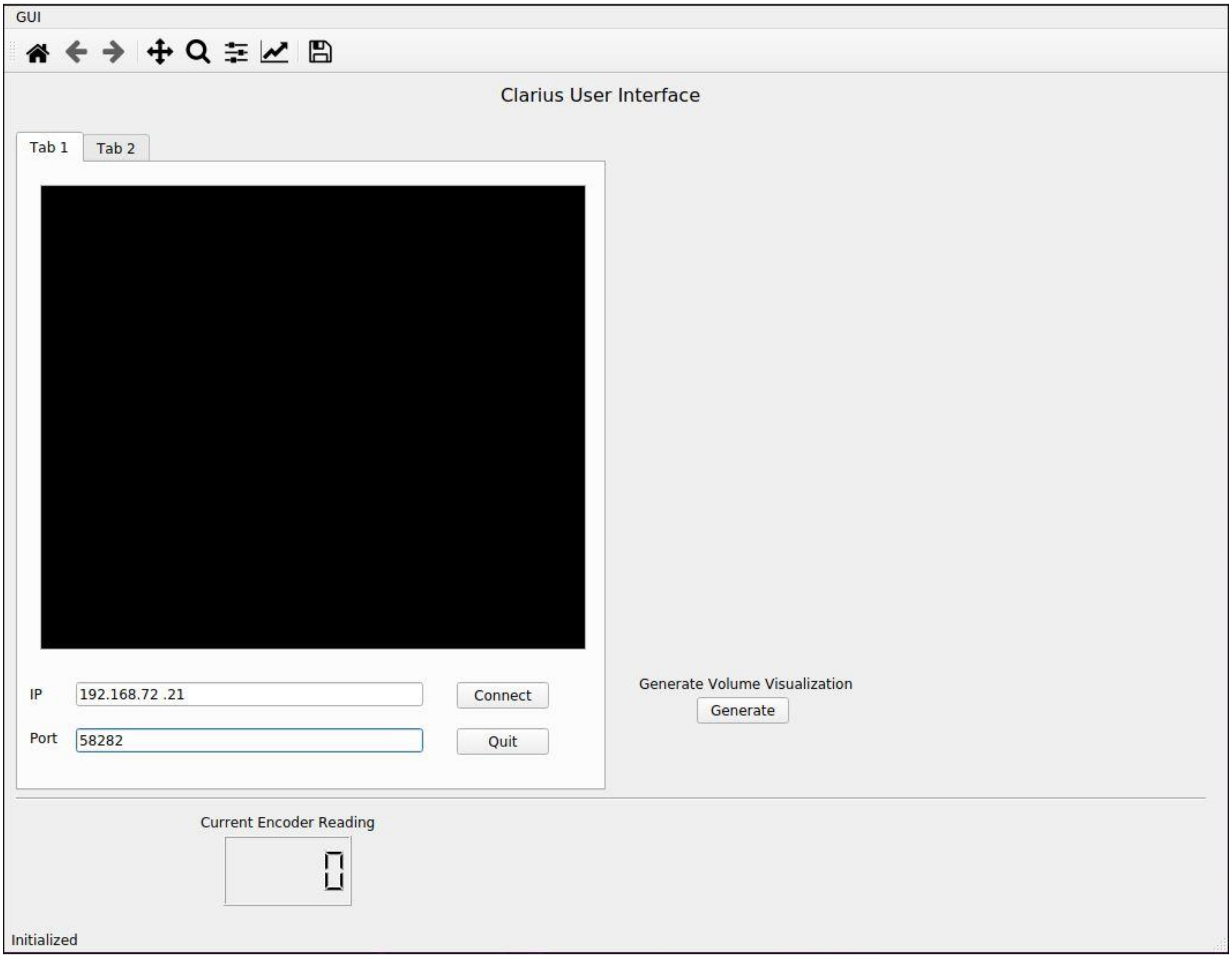

Figure 46: Stream Live Ultrasound Images with GUI

Figure 45 above demonstrates the ability to view live ultrasound images with Tab 1 in the GUI. The user starts by entering the IP address and Port number at which the Clarius probe is connected. After clicking "Connect" the GUI utilizes the Clarius Cast API and the PySideListener module to stream live ultrasound images from the probe. Since we were unable to access the Clarius probe while documenting the results, you can currently only see a black window instead of an ultrasound image. The GUI also implements a status bar that can be seen in the bottom of the image. The status is set to “initialized” once the GUI is launched, which means that it is ready to establish a connection to the probe. In the case that there is an unsuccessful connection to the Clarius probe, the status is updated to alert “failed to connect to IP address”. This can be seen in Figure 40 below. In this case, the “connect” button is updated to read “Retry” and the user can try to establish a new connection to the probe.

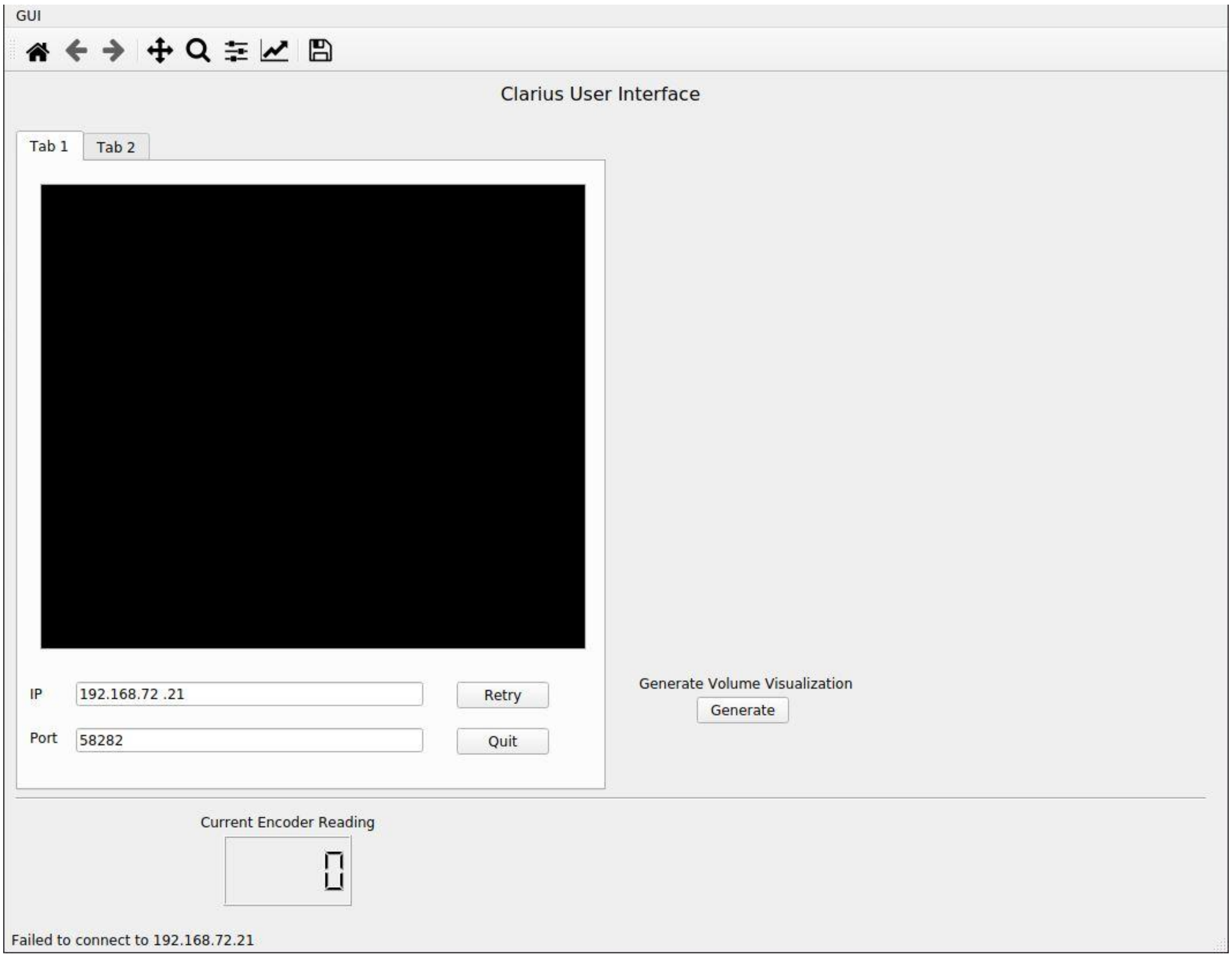

Figure 47: Demonstrating Clarius Connection States

Tab 2 in the GUI contains the SliceViewer that allows the user to view offline image data. It also contains functionality to collect individual images slices and raw IMU data. Like the functionality with Tab 1, the user needs to enter the IP address and port number to establish a connection to the Clarius probe. Once done, the user clicks the "Start Collection" to start collecting image slices and raw IMU data from the probe, including orientation data. During this time, the user should conduct a sweep of the target area and then click "Stop Collection". Using the data_acquisition_pipeline module, image slices and raw IMU data are collected from the probe during the sweep motion. The image slices are saved to a directory that can then be used to view offline with the SliceViewer. The image seen in Figure 41 below is an example of an image slice displayed with the SliceViewer. The user can scroll through different images by clicking 'J' (for previous slice) and 'K' (for next slice) on their keyboard.

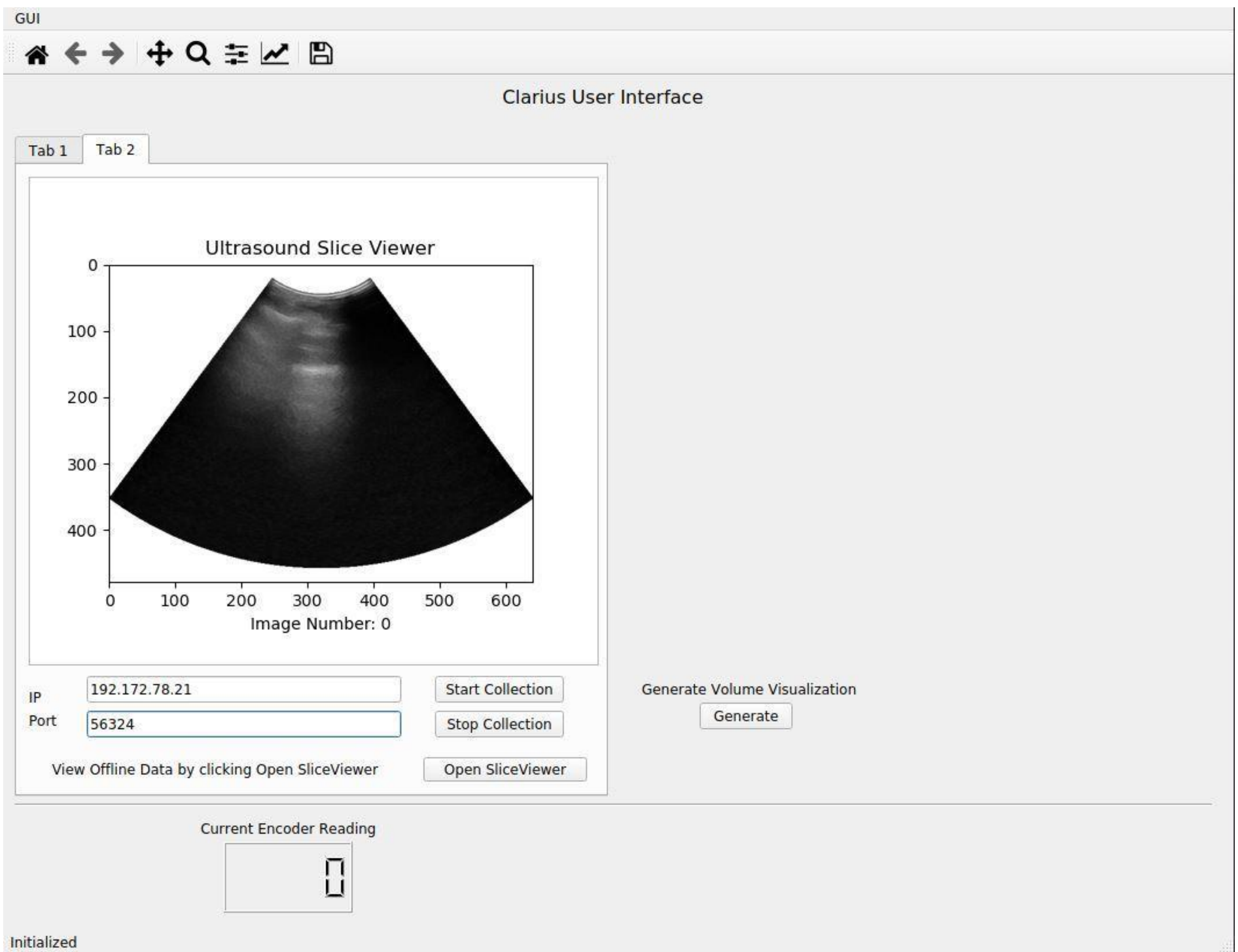

Figure 48: Collecting Raw Data and Demonstrate SliceViewer

Figure 47 shown below showcases the several images' slices collected during the sweep, with their individual time stamps. These image slices can then be loaded and viewed at any time using the SliceViewer in Tab 2 of the GUI.

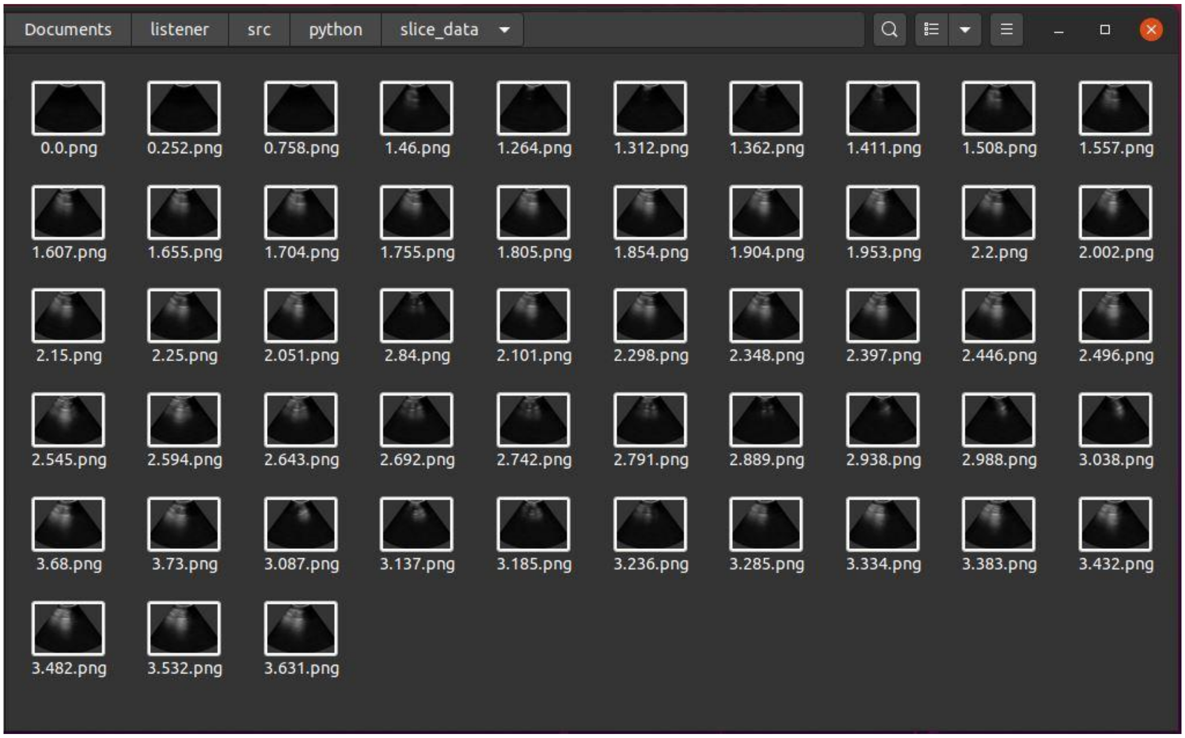

Figure 49: Images Slices Collected During Sweep

Similarly, Figure 49 shown below showcases the raw IMU data collected during the sweep. There are 9 DOF IMU data collected including data from accelerometer, gyroscope, magnetometer, and orientation data.

	A	B	C	D	E	F	G	H	I	J	K	L	M	N	O
1	acc_x	acc_y	acc_z	gyro_x	gyro_y	gyro_z	mag_x	mag_y	mag_z	quaternion_w	quaternion_x	quaternion_y	quaternion_z	rate	time
2	-0.08	-0.07	-1.03	-0.17	-0.03	0.03	0.28	0.25	-0.07	0.95	0.06	-0.02	-0.29	###	0.00
3	0.23	-0.02	-1.12	-1.06	1.16	-0.11	0.37	0.27	-0.08	0.98	-0.03	0.05	-0.36	3.97	0.25
4	0.28	0.72	-0.61	-1.35	0.86	-0.07	0.42	0.40	0.05	0.67	-0.15	0.44	-0.65	1.98	0.76
5	0.47	0.85	0.02	-0.71	0.57	-0.09	0.45	0.41	0.21	0.51	-0.17	0.71	-0.59	1.98	1.26
6	0.53	0.97	0.22	-0.15	-0.05	-0.04	0.57	0.44	0.36	0.55	-0.21	0.85	-0.63	20.83	1.31
7	0.61	1.12	0.20	0.28	-0.62	0.02	0.66	0.51	0.45	0.67	-0.29	0.98	-0.69	20.00	1.36
8	0.61	1.09	0.10	0.43	-0.85	0.12	0.67	0.49	0.42	0.69	-0.32	0.92	-0.63	20.41	1.41
9	0.62	1.05	0.01	0.43	-0.71	0.11	0.66	0.50	0.42	0.73	-0.36	0.88	-0.59	20.41	1.46
10	0.66	1.15	-0.02	0.27	-0.32	0.05	0.73	0.52	0.44	0.82	-0.42	0.92	-0.61	20.83	1.51
11	0.61	1.07	0.04	0.13	-0.10	0.19	0.68	0.50	0.41	0.79	-0.42	0.86	-0.55	20.41	1.56
12	0.62	1.05	0.10	0.07	-0.24	0.14	0.66	0.49	0.41	0.80	-0.43	0.83	-0.52	20.00	1.61
13	0.63	1.03	0.01	0.21	-0.44	0.06	0.68	0.49	0.39	0.82	-0.46	0.81	-0.49	20.83	1.66
14	0.62	1.05	-0.10	0.06	-0.19	0.08	0.68	0.48	0.41	0.84	-0.48	0.79	-0.46	20.41	1.70
15	0.69	1.14	-0.14	-0.17	0.16	0.08	0.73	0.52	0.46	0.92	-0.53	0.85	-0.49	19.61	1.76
16	0.67	1.08	-0.08	-0.30	0.52	0.14	0.69	0.49	0.42	0.86	-0.50	0.81	-0.46	20.00	1.81
17	0.66	1.02	0.00	-0.45	0.70	0.22	0.67	0.48	0.44	0.84	-0.49	0.81	-0.45	20.41	1.85
18	0.66	1.00	0.08	-0.50	0.80	0.39	0.68	0.48	0.45	0.82	-0.47	0.83	-0.44	20.00	1.90
19	0.68	0.99	0.25	-0.40	0.61	0.29	0.68	0.48	0.43	0.80	-0.46	0.86	-0.44	20.41	1.95
20	0.73	1.08	0.35	-0.08	0.07	0.09	0.73	0.50	0.49	0.86	-0.51	0.94	-0.46	20.41	2.00
21	0.66	1.03	0.30	0.17	-0.69	-0.03	0.69	0.49	0.44	0.82	-0.51	0.87	-0.41	20.41	2.05
22	0.69	1.02	0.12	0.48	-1.08	0.09	0.69	0.48	0.45	0.84	-0.53	0.82	-0.37	20.00	2.10
23	0.68	1.00	-0.08	0.45	-0.97	0.21	0.70	0.47	0.43	0.87	-0.55	0.78	-0.33	20.41	2.15
24	0.69	0.97	-0.15	0.01	-0.32	0.16	0.70	0.47	0.40	0.89	-0.56	0.76	-0.31	20.00	2.20
25	0.77	1.05	-0.12	-0.29	0.22	0.09	0.77	0.50	0.44	0.97	-0.60	0.82	-0.33	20.00	2.25
26	0.76	1.03	0.01	-0.48	0.64	0.01	0.71	0.48	0.42	0.90	-0.56	0.79	-0.32	20.83	2.30
27	0.73	1.00	0.14	-0.48	0.61	0.05	0.69	0.47	0.43	0.87	-0.55	0.80	-0.32	20.00	2.35
28	0.74	0.99	0.16	-0.25	0.42	0.14	0.71	0.46	0.43	0.85	-0.54	0.81	-0.32	20.41	2.40
29	0.74	0.94	0.07	-0.09	0.47	0.14	0.69	0.46	0.44	0.84	-0.54	0.82	-0.32	20.41	2.45
30	0.76	1.05	0.00	-0.02	1.04	0.16	0.75	0.49	0.49	0.90	-0.58	0.90	-0.35	20.00	2.50
31	0.66	0.97	0.14	-0.08	1.71	0.18	0.69	0.47	0.46	0.83	-0.52	0.88	-0.35	20.41	2.55
32	0.66	0.88	0.39	-0.17	1.91	-0.05	0.68	0.46	0.49	0.77	-0.49	0.91	-0.37	20.41	2.59
33	0.72	0.99	0.58	0.19	1.39	-0.46	0.71	0.50	0.53	0.80	-0.52	1.01	-0.42	20.41	2.64
34	0.64	1.04	0.40	0.41	0.32	-0.39	0.61	0.45	0.45	0.70	-0.49	0.89	-0.38	20.41	2.69

Figure 50: Raw IMU Data Collected During Sweep

Evaluation Criteria:

In terms of evaluation criteria, it is important to test the GUI across several parameters to make sure that the user is receiving meaningful information that maximizes their utility and aids the effectiveness of the procedure being conducted. When evaluating a GUI, it is important to conduct empirical evaluations with the end users, but also conduct heuristic evaluations based on a set of guidelines. The list below contains a set of heuristic evaluation parameters that need to be assessed to measure the effectiveness of the GUI at providing the user all the information needed during an ultrasound procedure.

Table 6: Evaluation Criteria

Heuristic	**Explanation**
Applicability	The most important criteria to test the GUI is its ability to provide relevant information to the user that benefits a process. With our GUI, we would evaluate it based on image quality of ultrasound scans, the accuracy of encoder readings at letting the user know of the current needle orientation, and the effectiveness of the volume visualization at providing additional views that help the user during a procedure
Visibility of System Status	The GUI should always keep the user informed about what is going on. For instance, the status bars at the bottom GUI alert the user of the current connection status to the Clarius probe
User control and freedom	The GUI should support undo and redo actions and allow the user to override the system
Error Prevention	The GUI should as much as possible prevent the possibility of errors occurring in the first place.
Flexibility and ease of use	The GUI should provide all the information organized well in one place. The user should not have to go looking for information.
Aesthetic and minimalist design	All user content should be relevant to the task and there should be no crowding of information

Iteration 2 Software Development:

The current iteration of the software builds upon our goal to provide a packaged solution that would provide a user with all the information they need, presented in an accessible manner, so that they can effectively carry out their intended procedures. The previous iteration of the software allowed the user to view high-quality ultrasound images taken during a procedure, while also being able to load previously collected data to view offline when not connected to the ultrasound probe. The current iteration of the software adds additional usability and functionality to enable users to view orientation data of the needle as they manipulate the needle and the viewing angle of ultrasound scans. Additionally, users can now better visualize the effect that rotating the mirror angle on our attachment has on the region that ultrasound data is being collected from. This can be done by visualizing the ultrasound scans in a three-dimensional space, where the ultrasound images are rotated along the plane where the mirror angle is being rotated.

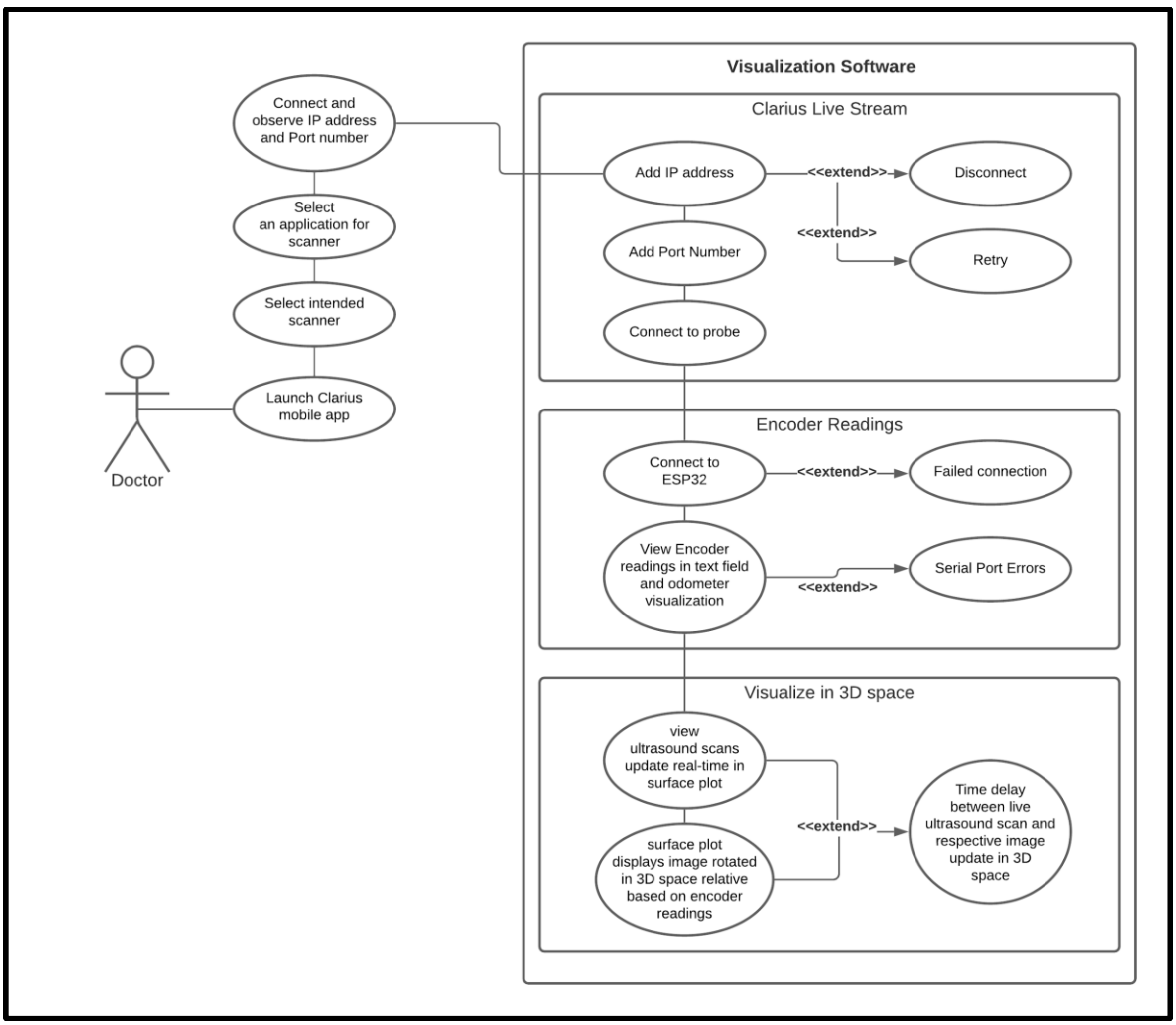

Figure 51: Use Case Diagram for Visualization Software

Implementing these additional functionalities in the software, resulted in a more complex system. To help the user better understand how to use the application and the general flow of events, we created the use case diagram as shown above in Figure 50. The use case diagram showcases one possible scenario, and the flow of events, where a doctor would use our system to visualize ultrasound data during a procedure. The flow of events can be better explained with the help of the textual use case description below. The textual use case describes certain entry conditions that the user must satisfy to be able to use the visualization software, the exit conditions for when the user has completed their intended use, the general flow of events while using the application.

Doctor Textual Use Case:

1. Name: Doctor use case
2. Participating Actors: Doctor
3. Entry Condition:
    a. Doctor has Clarius mobile application installed and has a Clarius scanner appropriate for the intended use.
    b. Doctor can successfully connect to the Clarius probe and the ESP32.
4. Exit Condition:
    a. Doctor has viewed all relevant information and does previous data is not required.
    b. Doctor has completed the procedure.
5. Flow of Events:
    a. The doctor launches Clarius mobile application
    b. The doctor selects the correct Clarius scanner for the procedure and selects the intended application in the Clarius Mobile app based on the body region being scanned. For instance, the doctor selects ‘abdomen’ under the applications menu.
    c. The doctor notes the IP address and Port number that the Clarius probe is connected through.
    d. The doctor launches the visualization software and enters the IP address and Port Number in the relevant fields in the visualization software. The doctor proceeds to connect to the probe from the application.
    e. The doctor can connect to the Clarius probe and view a live stream of ultrasound scans as he performs the procedure.
    f. The doctor can view encoder readings and determine the optimal needle orientation before insertion.
    g. The doctor can view real-time ultrasound scans in a three-dimensional space.
6. Alternate Flow of Events:
    a. Clarius probe fails connection. IP address and Port number need to be re-entered.
    b. Unable to connect to the ESP32. Serial connection needs to be re-established.
    c. Time delay between ultrasound scans appearing and visualizing them in three-dimensional space exist. Application needs to be restarted.

Updated Software Architecture:

Given the added functionalities to the software, there were several additional classes and methods added to the system. These can be visualized effectively with the help of class diagrams that showcase the structure of the system and represent the object's attributes, operations, and associations. The ClariusGUI module handles the main workflow of the application and is the central module where data is being passed through. The ClariusGUI module handles launching the GUI, streaming live ultrasound scans, updating current encoder readings, and visualizing ultrasound scans in a three-dimensional space.

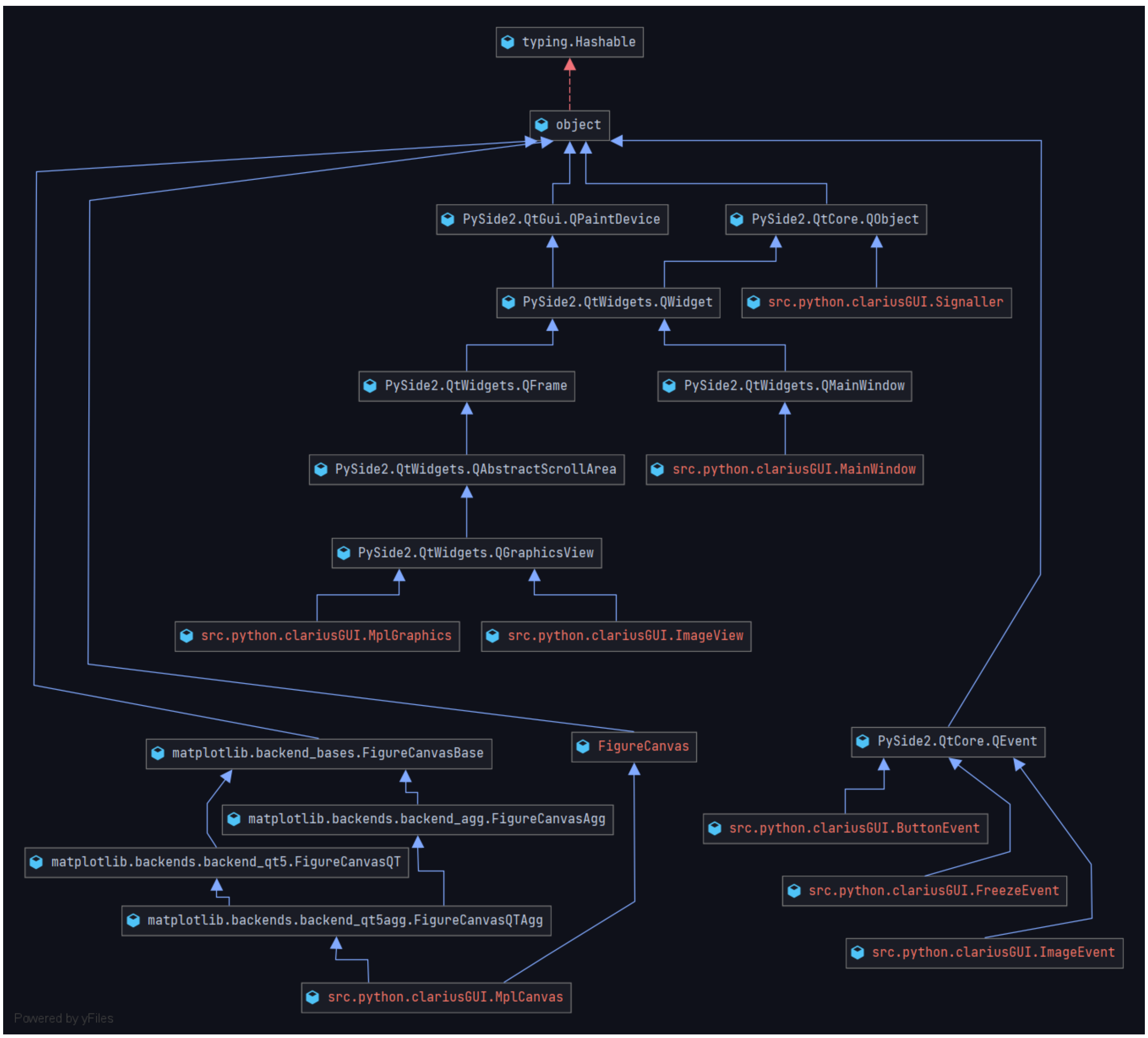

Figure 52: ClariusGUI Class Diagram

As shown above, Figure 51 demonstrates the way that classes and packages within the ClariusGUI module are structured and the way that they interact with one another. Each of the classes shown in red, is responsible for handling a key task in the visualization software. The

MplCanvas utilizes a FigureCanvas to draw the surface plot axes that are used to display ultrasound images in a three-dimensional space. The classes ImageEvent, FreezeEvent, and ButtonEvent are event handlers that carry out specific actions whenever a new ultrasound image is streamed, when an image is frozen, and when certain buttons on the GUI are clicked, respectively. The class MplGraphics handles drawings and updating plots of ultrasound images in the SliceViewer used for offline viewing of scanned ultrasound images. The class ImageView handles drawing the ultrasound image in the QGraphicsView by setting new incoming ultrasound images, redrawing them, resizing the scan converter, image, and scene, and drawing a black background to accurately display the image. The class Signaller manages custom events posted from callbacks, and then relays signals to the main widget to carry out the intended application. Some of these classes, including the event handlers, ImageView, and Signaller, were adapted from the Clarius Listener API module named PySideListener. A clearer class diagram for the PySideListener module can be seen in Figure 52 as shown below.

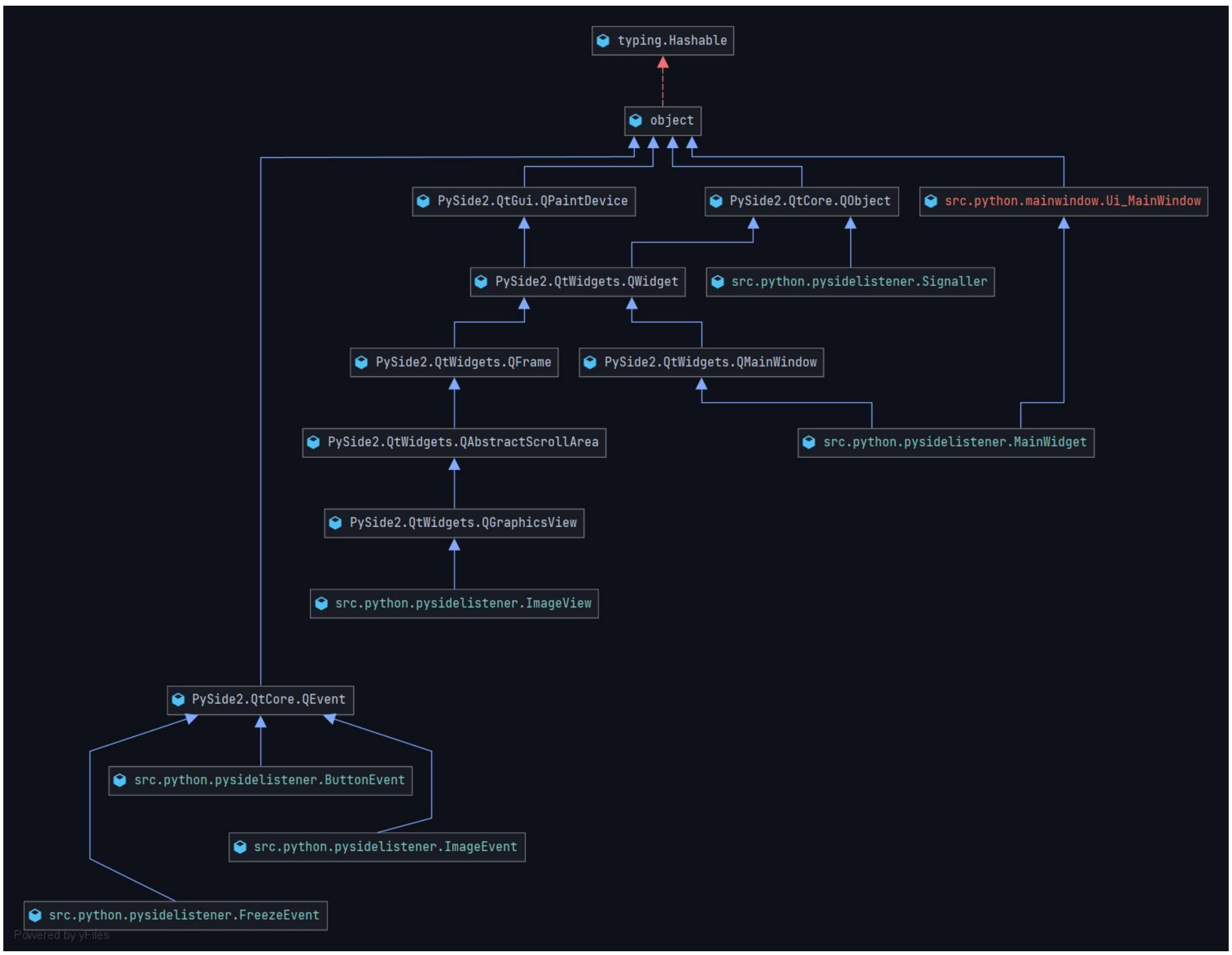

Figure 53: PySideListener Class Diagram

Now that class diagrams for the ClariusGUI module and PySideListener have been explored, it also useful to visualize how other helper classes such as ControlArduino, View3D, SliceViewer, and Data_acquisition_pipeline interact with the ClariusGUI module. Refer to Page 59 for details about the functionality of the SliceViewer and Data_acquisition_pipeline classes.

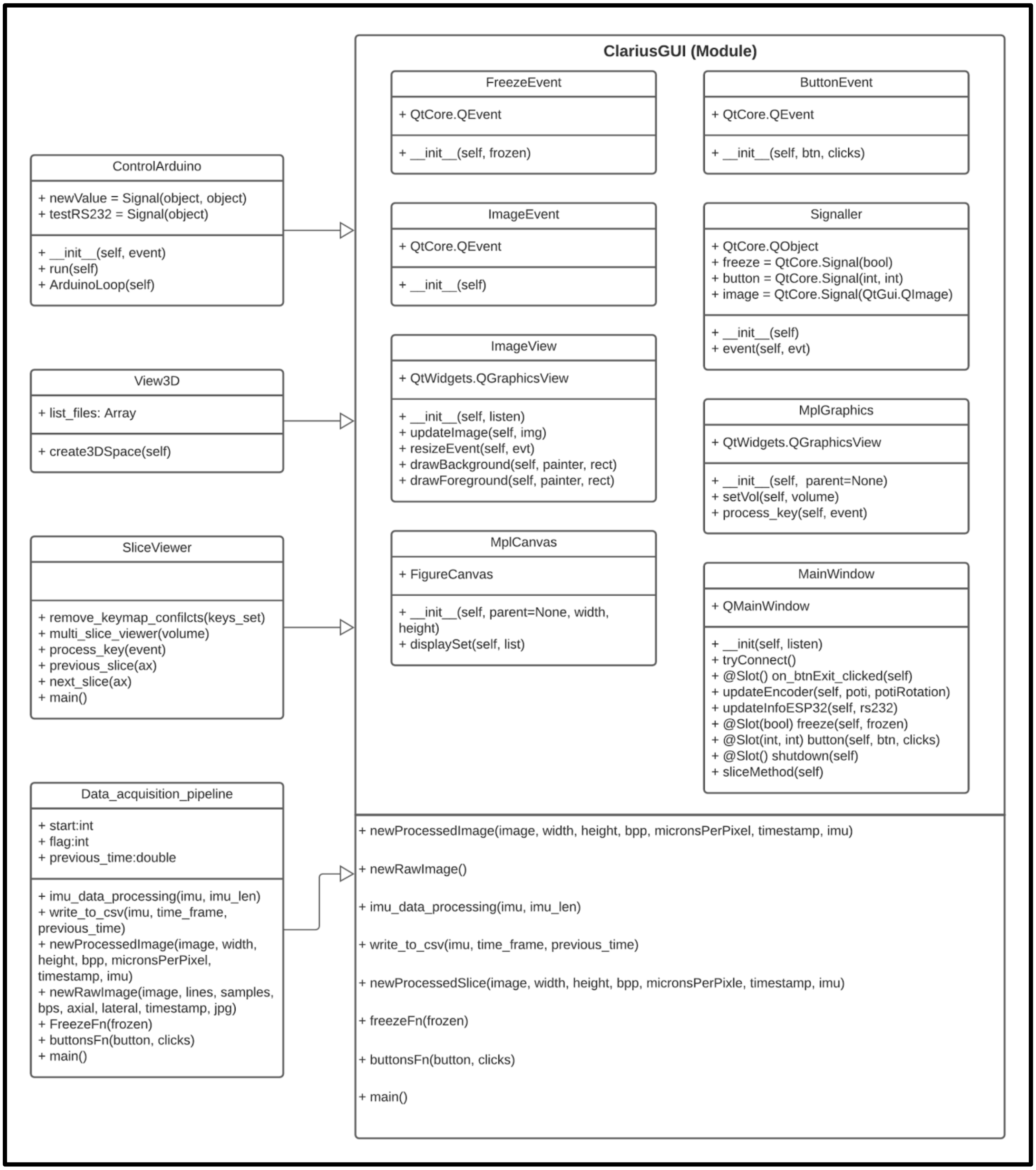

Figure 54: Class Diagram for Whole Application

As seen in the detailed class diagram shown in Figure 53 above, the ClariusGUI module interacts with and utilizes functionality from several other classes. Building functionality from the previous software interaction, the current iteration added the view3D and ControlArduino classes to the system. The ControlArduino class has functionality to read data from the encoder through the serial port and display it in the GUI. Firstly, an instance of the ControlArduino class controller is created in the ClariusGUI module. Thereafter, a thread is started to get data from the ESP32 through the serial port and the UpdateEncoder function is called to get new integer values between 0 and 1023 showcasing the new angle of the needle. The View3D class handles functionality for drawing and updating a surface plot to visualize ultrasound images in a three-dimensional space. As the ImageView class in ClariusGUI updates with incoming ultrasound scans from the Clarius probe, the View3D class updates the surface plot to visualize the image in the 3D space and with angle information from the encoders.

Iteration 2 Experimental Results and Demo:

The current iteration of the visualization software builds upon the idea of designing the GUI in a way that maximizes the screen usage and provides the user with relevant information presented in a modular fashion. The GUI now has functionality that enables users to view live ultrasound images being streamed from the Clarius scanner, view real-time encoder readings as the mirror and viewing angles are changed, and visualize the real-time ultrasound scans in a three-dimensional space. The following section showcases what each of the functionalities looks like in the GUI.

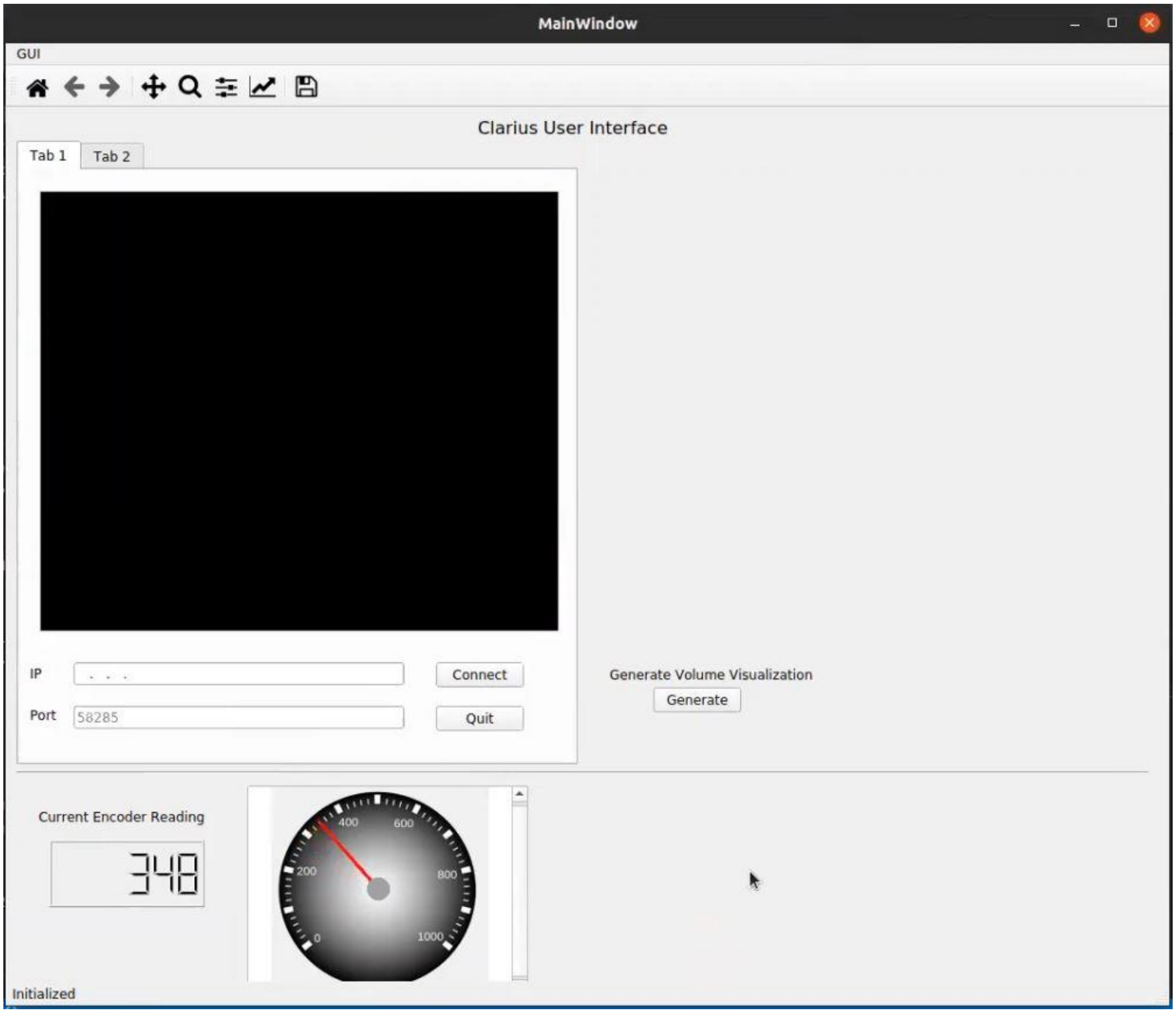

Figure 55: GUI Displaying Real-Time Encoder Readings

Figure 54, as shown above, displays the encoder readings and an odometer visualization to provide a more user-friendly method of viewing angle information. On launch of the application, the software tries to connect to the ESP32 present on the PCB that is fixed on the probe's attachment. Data is transferred from the ESP32 using listeners receiving encoder data through a Serial Port. As the user manipulates the needle angle, the corresponding encoder readings are updated on the GUI as seen in Figure 54. This way the user can visualize and note the optimal angle for needle insertion. As seen in Figure 54, the encoder reading of 348 degrees is also updated in the odometer visualization, which provides a more user-friendly method of viewing the change in angle readings over a given time, since solely tracking numbers is much more tedious.

Figure 55, as shown below, further demonstrates a holistic view of visualization software being used to stream ultrasound images and view angle information simultaneously. The image in the top-right corner of Figure 55 demonstrates the encoder readings being shown on the TFT display on the PCB fixed to the probe's attachment. As seen, the TFT display showcases an encoder reading of 154.69 degrees. The encoder reading can also be seen in the GUI that showcases an encoder reading of 155 degrees on the label and the odometer visualization. As seen in Figure 55, the system was also tested to make sure that it works well while wirelessly streaming ultrasound images from the Clarius scanner and reading encoder data through the serial port. Although there is a minute delay between encoder readings on the TFT display and GUI (the difference between readings of 154.69 degrees and 155 degrees), overall, the system works well to showcase all the components without any image freezing or major data lags.

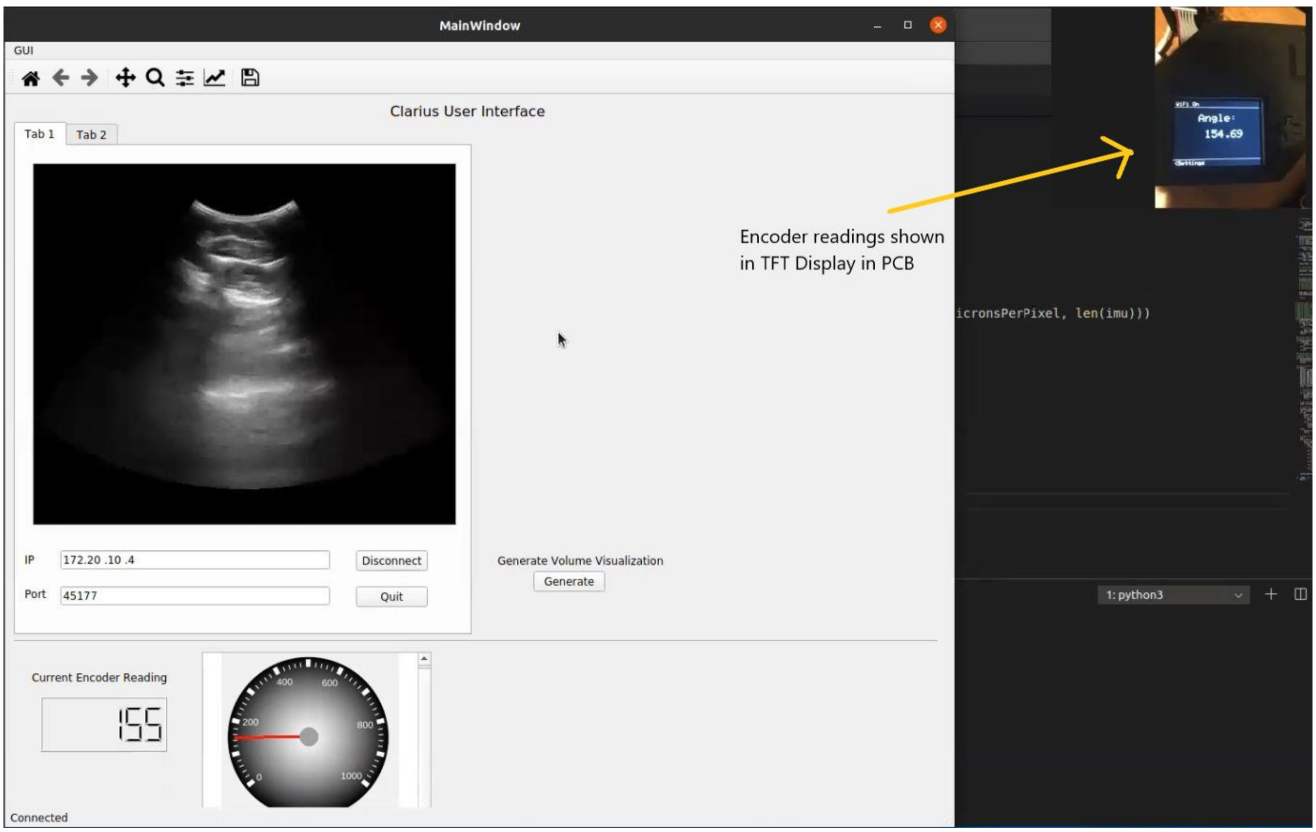

Figure 56: Encoder Readings Along Live Stream

Figure 56, as shown below, showcases the ultrasound scans presented in a three-dimensional space. As seen in the plot on the right-hand side of Figure 56, the ultrasound image associated with a rotation of 155 degrees is plotted in a three-dimensional mesh grid, that has the exact dimensions as the ultrasound image. This way, the user can better visualize ultrasound scans collected along the entire region that the changing mirror angle covered. Currently, the image plotted in the 3D mesh grid does not showcase a rotation, but only updates with current ultrasound images.

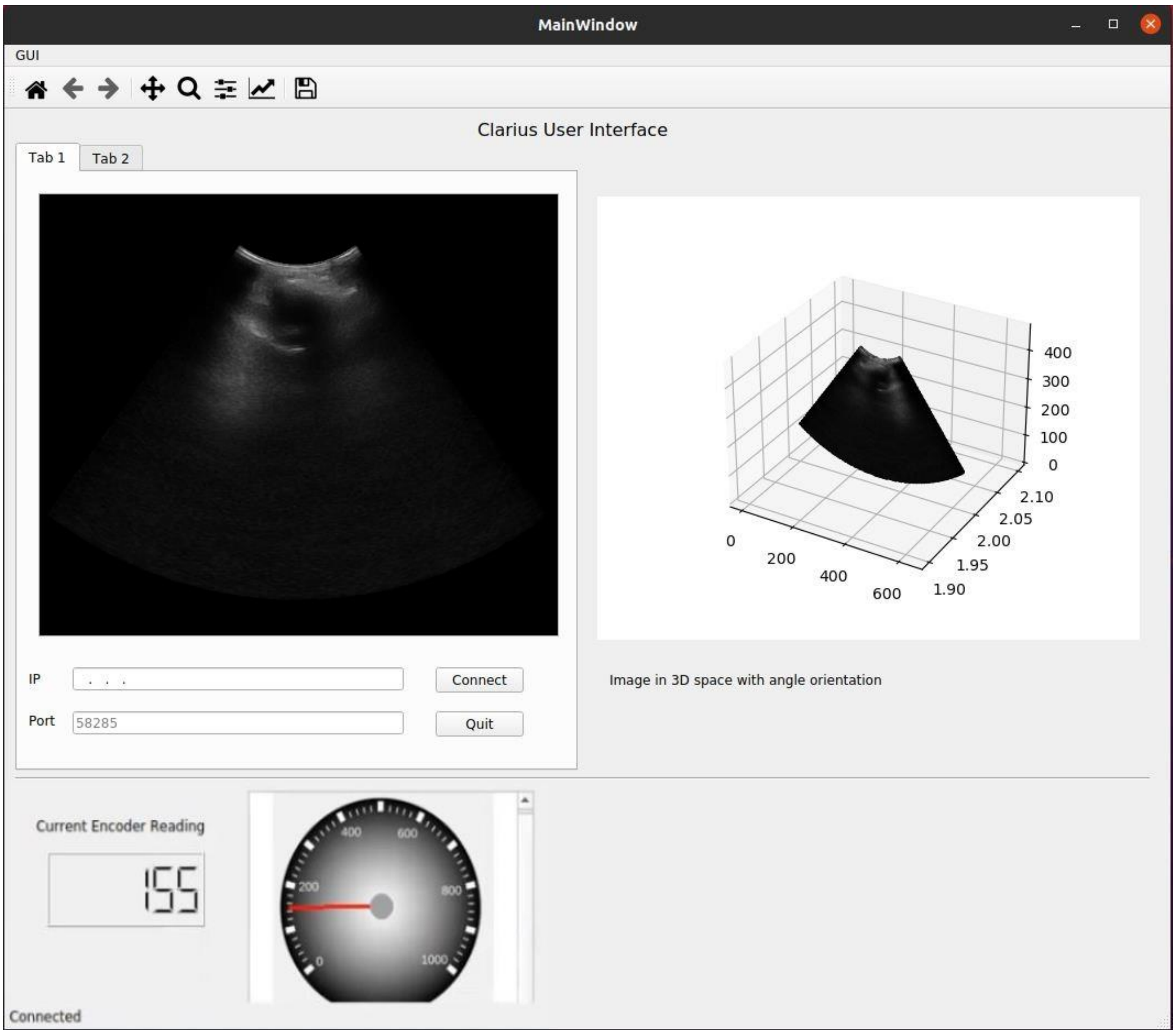

Figure 57: Ultrasound Image in 3D Space

Iteration 3 Software Development:

Iteration 3 of the software further builds upon our goal to provide a packaged solution that complements our device and provides users with useful information, all accessible in one place, so that they can carry out their procedures effectively. The previous iteration of the software added additional usability and functionality to enable users to view orientation data of the needle as they manipulate the needle as well as better visualize the effect that rotating the mirror angle on our attachment has on the region that ultrasound data is being collected from. This was done by visualizing the ultrasound scans in a three-dimensional space, where the ultrasound images are rotated along the plane where the mirror angle is being rotated.

The current iteration of the software builds upon this feature by implementing images in the 3D space visualization to rotate with an angle corresponding to encoder readings. By doing so, the user would have a clearer idea of how manipulating the mirror angle influences the US image and region being scanned. Furthermore, functionality was added so that images in the 3D mesh grid update real-time with incoming US images from the Clarius scanner. The images are also synchronized with incoming encoder readings, so that they can be plotted in a three-dimensional space with the correct orientation. The use case diagram on Page 50, demonstrates an example of the workflow that a typical user might have using our system. One of the key goals of iteration 3 of software development was to the test performance of the GUI while displaying a live stream of ultrasound images, reading encoder values from the serial port, and plotting ultrasound images in a 3D space simultaneously. An analysis of software performance can be seen in the discussion section.

Updated Software Architecture:

With the added functionalities to the software, there were several additional classes and methods added, as well as modified. These can be visualized effectively with the help of class diagrams that showcase the structure of the system and represent the object's attributes, operations, and associations. The ClariusGUI module handles the main workflow of the application and is the central module where data is being passed through. Since the last iteration, the view3D class was removed, and replaced by the Mpl3DPlot class within the ClariusGUI module. This was done to implement real-time plotting of ultrasound images from the Clarius. The Signaller and handler for new incoming ultrasound images was also updated so that whenever a new image is processed, the update_plot function within Mpl3Dplot is called, and the image is plotted in a 3D space. The image is also plotted with its corresponding encoder reading to provide the user with an accurate depiction of the angle at which the scanned area is being visualized. The changes made to the system can be visualized with the class diagram shown below:

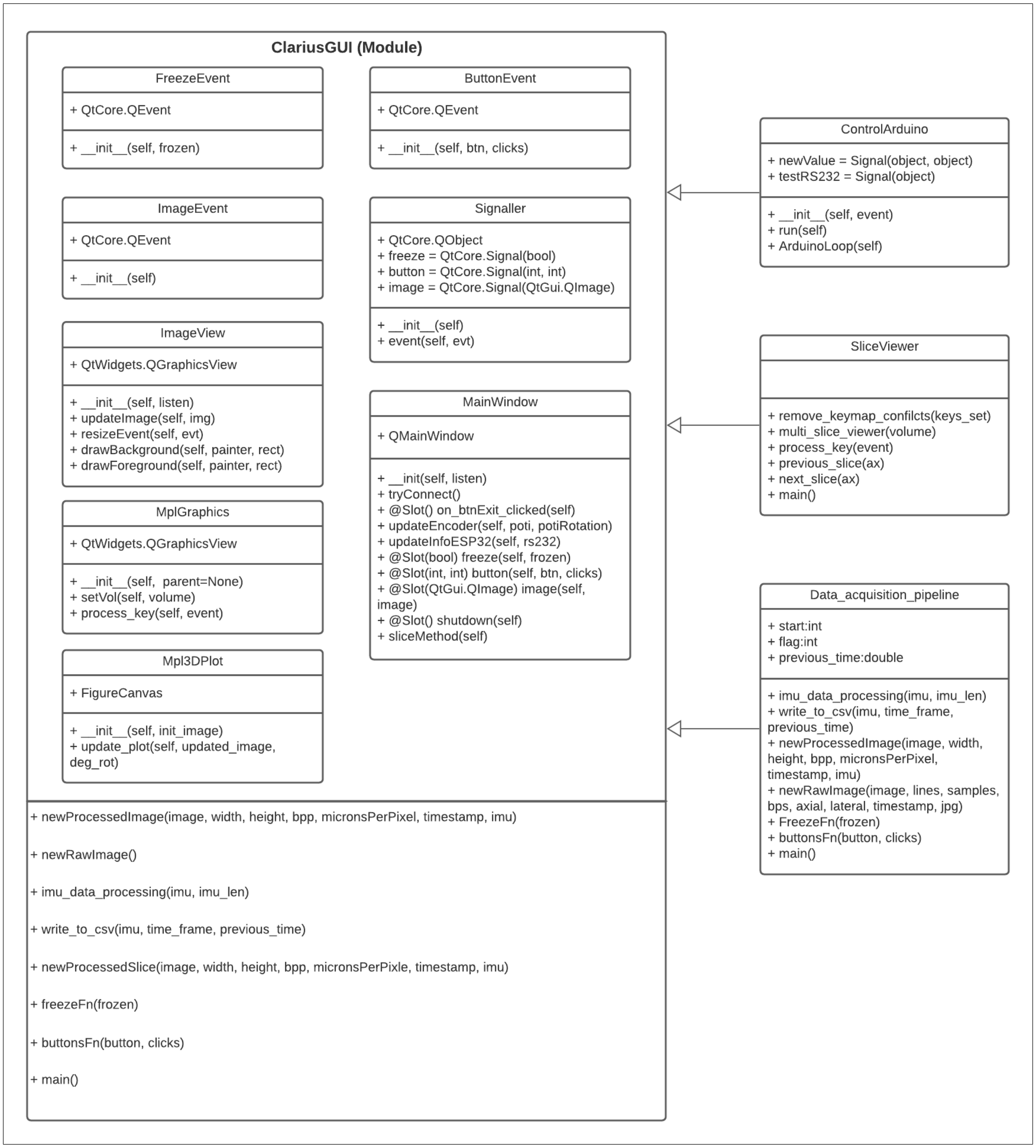

Figure 58: Class Diagram for Whole Application

Iteration 3 Experimental Results and Demo:

The Iteration 3 of the visualization software builds upon the idea of designing the GUI in a modular fashion so that the user has easy access to all the information that they need during the procedure. The GUI now has functionality that enables users to view live ultrasound images being streamed from the Clarius scanner, view real-time encoder readings as the mirror and viewing angles are changed, and visualize the real-time ultrasound scans in a three-dimensional space with their corresponding angle orientation.

This was implemented in the Mpl3Dplot class in the ClariusGUI module so that real-time images from the Clarius and incoming encoder readings could be utilized to plot the ultrasound images in a 3D space. Each incoming ultrasound image is plotted in a 3D space, with its corresponding angle value, using the Matplotlib plot_surface function. Although the image is plotted in a 3D space, the rotation for each image is performed along a 2D plane using 2D Affine Transformations. Each image is rotated based on its corresponding encoder value, read from the serial port. The angle of rotation is meant to mimic the rotation of the needle so that the user can easily visualize exactly what angle and plane the image was collected from, as they are manipulating the knob on the device. The mirror has a base angle of 45 degrees, which is the zero-position of the encoder. Therefore, the encoder records readings between -20 degrees and +20 degrees. A positive rotation on the device, will result in the ultrasound image being rotated to the left in the 3D space. Similarly, a negative rotation on the device, will result in the ultrasound image being rotated to the right in the 3D space.

Figure 56, as shown below, showcases the ultrasound scans presented in a three-dimensional space. As seen in the plot on the right-hand side of Figure 56, the ultrasound image associated with a rotation of 18 degrees is plotted in a three-dimensional mesh grid, that has the exact dimensions as the ultrasound image. This way, the user can better visualize ultrasound scans collected along the entire region that the changing mirror angle covered. You can also see how the image in the 3D space reflects the 18-degree rotation. Similarly, Figure 57 shows a negative rotation of -9 degrees, which is reflected in the 3D space by the image rotating slightly to the right.

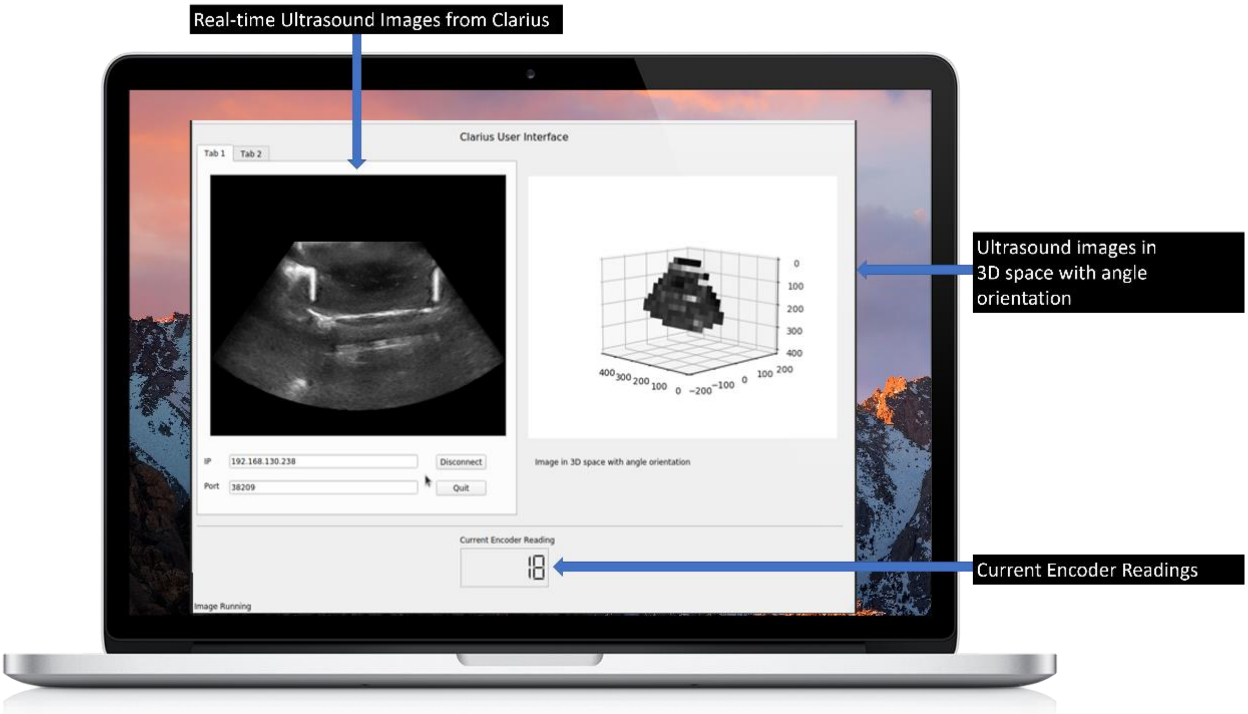

Figure 59: GUI Displaying US Image with Positive Degree Rotation.

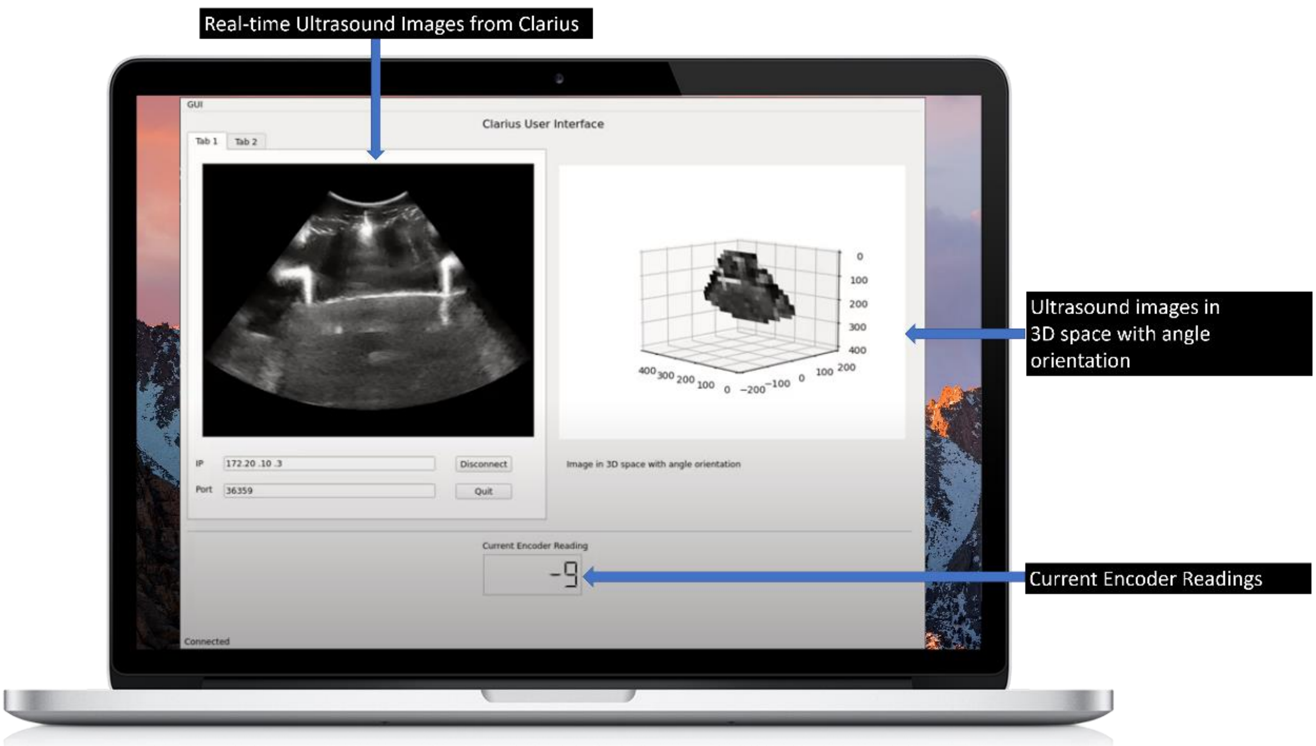

Figure 60: GUI Displaying US Image with Negative Degree Rotation.

Testing and Validation:

After completing the design process and adding all the required functionality to our device, we aimed to integrate all the various components and test the system's performance to make sure that we could accomplish our goal of creating a device that can guide the needle insertion path by reflecting ultrasound waves in-line with a needle. The following sections cover the testing setup we implemented, the ultrasound images we received from phantom tests, and the results from hardware and software testing.

Testing Setup:

The device was designed for its lower half to be submerged in gel or water, keeping the electronics above the water. This provides a medium for sound to travel through between the probe, mirror, and phantom. Without the device submerged, the US image would not have enough detail to validate our system, therefore we designed a custom water tank.

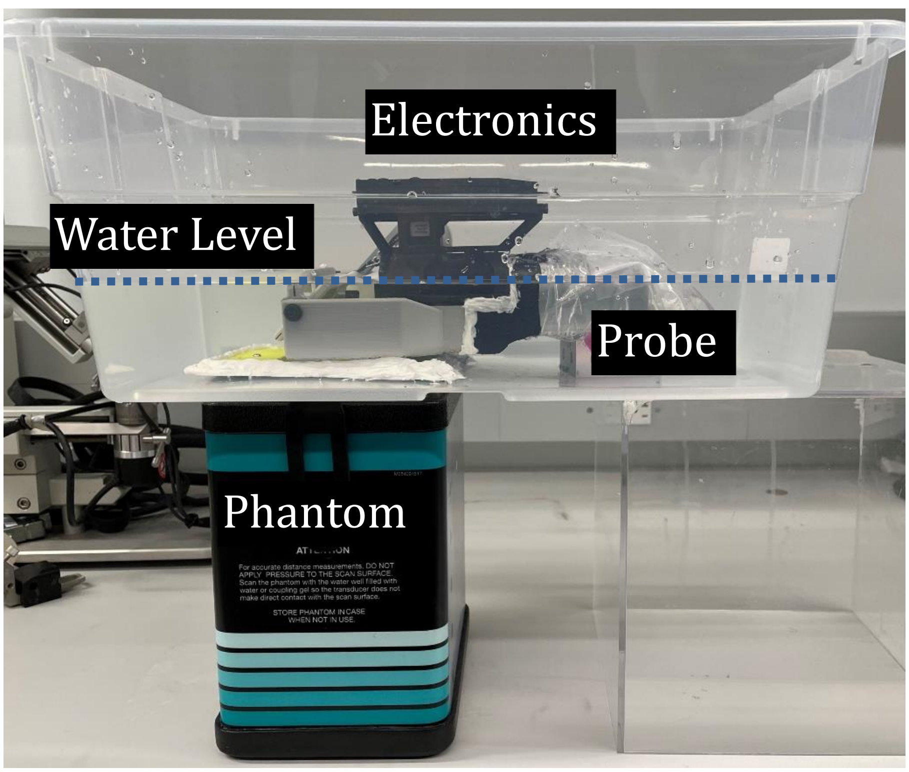

Figure 61: Testing Setup

As shown in the figure above, the probe and mirror mechanism can be submerged, with the electronics sufficiently above the water's surface. Additionally, with the assistance of Yichuan, we repurposed a plastic container to have a 3D printed pass-through for the US waves which was sealed with silicone glue. The pass-through allowed plastic wrap to be used rather than the US waves passing directly through the thicker plastic of the container.

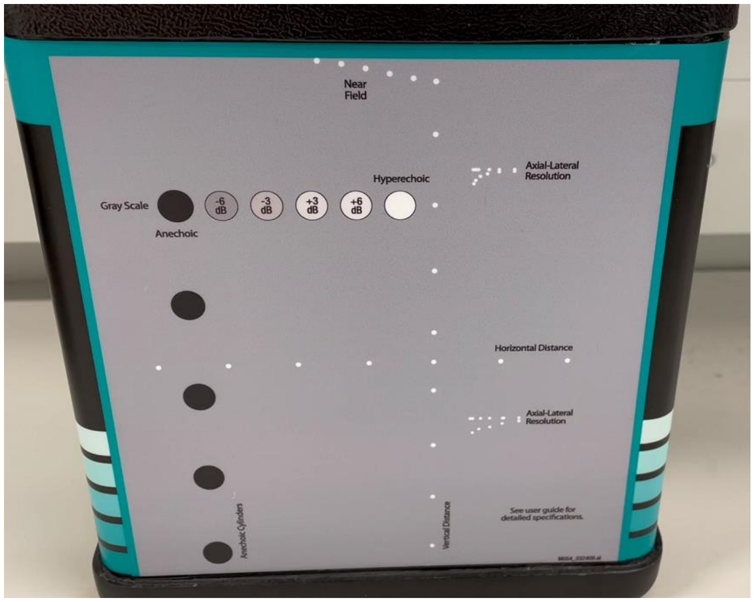

Figure 62: Phantom Cross Section

In the Medical Fusion Lab, we used a general US phantom to test the device. The white dots depicted in the figure above indicate all the possible points that can be viewed by the US probe. It is a reliable way of assessing the depth, width, and quality of the ultrasound image.

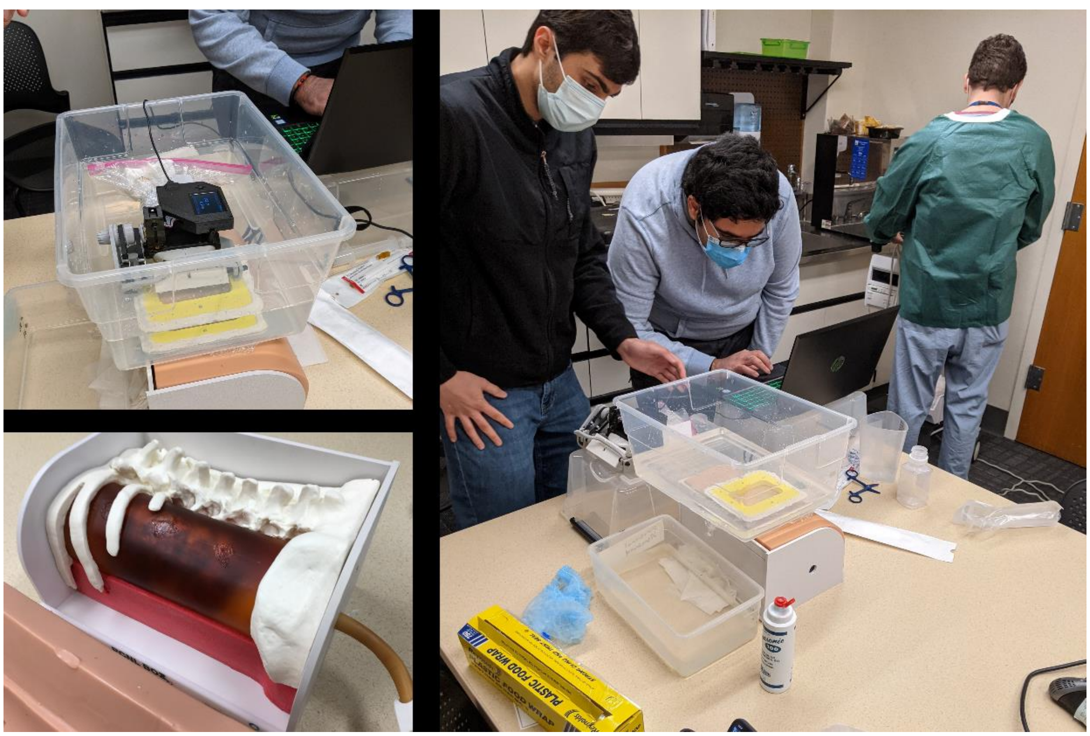

Figure 63: Testing Configuration at UMass Memorial Hospital

Thanks to Dr. Igor Sorokin and UMass Memorial Hospital, we were able to test the functionality of our device on a kidney phantom. In the bottom left of Figure 63, the kidney and bone phantom with the skin phantom removed is showcased. Above, as well as to the right, the general test setup can be viewed.

Ultrasound Scans:

We utilized the testing setup described in the section above to test and validate that our system was able to reflect ultrasound images using a mirror. We also tested ultrasound image quality and the depth of penetration that we were able to receive with our system.

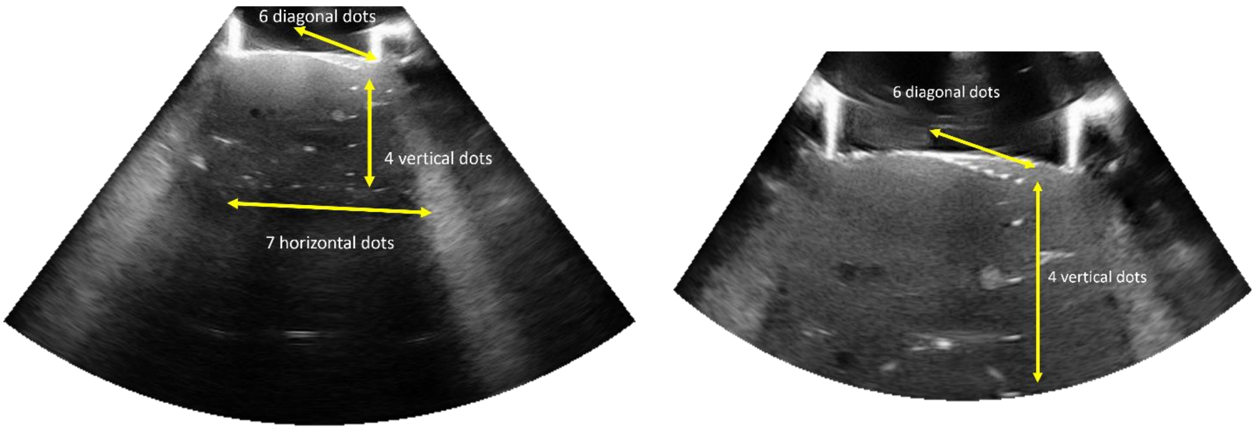

Figure 64: Image Results with Ultrasound Phantom

The images shown in Figure X above were collected using our GUI while testing the system on the ultrasound phantom displayed in Figure X. The pattern of dots seen in the ultrasound scans in Figure X demonstrate that our system was successful at reflecting ultrasound waves with a mirror. While performing the test, our device was placed in a water tank above the ultrasound phantom to provide a medium for the ultrasound waves to travel through from the probe to the phantom. The device and electronics were connected to the GUI to stream real-time ultrasound images and collect ultrasound data.

The 6 diagonal dots shown in the image relate to the upper-portion of the ultrasound phantom, validating that our needle-mirror mechanism is effective. The 4 vertical dots, and 7 horizontal dots prove that the system has sufficient depth of penetration and can visualize objects with a depth of up to 32 centimeters.

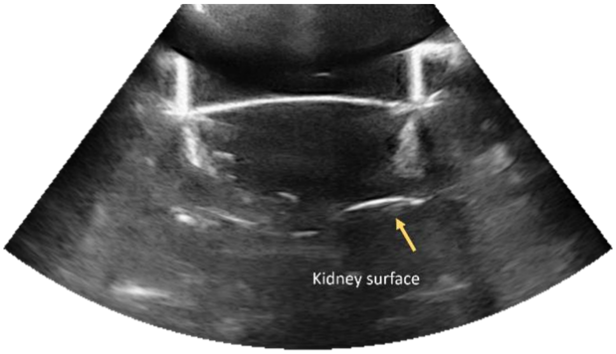

Figure 65: Image Result with Kidney Phantom

The image shown in Figure X above was collected while testing our system on a kidney phantom, as shown in Figure X. Visualizing the kidney phantom with the system was a lot more challenging than with the ultrasound phantom. The system had sufficient depth of penetration to view the surface of the kidney as seen in the ultrasound image above.

Angular Accuracy:

The device can rotate the needle and mirror with a 2:1 ratio, however, we also experienced measurable error. Across larger rotations we observed no more than 5.8 % error, so for the purposes of our testing this presented no issue.

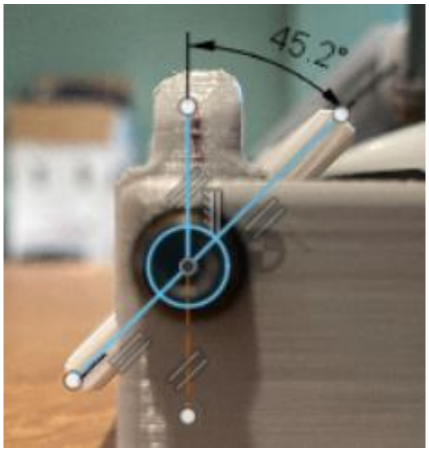

Figure 66: Side View of Needle/Mirror Center Position

We observed a baseline error of 0.44% at the center position. As can be seen in the Figure above, the desired angle between the needle and mirror at the center position is 45°, and our device was measured to have an actual angle of 45.2°.

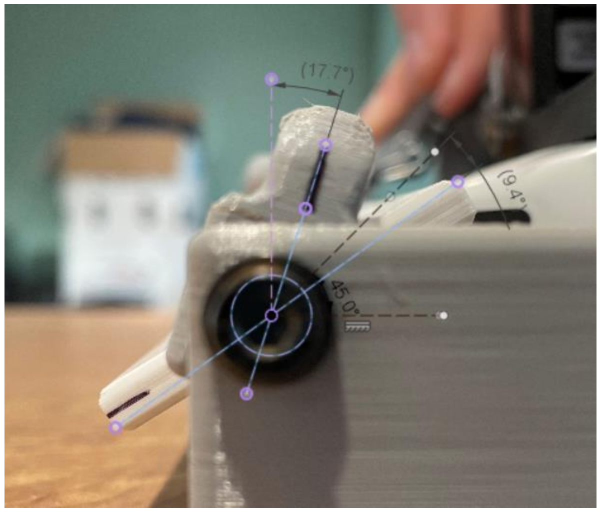

Figure 67: Angle Measurements of Rotation Test

The figure above showcases the needle and mirror mechanism as the needle is rotated 17.7° to the right, which should result in an 8.85° rotation of the mirror given that it is half of the needle's rotation. We observed the actual rotation to be 9.36°, meaning the error was 5.8%.

Angle Visualization:

During our testing procedures, we also tested the GUI's capability to visualize ultrasound images in a 3D space with angle orientation. With testing we were able to validate the software was able to handle streaming real-time ultrasound images, reading encoder values from the serial port, and plotting ultrasound images in a 3D space with their corresponding angle orientation. As seen in Figure X below, images in the 3D space can plotted through a sweep of 40 degrees (20 degrees each way about the origin), allowing for better visualization of the scanner area.

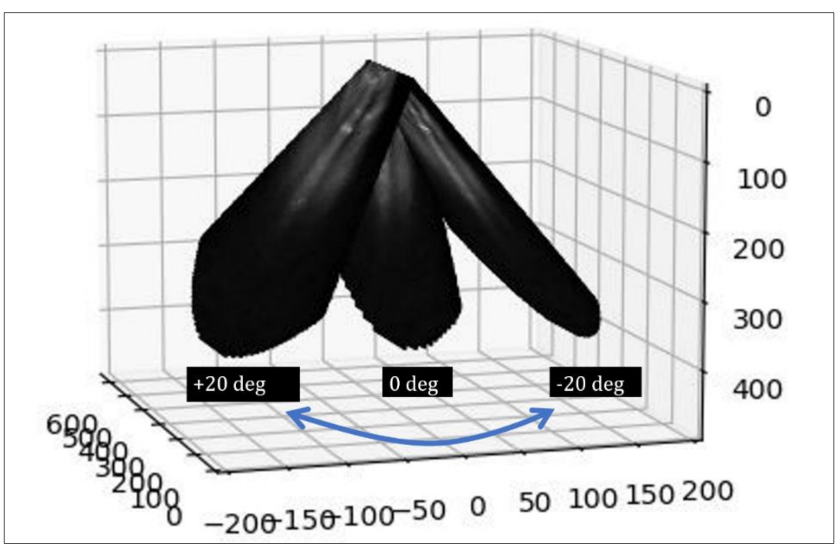

Figure 68: Angle Range for US Images in 3D Space

Discussion and Future Work:

Belt Drive Mechanism:

The belt drive system proved to be a successful solution to create a 2:1 ratio. We had originally planned to use a gear system; however, this would have been very complex to implement with the constraint that the two driven belt wheels must be rotating along the same axis. Our belt drive solution solved this issue and after multiple iterations we were able to achieve proper belt tension and suitable angular accuracy. We believe this system could be further improved with sturdier components, however the most pressing issue with the system is how to make it more modular. In a hospital setting, the portion touching the patient would ideally be disposable and replaced a sterilized part, but our current design is built as one large unit. If the belt drive system can be protected and separated from the needle and mirror components, this would substantially improve the device’s usability.

PCB:

The PCB functioned very well and enabled the use of a serial connection and clear encoder readings in a compact form. The menu navigation is smooth and intuitive, and the PCB can be easily incorporated in a future design of the device. With that said, a valuable extension of the project would be to make the electronics powered with an on-board battery as we had initially planned and use a wireless connection to stream encoder readings. This would allow the device to be entirely wireless.

Enclosure:

Our design functioned as a proof of concept and validated that the system works, however a great deal of work would be required to make the device practical. Currently, the lower half of the device must be submerged in water or gel to provide a medium for the US waves to pass through, but ideally this could be redesigned to have a small disposable enclosure only surrounding the mirror and needle. This would allow a practitioner to use the device on a patient without a large water tank or submerging the patient.

3D Visualization:

The current implementation of the 3D visualization allows users to visualize ultrasound images in a 3D space with their angle orientation, thus giving users a better understanding of the scanned area. With our current system, incorporating 3D visualization for real-time ultrasound images created latency issues due to our system set-up and the way that data is being processed. Submerging the device under water and poor network connection due to the use of mobile hotspots lead to ultrasound images being updated at an uneven rate, and even freezing at times. More importantly, plotting ultrasound images in the 3D space needs to be optimized to prevent latency issues. Having the GUI stream real-time ultrasound images from the Clarius, while reading encoder data from the serial port and plotting images in a 3D surface plot can be a strenuous process. The 3D plotting can be optimized to update the same image, instead of updating the plot each time a new ultrasound image is received. With the current setup, there can sometimes be a latency of about 2 seconds between updates of the ultrasound image and plotting the image in a 3D space. The recommended next step for the 3D visualization would be implement elevational beamforming so that a 3D volume can be generated for ultrasound scans. Performing beamforming would both improve image quality and help the user visualize depth information instead of just looking at a 2D scan.

System Performance:

With our current setup, the device needs to be submerged under water, due to a lack of an enclosure. Placing the device under water created network performance issues for the Clarius probe, which meant there was increased delays in the rate at which ultrasound images were streamed to the GUI. There were also increased occurrences of the Clarius phone application freezing due to poor network performance. Another factor contributing to network issues was the need to use an external mobile hotspot when connecting to the Clarius probe. To connect to the probe, both the mobile and pc running the GUI must be on the same Wi-Fi network. Due to restrictions with the WPI network, this meant that we needed to use a mobile hotspot every time we needed to test the system. Given the network inconsistencies associated with the hotspots, it would be recommended to get a router so that a consistent network connection can be established.

Transition to Human Testing:

The current device is capable of the basic functions we needed, however, for animal or eventually human testing, many improvements would need to be made. Firstly, in terms of practicality and usability, a proper enclosure is necessary to avoid the need for the device to be fully submerged. Ideally this could be a detachable and disposable component that houses the needle sheath and mirror and is filled with water or gel. This way the medium for US waves is maintained but packaged in a much smaller form factor. This ties into the issue of sterility because there cannot be any risk of transmitting anything between patients. If the device is redesigned and fabricated with sterility in mind, it could be suitable for human testing.

Another important step before transitioning to animal/human testing would be test the accuracy of the needle insertion process with our system. This includes a test to check the error between expected needle tip location and the actual needle tip location. Additionally, a test on a kidney phantom where a calyx of a kidney can be used would validate that the accuracy is sufficient for live trials. Finally, for the GUI to provide the practitioner with the desired telemetry and 3D visualization, latency issues will need to be improved.

Conclusion:

In conclusion, with this project we designed a system that would provide the benefits of ultrasound image guidance, needle stability, as well as added degrees of freedom for the operator to manipulate the needle. This project laid the groundwork for future projects to continue with ample opportunity to expand our research. This project could help improve clinical outcomes of needle guided intervention procedures and be adapted to a wide spectrum of needle guided intervention procedures other than PCNL. We hope that our work will eventually be utilized in a clinical setting and have a significant impact on improving clinical outcomes for needle guided intervention procedures.

References

[1] S. V. Reddy and A. B. Shaik, "Outcome and complications of percutaneous nephrolithotomy as primary versus secondary procedure for renal calculi," 2016. [Online]. Available: https://www.ncbi.nlm.nih.gov/pmc/articles/PMC4871386/#:~:text=PCNL .

[2] Radiological Society of North America (RSNA) and American College of Radiology (ACR), "Ultrasound (Sonography)," [Online]. Available: https://www.radiologyinfo.org/en/info.cfm?pg=genus.

[3] Clarius Mobile Health, "YouTube," 30 August 2016. [Online]. Available: https://www.youtube.com/watch?v=cI7ULKNhVcw.

[4] M. Nadrljanski, "Physical principles of ultrasound: Radiology Reference Article," [Online]. Available: https://radiopaedia.org/articles/physical-principles-of-ultrasound-1?lang=us.

[5] C. Chan, "A Needle Tracking Device for Ultrasound Guided Percutaneous Procedures," *Ultrasound in Medicine and Biology*, 9 November 2005.

[6] P. L. Rodrigues and N. F. Rodrigues, "Kidney Targeting and Puncturing During PCNL," July 2013. [Online]. Available: https://core.ac.uk/download/pdf/192109809.pdf.

[7] V. Arumuham, "A guide to percutaneous nephrolithotomy," 01 July 2019. [Online]. Available: https://www.urologynews.uk.com/features/features/post/a-guide-to-percutaneous-nephrolithotomy.

[8] F. C. Ng, W. L. Yam, T. Y. Lim, J. K. Teo and S. K. Lim, "Ultrasound-guided percutaneous nephrolithotomy: Advantages and limitations," 2017. [Online]. Available: https://www.ncbi.nlm.nih.gov/pmc/articles/PMC5577331/.

[9] K. J. Chin and A. Perlas, "Needle Visualization in Ultrasound-Guided Regional Anesthesia: Challenges and Solutions," 2008. [Online]. Available: https://edus.ucsf.edu/sites/edus.ucsf.edu/files/wysiwyg/Needle .

[10] H. J. Scholten, A. Pourtaherian, N. Mihajlovic, H. Korsten and R. Bouwman, "Improving needle tip identification during ultrasound-guided procedures in anaesthetic practice," 22 May 2017.

[11] L. J. Brattain, "Simple and Effective Ultrasound Needle Guidance System," in *International Conference of the IEEE EMBS, 33rd Annual International Conference of IEEE EMBS*, 2011.

[12] C. Hastings, "Iris Needle Guidance for Lumbar Punctures: Interview with Dev Mandavia, CEO of Ethos Medical," Medgadget, 18 March 2020. [Online]. Available: www.medgadget.com/2020/03/iris-needle-guidance-for-lumbar-punctures-interview-with-dev-mandavia-ceo-of-ethos-medical.html.

[13] S. Honigmann, "EpiGuide 2D: Visibility Assessment of a Novel Multi-Channel out-of-Plane Needle Guide for 2D Point-of-Care Ultrasound," in *International Society for Optics and Photonics*, 2019.

[14] S. Kwong, "Elevation Direction Focusing in Ultrasound Transducer Arrays - Siemens Medical Systems, Inc.," *FPO IP Research & Communities,* 13 February 1996.

[15] Telemed, "Research RF Data," *Telemed,* 2020.

[16] "Basic principle of medical ultrasonic probes (transducer)," [Online]. Available: https://www.ndk.com/en/sensor/ultrasonic/basic02.html.

[17] A. S. F. &. J. D. Carovac, "Application of ultrasound in medicine," September 2011. [Online]. Available: https://www.ncbi.nlm.nih.gov/pmc/articles/PMC3564184/.

[18] C. M. Doherty and R. B. Forbes, "Diagnostic Lumbar Puncture".

[19] M. Jonathan Cluett, "Are Ultrasound-Guided Injections Worth the Expense?," [Online]. Available: https://www.verywellhealth.com/ultrasound-guided-injections-2549577.

[20] Science Direct, "Percutaneous Nephrolithotomy," [Online]. Available: https://www.sciencedirect.com/topics/medicine-and-dentistry/percutaneous-nephrolithotomy.

[21] R. Singla, "Interdisciplinary Development and Evaluation of a Novel Needle Guide for Ultrasound-Guided Lumbar Epidural Placement," *BMJ Innovations,* 13 October 2020.

[22] "The Relevance of Needle Visibility in Intervention Procedures," [Online]. Available: https://www.esaote.com/en-US/clinical-solutions/therapy-and-interventional/relevance-of-needle-visibility-in-intervention-procedures/.

[23] S. J. Wisniewski and M. B. Hurdle, "Ultrasound-Guided and Fluoroscopically Guided Joint Injections," *Spinal Injections &amp Peripheral Nerve Blocks,* pp. 224-231.

[24] Verasonics, Inc., "Verasonics Transducers," *Verasonics.*

Appendix A: C-Term Development Timeline

Table 7: C Term Hardware Development Timeline

Order	TASK TITLE	START DATE	DUE DATE	DURATION
C Term	Iteration 4 Development and Testing			
1	Solder components to PCB	12/13/2020	12/16/2020	4
2	Sketch iteration 4 with elevated electronics	12/16/2020	12/26/2020	11
3	Purchase timing belts, tensioner wheels, and water tank	12/16/2020	1/1/2021	18
4	CAD Iteration 4	1/28/2021	2/5/2021	8
5	3D print and assemble Iteration 4	2/5/2021	2/12/2021	7
6	Configure Iteration 4 with software	2/5/2021	2/19/2021	14
7	Test Iteration 4	2/19/2021	2/26/2021	7
8	Adjust, tune, and improve device accuracy	2/26/2021	3/18/2021	19

Table 8: C Term GUI Development Timeline

Order	TASK TITLE	START DATE	DUE DATE	DURATION
C Term	Volume Visualization and integration with hardware			
1	Modifications to GUI to improve user control and accessibility	12/13/2020	12/28/2020	15
2	Implement image reconstruction and 3D volume visualization	12/28/2020	1/28/2021	30
3	Test and Validate B-term progress with Clarius	1/28/2021	2/5/2021	7
4	Ability to view Volume data based on device orientation	2/2/2021	2/15/2021	13
5	Integrate with electronics to display encoder readings. In GUI	2/12/2021	2/21/2021	7
6	Configure Iteration 4 with software	2/5/2021	2/25/2021	14
7	Test overall GUI functionality and image quality once integrated with hardware	2/19/2021	2/26/2021	7
8	Adjust, tune, and improve device accuracy	2/26/2021	3/18/2021	19

Appendix B: D-Term Development Timeline

Table 9: D Term Hardware Development Timeline

Order	TASK TITLE	START DATE	DUE DATE	DURATION
D Term	Iteration 4 improvements and testing			
1	Finalize adjustments to iteration 4 tensioning system and sufficiently test angular accuracy (6+ times)	3/21/2021	3/31/2021	10
2	Setup testing environment with water tank and test how accurately the user can determine the position of the needle tip.	3/31/2021	4/7/2021	7
3	Test device using a phantom material. Gather footage and collect data about efficacy. Test integration with software.	4/14/2021	4/25/2021	11
4	Prepare for MQP Project Presentation Day	4/25/2021	4/30/2021	5
5	Final improvements and testing with software	4/30/2021	5/5/2021	5
6	Work on Final MQP Report	5/2021	5/12/2021	7

Table 10: D Term GUI Development Timeline

Order	TASK TITLE	START DATE	DUE DATE	DURATION
D Term	Visualization in 3D space and integration with hardware			
1	Enable plot to rotate in 3d space based on encoder value	3/24/2021	3/31/2021	7
2	Work on updating rotated image real-time	3/31/2021	4/7/2021	7
3	Test performance for the whole system and work on error-handling. Integrate and test software with hardware from iteration 4	4/7/2021	4/14/2021	7
4	Test entire system with phantom in water tank	4/14/2021	4/22/2021	8
5	Prepare for MQP Project Presentation Day	4/23/2021	4/30/2021	7
6	Final GUI improvements and testing with hardware	4/30/2021	5/5/2021	5
7	Work on Final MQP Report	5/2021	5/12/2021	7